

2020年度測位航法学会 全国大会 セミナー②

RTK および PPP 技術の応用と実習

Theory and Practice of RTK/PPP Technology

 Tokyo Univ. of Marine Science and Technology (TUMSAT)

Tomoji TAKASU

2020-07-16 @Zoom meeting (online)

Timetable

July 16, 2020

1	Introduction of RTK/PPP	9:30-10:20
2	Theory of PTK/PPK	10:30-11:20
3	RTK/PPK Practice	11:30-12:30
	Lunch Break	12:30-13:30
4	Theory of PPP	13:30-14:20
5	PPP Practice	14:30-15:20
6	Advanced Topics	15:30-16:30

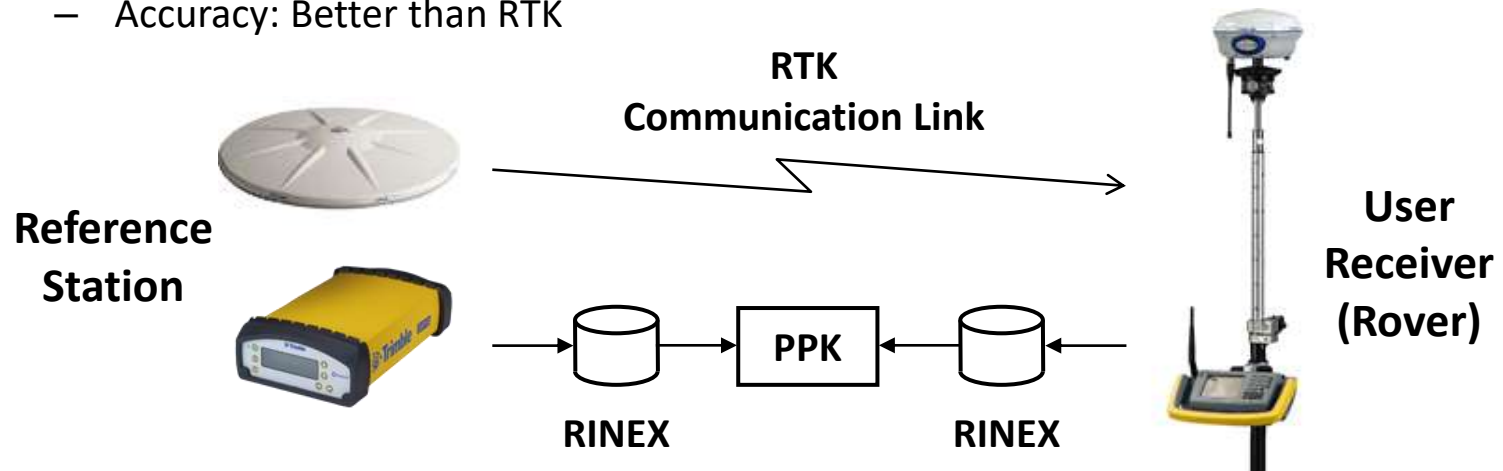
1.
Introduction of RTK/PPP

Code vs Carrier-Based Positioning

	SD (standard positioning, code-based)	PP (precise positioning, carrier-based)
Observables	Pseudorange (Code)	Carrier-Phase + Pseudorange
Receiver Noise	30 cm	3 mm
Multipath	30 cm - 30 m	1 - 3 cm
Sensitivity	High (<20dBHz)	Low (>35dBHz)
Discontinuity	No Slip	Cycle-Slip
Ambiguity	-	Estimated/Resolved
Receiver	Low-Cost (~\$100)	Expensive (~\$20,000)
Accuracy (RMS)	3 m (H), 5 m (V) (Single) 1 m (H), 2 m (V) (DGPS)	5 mm (H), 1 cm (V) (Static) 1 cm (H), 2 cm (V) (RTK/PPK)
Application	Navigation, Timing, SAR,...	Survey, Mapping, ...

RTK/PPK

- **RTK (Real-time Kinematic)**
 - Real-time Position of Rover Antenna
 - Transmit Reference Station Data to Rover via Comm. Link
 - OTF (On-the-Fly) Integer Ambiguity Resolution
 - Typical Accuracy: 1 cm + 1ppm x BL RMS (Horizontal)
- **PPK (Post-processing Kinematic)**
 - Post-processed Position of Rover Antenna
 - Rover and Reference Station Data provided by Standard RINEX Formats
 - Accuracy: Better than RTK



RTK/PPK Applications



Geodetic Survey



**Construction Machine
Control**



Precision Agriculture



Self-driving Car

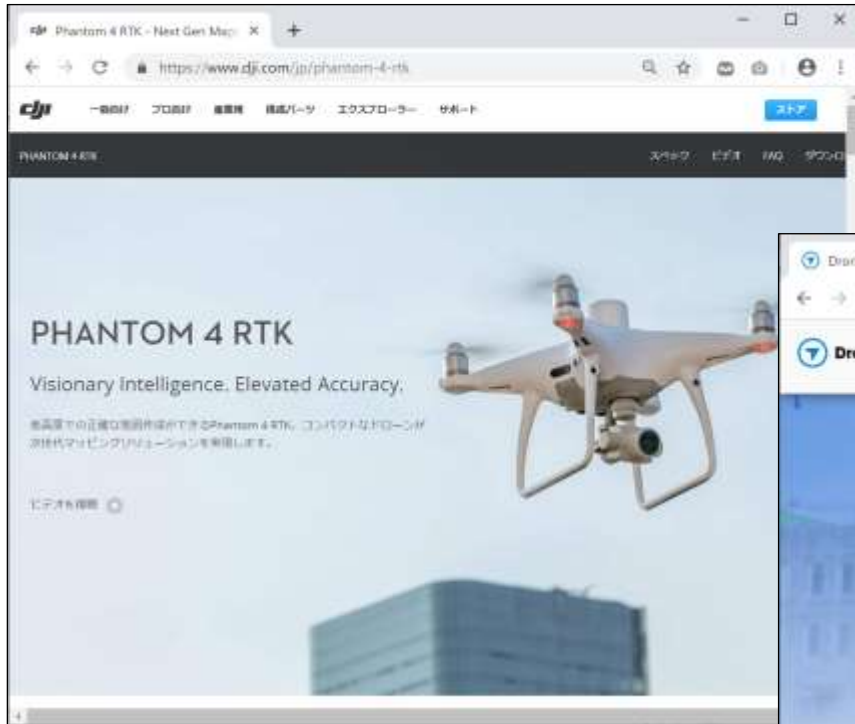


Mapping

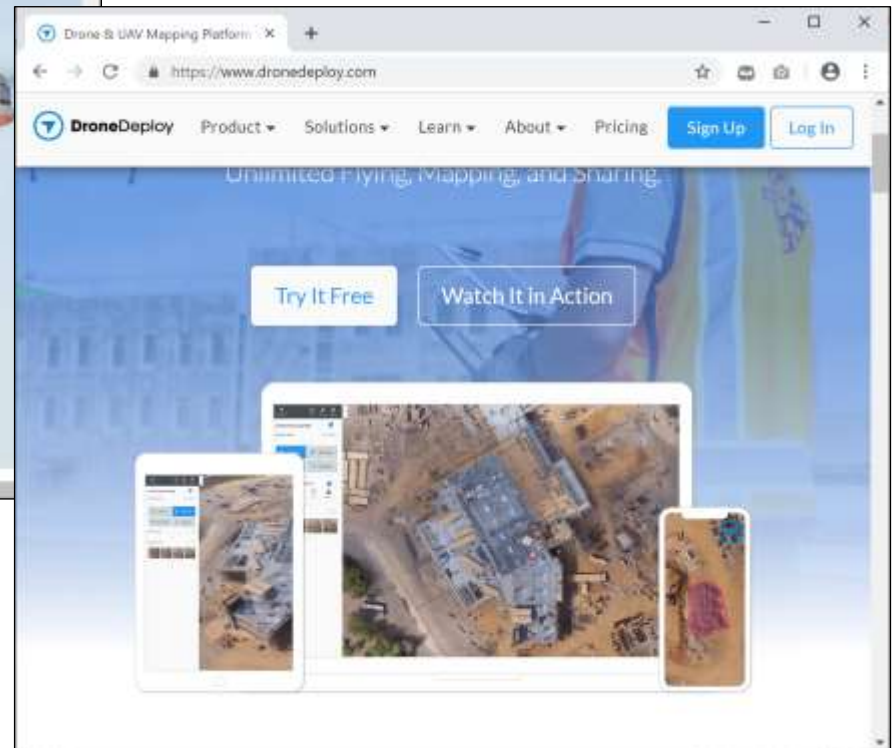


UAV (Drone)

UAV (Drone) with RTK/PPK



<https://www.dji.com/jp/phantom-4-rtk>



<https://www.dronedeploy.com/>

PPP (Precise Point Positioning)

- **Historical View**
 - **Firstly introduced in 1990s** to analyze data of large GPS station N/W ^[1]
 - **Conventionally PP** with IGS precise ephemerides since 1990s
 - Several **RT-PPP services have launched via GEO satellite links** since 2000s
 - Recently improving accuracy with **multi-constellation GNSS and PPP-AR**
 - **Convergence time is still an issue** for some applications even in 2019

[1] J. F. Zumberge et al., Precise point positioning for the efficient and robust analysis of GPS data from large networks, Journal of Geophysical Research, 1997

	RTK	PPP
Base Station	Required	Not required
Area Coverage	Local (< 30 km)	Global (worldwide)
Accuracy (HRMS)	1 ~ 4 cm	2 ~ 5 cm
Convergence Time	< 60 s	15 ~ 45 min

PPP Applications



Automated Farming



**Offshore Construction/
Mining**



Drone/UAV



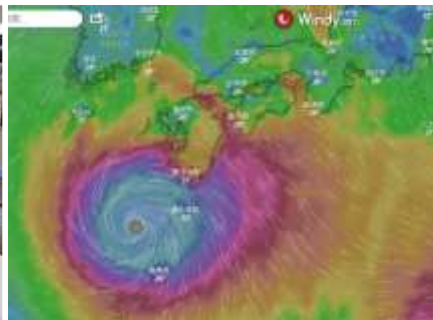
**ADAS/
Autonomous Driving**



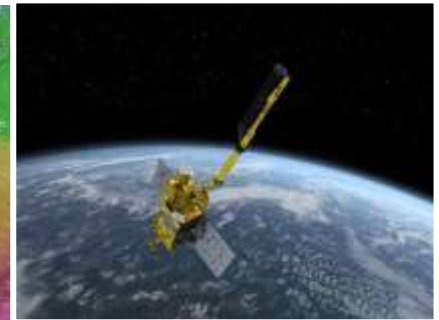
Tsunami Warning



Precise Time Transfer

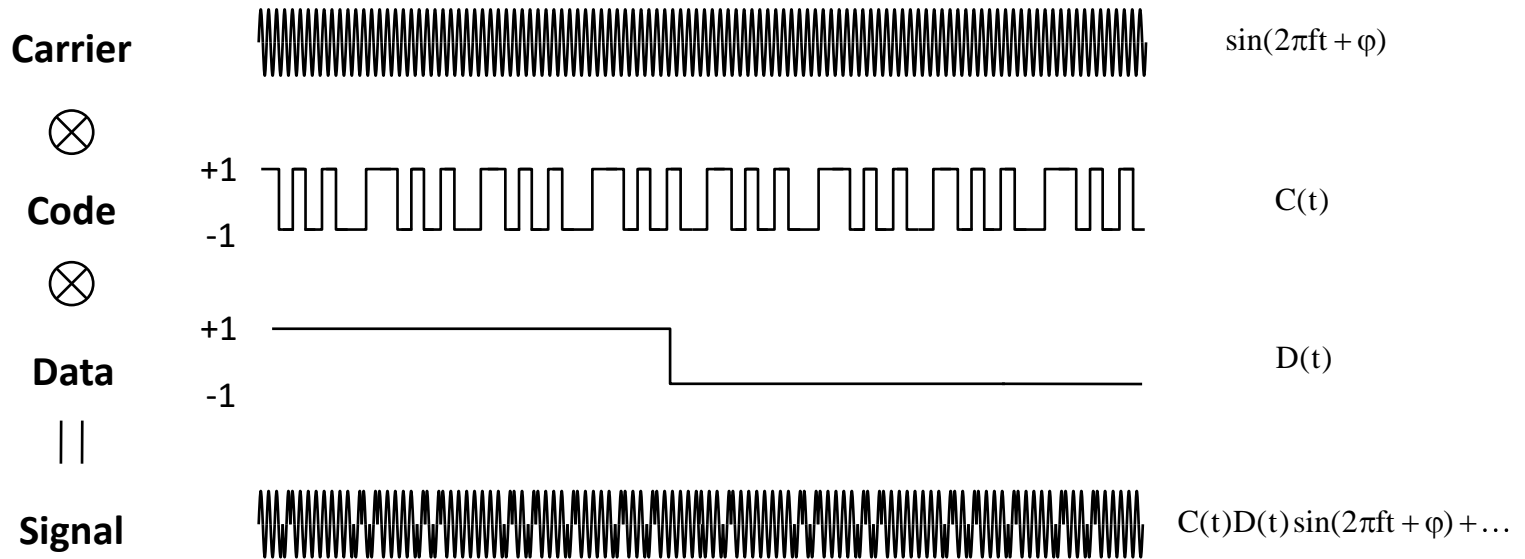


**Weather Forecast
(GNSS Meteorology)**

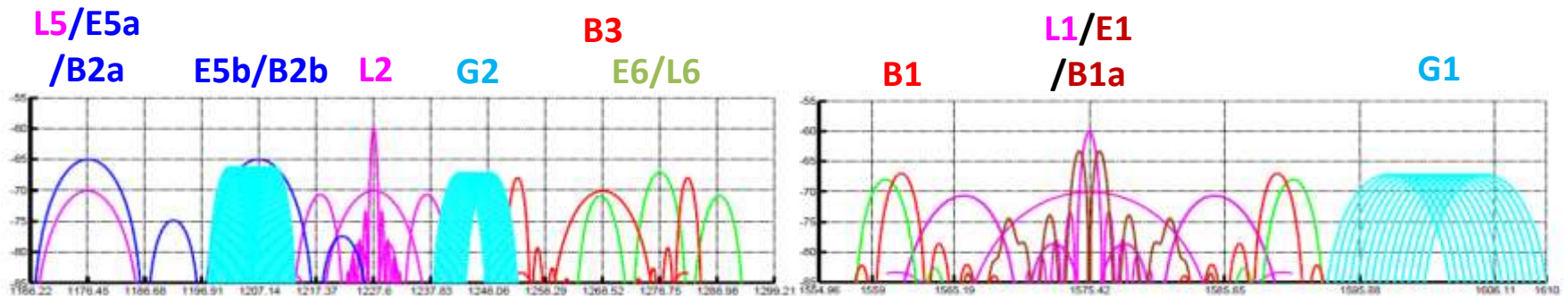


Satellite POD

GNSS Signal Structure

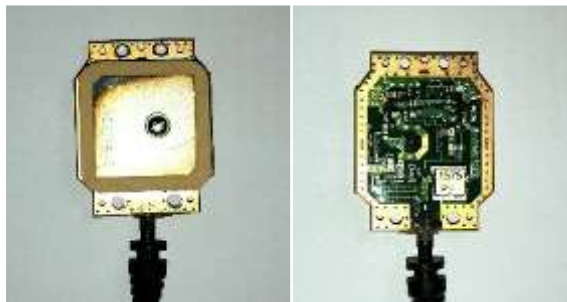


GNSS Signal Spectrum ^[1]



[1] Y.Yang, COMPASS: View on Compatibility and Interoperability, 2009

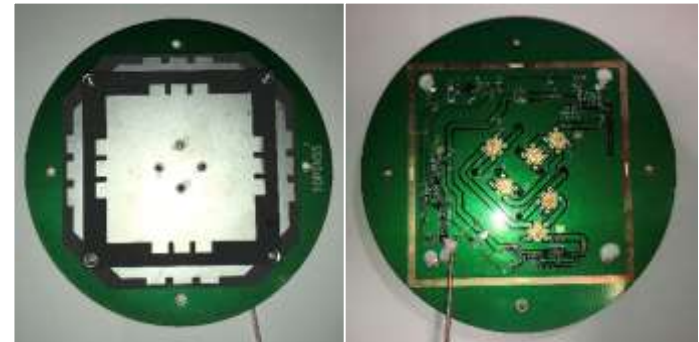
GNSS Antennas



Patch Antenna (L1)



Helix Antenna
(L1+L2)



Patch Antenna (L1+L2)

GNSS Receivers (1)



My receiver collections

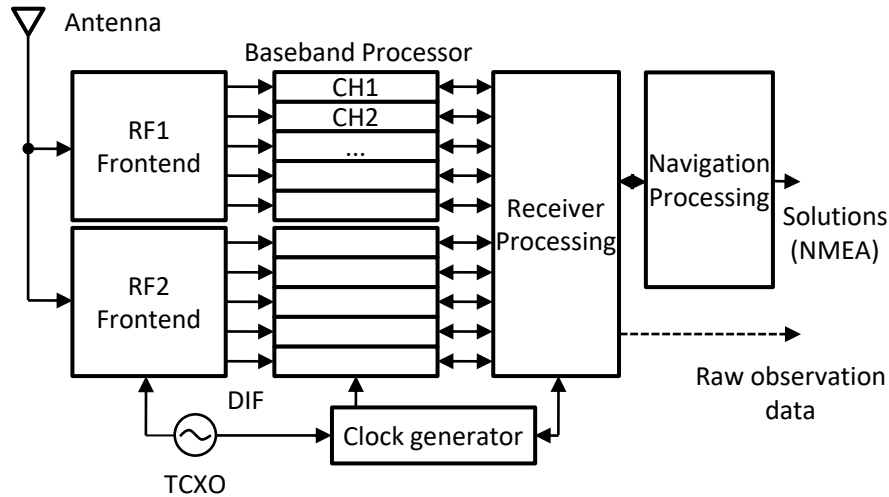


NovAtel OEMV-3



Trimble BD982

GNSS Receivers (2)

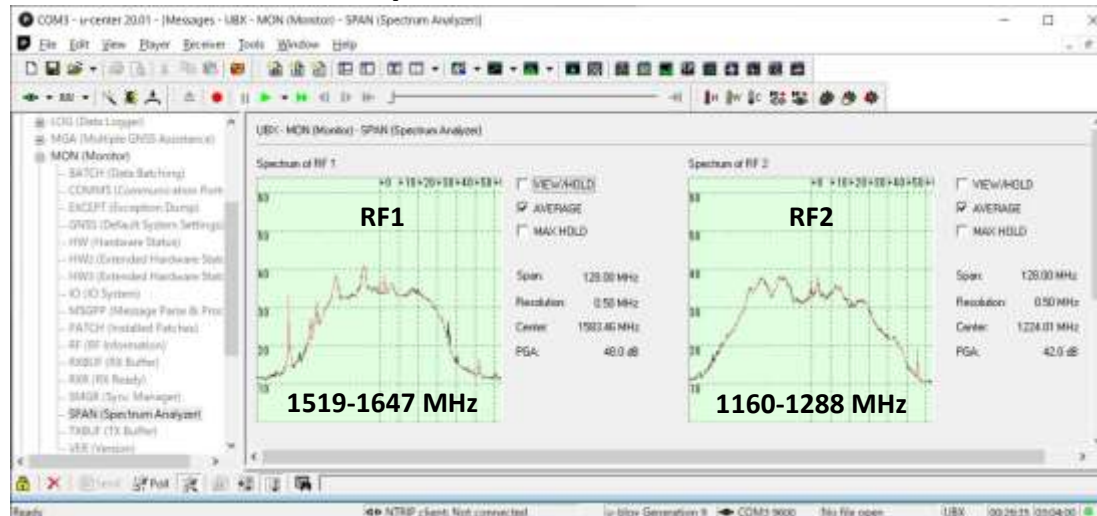


Mini-EVK of u-blox ZED-F9P [1]



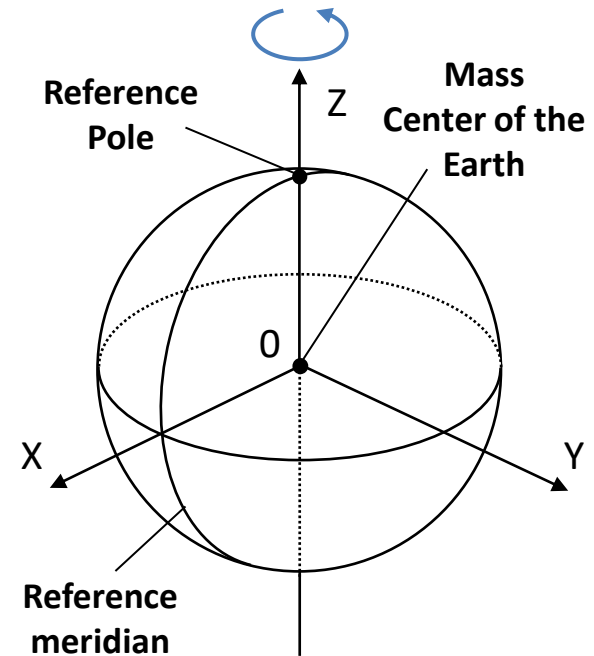
[1] <https://www.u-blox.com>

IF Spectrum of ZED-F9P [1]



Coordinate Systems

- **ECEF (earth-centered earth-fixed)**
 - ITRF
 - WGS84 (GPS)
 - PZ90.14 (GLONASS)
 - JGS (QZSS)
 - JGD (Japan, GSI) ...
- **Latitude, Longitude and Height**
 - Latitude: geodetic, geocentric
 - Height: orthometric, ellipsoidal
- **ECI (earth-centered inertial)**
 - J2000.0 (equatorial coordinate system)
 - ICRF (international celestial reference frame)



ECEF Definitions

ITRF

- **International Terrestrial Reference Frame**

- A "Realization" of ITRS developed and maintained by IERS
- GNSS, VLBI, SLR, DORIS site position/velocity, EOP, PSD (SINEX)
- ITRF2014, ITRF2008, ITRF2005, ITRF2000, ITRF97, ITRF96, ...

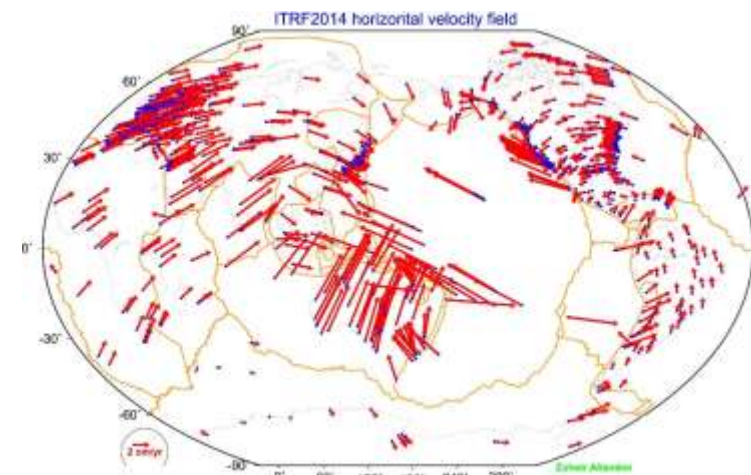
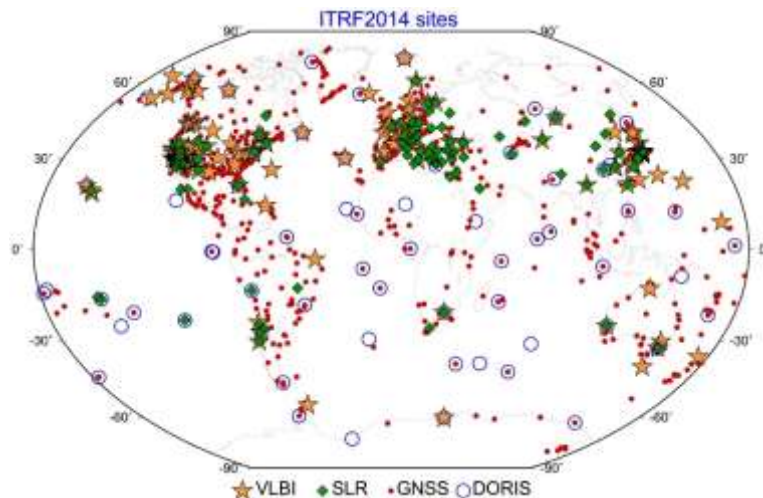
VLBI: Very Long Baseline Interferometry

SLR: Satellite Laser Ranging

DORIS: Doppler Orbit determination and Radiopositioning Integrated on Satellite

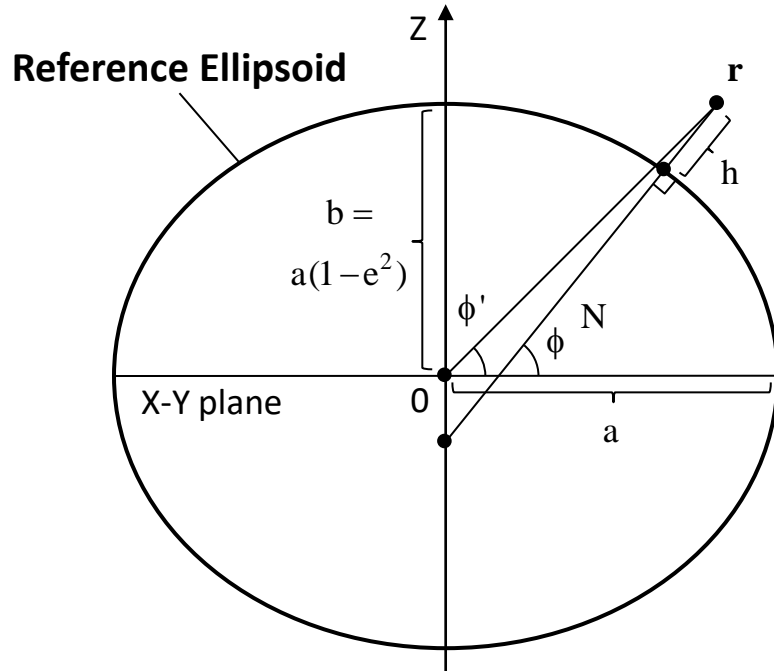
ITRS: International Terrestrial Reference System

IERS: International Earth Rotation Service



Z.Altamimi et al., ITRF2014: A new release of the International Terrestrial Reference Frame modeling nonlinear station motion, JGR Solid Earth, 2016

Latitude, Longitude and Height



Lat/Lon/Hgt -> ECEF-XYZ

$$e^2 = f(2 - f)$$

$$N = \frac{a}{\sqrt{1 - e^2 \sin^2 \phi}}$$

$$\mathbf{r} = \begin{pmatrix} x \\ y \\ z \end{pmatrix} = \begin{pmatrix} (N + h) \cos \phi \cos \lambda \\ (N + h) \cos \phi \sin \lambda \\ (N(1 - e^2) + h) \sin \phi \end{pmatrix}$$

ECEF-XYZ -> Lat/Lon/Hgt

$$R = \sqrt{x^2 + y^2}, \phi_0 = 0$$

$$\phi_{i+1} = \arctan \left(\frac{z}{R} - \frac{ae^2 \tan \phi_i}{R \sqrt{1 + (1 - e^2) \tan^2 \phi_i}} \right)$$

$$\phi = \lim_{i \rightarrow \infty} \phi_i$$

$$\lambda = \text{ATAN2}(y, x)$$

$$h = \frac{R}{\cos \phi} - \frac{a}{\sqrt{1 - e^2 \sin^2 \phi}}$$

	GRS80	WGS84
a	6378137 m	6378137 m
f	1/298.257222101	1/298.257223563
b	6335439.32708 m	6335439.32729 m

- a** : Semi-major axis length (m) **f** : Flattening
phi-prime : Geocentric latitude **lambda** : Longitude
phi : Geodetic latitude **h** : Ellipsoidal height

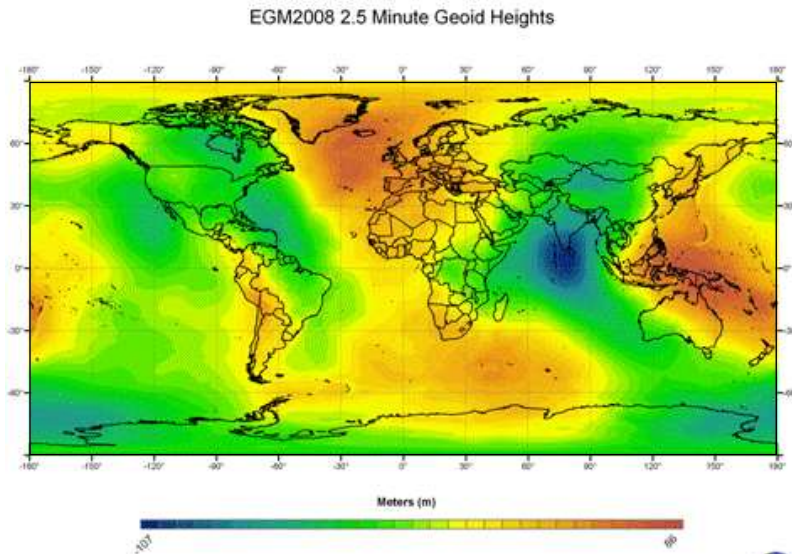
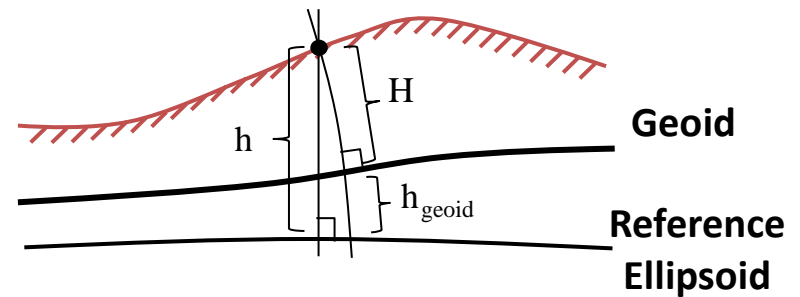
Heights

$$H \approx h - h_{\text{geoid}}(\phi, \lambda)$$

H : Orthometric height (m)

h : Ellipsoidal height (m)

h_{geoid} : Geoid height (m)

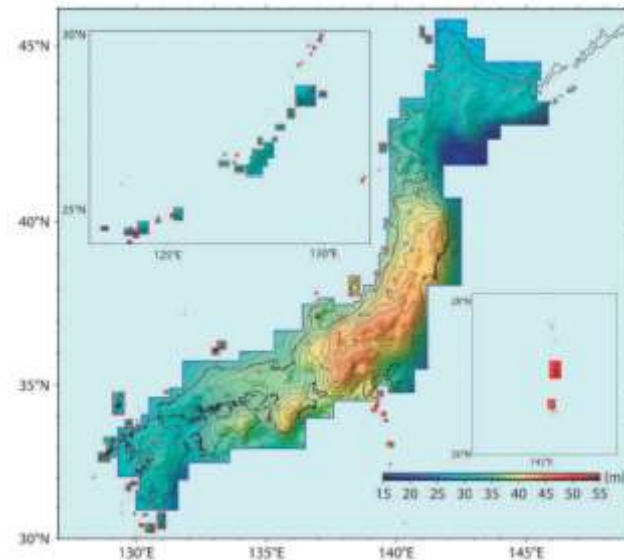


NGA - GeoSciences Division

EGM2008 Geoid



https://earth-info.nga.mil/GandG/wgs84/gravitymod/egm2008/egm08_wgs84.html

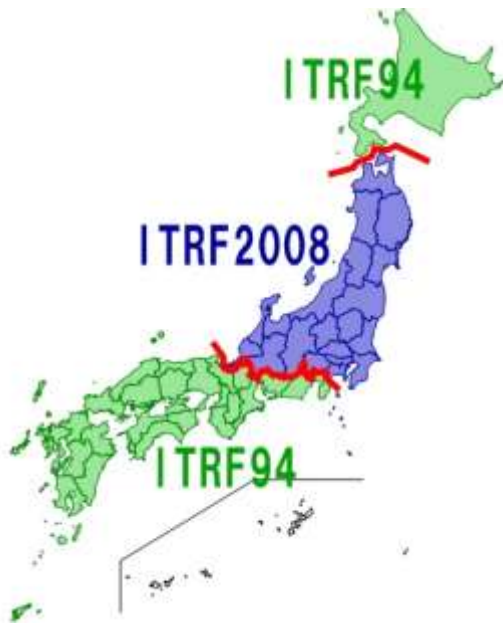


GSIGEO2011 (Ver.2) Geoid

https://www.gsi.go.jp/buturisokuchi/grageo_geoidseika.html

Japanese Geodetic Datum

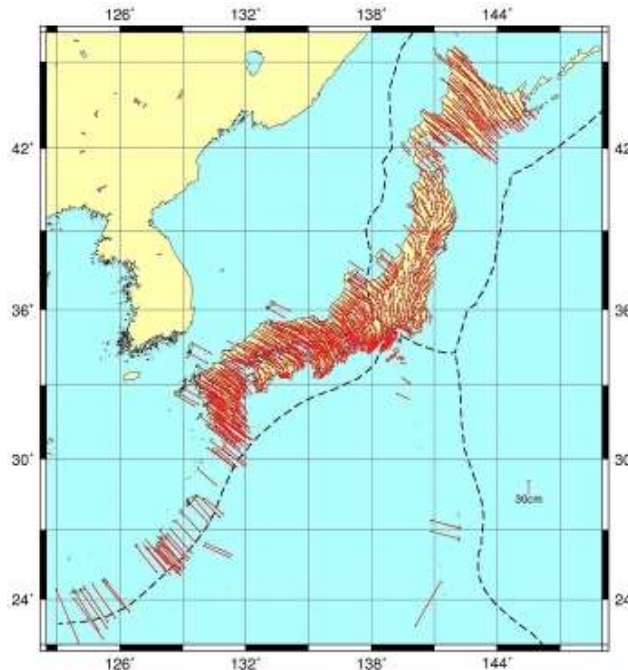
Tokyo -> JGD2000 ->
JGD2011



JGD2011 (GSI)

<http://club.informatix.co.jp/?p=998>

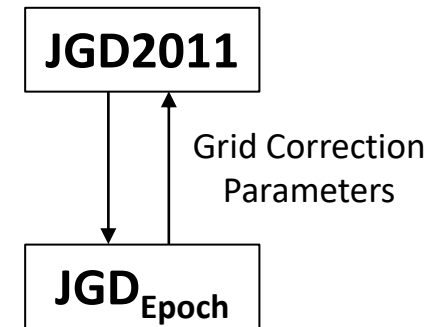
Displacement of
Japanese Island



1997 -> 2009

<https://www.gsi.go.jp/sokuchikijun/semidyna01.html>

Semi-dynamic
corrections



<https://www.gsi.go.jp/sokuchikijun/semidyna03.html>

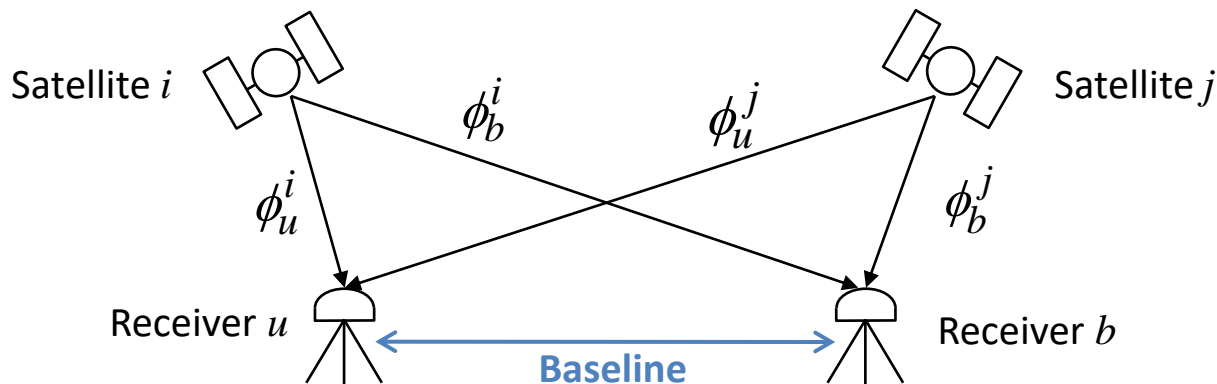
2. Theory of RTK/PPK

DD (Double-difference)

$$\begin{aligned}
 \Phi_{ub}^{ij} &\equiv \lambda((\phi_u^i - \phi_b^i) - (\phi_u^j - \phi_b^j)) \\
 &= \rho_{ub}^{ij} + c(dt_{ub}^{ij} - dT_{ub}^{ij}) - I_{ub}^{ij} + T_{ub}^{ij} + \lambda B_{ub}^{ij} + d_{ub}^{ij} + \varepsilon_{\Phi} \\
 &= \rho_{ub}^{ij} - I_{ub}^{ij} + T_{ub}^{ij} + \lambda N_{ub}^{ij} + d_{ub}^{ij} + \varepsilon_{\Phi} \\
 dt_{ub}^{ij} &= dt_u^{ij} - dt_b^{ij} = 0, dT_{ub}^{ij} = dT_{ub}^i - dT_{ub}^j \approx 0 \\
 B_{ub}^{ij} &= (\phi_{u,0}^i - \phi_0^i + N_u^i) - (\phi_{b,0}^i - \phi_0^i + N_b^i) - (\phi_{u,0}^j - \phi_0^j + N_u^j) + (\phi_{b,0}^j - \phi_0^j + N_b^j) = N_{ub}^{ij}
 \end{aligned}$$

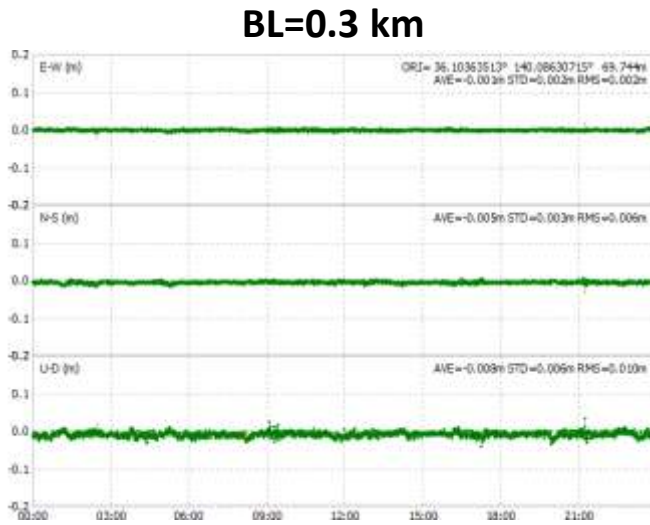
(short Baseline and same antenna type)

$$\Phi_{ub}^{ij} \approx \rho_{ub}^{ij} + \lambda N_{ub}^{ij} + \varepsilon_{\Phi} \quad I_{ub}^{ij} = I_{ub}^i - I_{ub}^j \approx 0, T_{ub}^{ij} = T_{ub}^i - T_{ub}^j \approx 0, d_{ub}^{ij} = d_{ub}^i - d_{ub}^j \approx 0$$

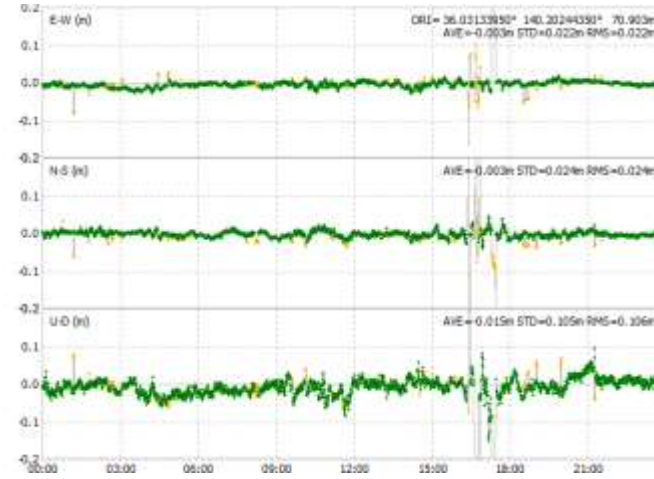


Effect of Baseline Length

RMS Error:
E: 0.2cm
N: 0.6cm
U: 1.0cm
Fix Ratio:
99.9%

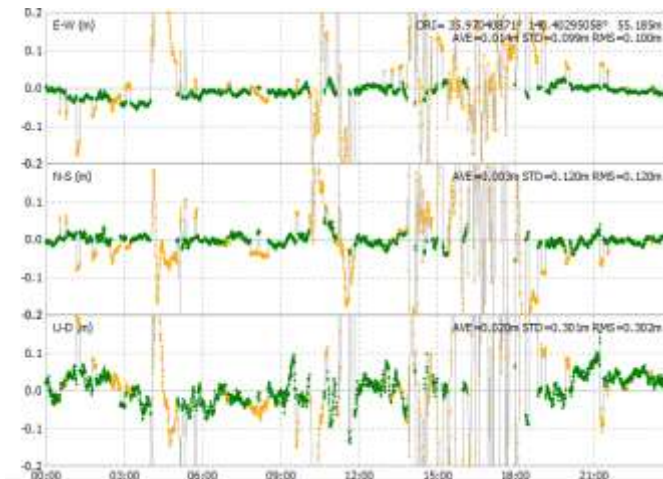


BL=13.3 km



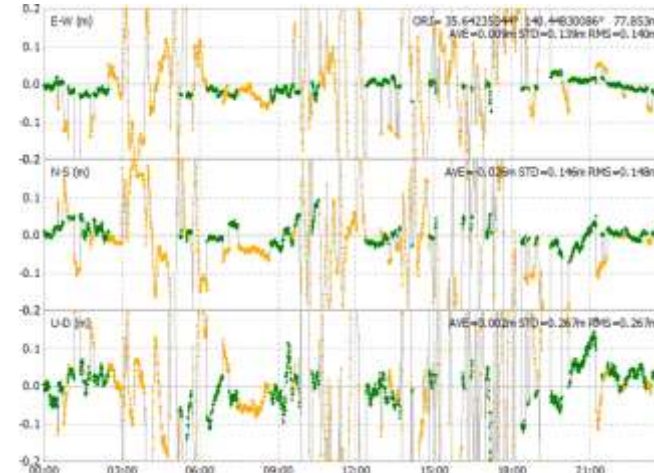
RMS Error:
E: 2.2cm
N: 2.4cm
U: 10.6cm
Fix Ratio:
94.2%

BL=32.2 km



RMS Error:
E: 10.0cm
N: 12.0cm
U: 30.2cm
Fix Ratio:
64.3%

BL=60.9 km



RMS Error:
E: 14.0cm
N: 14.8cm
U: 26.7cm
Fix Ratio:
44.4%

(24 hr Kinematic ● : Fixed Solution ● : Float Solution)

Ambiguity Resolution (AR)

Objectives of AR

More accurate solutions after proper AR (FIXED vs. FLOAT)

Faster solution convergence, ideally FIXED instantaneously

Carrier phase observables can be handled as precise pseudorange after AR

Initial phase terms should be eliminated for AR

Both of satellite and receiver initial phases do not have integer nature

DD (double difference) used for baseline processing like RTK

ZD (zero-difference) carrier-phase

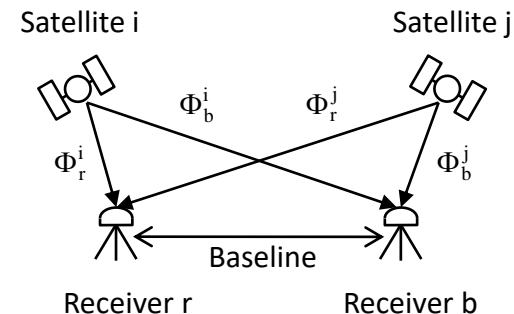
$$\Phi_r^s = \rho_r^s + c(dt_r - dT^s(t^s)) - I_r^s + T_r^s + d_r^s + \lambda d_{pw} + \lambda(\phi_{r,0} - \phi_0^s + N_r^s) + \varepsilon_\phi$$

DD (double-difference) carrier-phase for baseline processing

$$\Phi_{rb}^{ij} = \rho_{rb}^{ij} - I_{rb}^{ij} + T_{rb}^{ij} + d_{rb}^{ij} + \lambda d_{pw,rb}^{ij} + \lambda N_{rb}^{ij} + \varepsilon_\phi$$

$$\Phi_{rb}^{ij} \approx \rho_{rb}^{ij} + \lambda N_{rb}^{ij} + \varepsilon_\phi \quad (\text{short-baseline, same antenna})$$

- ρ_{rb}^{ij} : Difference between satellite i and j
- I_{rb}^{ij} : Difference between receiver r and b
- N_r^s : Integer ambiguity (cyc)
- ϕ_0^s : Satellite initial phase (cyc)
- $\phi_{r,0}$: Receiver initial phase (cyc)



FIXED Solution with AR

Typical AR Steps [1]

(1) $\mathbf{y} = \mathbf{H}\mathbf{x} + \boldsymbol{\varepsilon} = \mathbf{A}\mathbf{a} + \mathbf{B}\mathbf{b} + \boldsymbol{\varepsilon}$ ($\mathbf{a} \in \mathbf{Z}^n, \mathbf{b} \in \mathbf{R}^p$) Mixed-integer measurement models

(2) $\hat{\mathbf{x}} = \begin{pmatrix} \hat{\mathbf{a}} \\ \hat{\mathbf{b}} \end{pmatrix}, \mathbf{Q}_{\hat{\mathbf{x}}} = \begin{pmatrix} \mathbf{Q}_{\hat{\mathbf{a}}} & \mathbf{Q}_{\hat{\mathbf{a}}\hat{\mathbf{b}}} \\ \mathbf{Q}_{\hat{\mathbf{b}}\hat{\mathbf{a}}} & \mathbf{Q}_{\hat{\mathbf{b}}} \end{pmatrix}$ FLOAT solution and VC matrix by LSE or KF

(3) $\hat{\mathbf{a}} \rightarrow \check{\mathbf{a}}$ Mapping FLOAT to FIXED

(4) $\check{\mathbf{b}} = \hat{\mathbf{b}} - \mathbf{Q}_{\hat{\mathbf{b}}\hat{\mathbf{a}}} \mathbf{Q}_{\hat{\mathbf{a}}}^{-1} (\hat{\mathbf{a}} - \check{\mathbf{a}})$ FIXED solution

Mapping FLOAT to FIXED ($\hat{\mathbf{a}} \rightarrow \check{\mathbf{a}}$)

Integer Rounding (IR)

$$\check{\mathbf{a}} = [\hat{\mathbf{a}}] = ([\hat{a}_1], [\hat{a}_2], \dots, [\hat{a}_n])^T$$

Integer Bootstrapping (conditional sequential rounding) (IB)

$$\check{\mathbf{a}} = \left([\hat{a}_1], [\hat{a}_2 - \sigma_{21}\sigma_1^{-2}(\hat{a}_1 - \check{a}_1)], \dots, \left[\hat{a}_n - \sum_{i=1}^{n-1} \sigma_{n,i|I} \sigma_{i|I}^{-2} (\hat{a}_{i|I} - \check{a}_i) \right] \right)^T$$

Integer Least Squares (ILS)

$$\check{\mathbf{a}} = \arg \min_{\mathbf{a} \in \mathbf{Z}} (\hat{\mathbf{a}} - \mathbf{a})^T \mathbf{Q}_{\hat{\mathbf{a}}}^{-1} (\hat{\mathbf{a}} - \mathbf{a})$$

\mathbf{a} : Integer ambiguity parameters

\mathbf{b} : Other parameters

$\hat{\mathbf{a}}, \hat{\mathbf{b}}$: FLOAT solutions

$\check{\mathbf{a}}, \check{\mathbf{b}}$: FIXED solutions

$[x]$: Rounding to the nearest integer

$$\mathbf{Q}_{\hat{\mathbf{a}}} = \begin{pmatrix} \sigma_1^2 & \sigma_{12} & \cdots & \sigma_{1n} \\ \sigma_{21} & \sigma_2^2 & \cdots & \sigma_{2n} \\ \vdots & \vdots & \ddots & \vdots \\ \sigma_{n1} & \sigma_{n2} & \cdots & \sigma_n^2 \end{pmatrix}$$

[1] P. J. G. Teunissen and O. Montenbruck (eds.), Springer Handbook of Global Navigation Satellite Systems, 2017, Springer, Section 23

LAMBDA

Least-squares AMBiguity Decorrelation Adjustment [1]

A GNSS AR strategy by ILS estimator

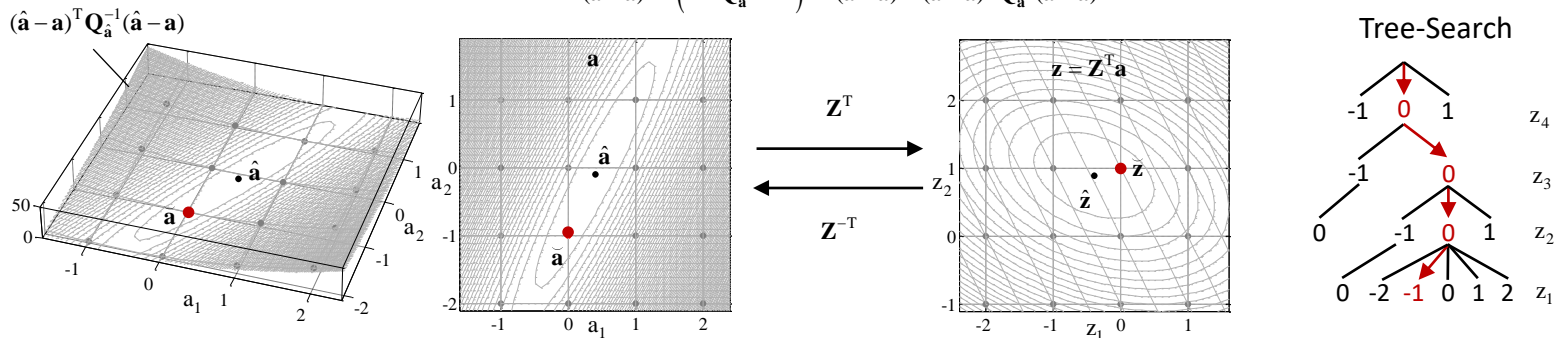
Shrinking integer search space with "decorrelation"

Skillful and efficient tree search strategy

Similar to "Closest Point Search with LLL Lattice Basis Reduction" Algorithm [2]

$$\begin{array}{ccc}
 \boxed{\begin{array}{l} \tilde{\mathbf{a}} = \arg \min_{\mathbf{a} \in \mathbb{Z}^n} (\hat{\mathbf{a}} - \mathbf{a})^T \mathbf{Q}_{\hat{\mathbf{a}}}^{-1} (\hat{\mathbf{a}} - \mathbf{a}) \\ \tilde{\mathbf{a}} = \mathbf{Z}^{-T} \tilde{\mathbf{z}} \end{array}} & \longleftrightarrow & \boxed{\begin{array}{l} \hat{\mathbf{z}} = \mathbf{Z}^T \hat{\mathbf{a}}, \mathbf{Q}_{\hat{\mathbf{z}}} = \mathbf{Z}^T \mathbf{Q}_{\hat{\mathbf{a}}} \mathbf{Z} \\ \tilde{\mathbf{z}} = \arg \min_{\mathbf{z} \in \mathbb{Z}^n} (\hat{\mathbf{z}} - \mathbf{z})^T \mathbf{Q}_{\hat{\mathbf{z}}}^{-1} (\hat{\mathbf{z}} - \mathbf{z}) \end{array}} \\
 \text{Z-transformation} & &
 \end{array}$$

$$\begin{aligned}
 (\hat{\mathbf{z}} - \mathbf{z})^T \mathbf{Q}_{\hat{\mathbf{z}}}^{-1} (\hat{\mathbf{z}} - \mathbf{z}) &= (\mathbf{Z}^T \hat{\mathbf{a}} - \mathbf{Z}^T \mathbf{a})^T (\mathbf{Z}^T \mathbf{Q}_{\hat{\mathbf{a}}} \mathbf{Z})^{-1} (\mathbf{Z}^T \hat{\mathbf{a}} - \mathbf{Z}^T \mathbf{a}) \\
 &= (\hat{\mathbf{a}} - \mathbf{a})^T \mathbf{Z} (\mathbf{Z}^{-1} \mathbf{Q}_{\hat{\mathbf{a}}}^{-1} \mathbf{Z}^{-T}) \mathbf{Z}^T (\hat{\mathbf{a}} - \mathbf{a}) = (\hat{\mathbf{a}} - \mathbf{a})^T \mathbf{Q}_{\hat{\mathbf{a}}}^{-1} (\hat{\mathbf{a}} - \mathbf{a})
 \end{aligned}$$



- [1] P. J. G. Teunissen, The least-squares ambiguity decorrelation adjustment: a method for fast GPS integer ambiguity estimation. Journal of Geodesy, 1994
- [2] E. Agrell, Closest point search in lattices, IEEE Transaction on Information Theory, 2002

Validation of AR

Acceptance Test after AR

Wrong AR much degrades the quality of the final (FIXED) solution

Need to maximize AR success probability and to minimize AR failure rate

Remain ambiguities FLOAT if the acceptance test failed and output FLOAT solution instead

Several acceptance tests are proposed: [1]

<p>Ratio Test</p>	<p>Difference Test</p>
<p>accept $\check{\mathbf{a}}$ if : $\frac{\ \hat{\mathbf{a}} - \check{\mathbf{a}}\ _{\mathbf{Q}_{\hat{\mathbf{a}}}}^2}{\ \hat{\mathbf{a}} - \check{\mathbf{a}}\ _{\mathbf{Q}_{\hat{\mathbf{a}}}}^2} \geq c$</p>	<p>accept $\check{\mathbf{a}}$ if : $\ \hat{\mathbf{a}} - \check{\mathbf{a}}\ _{\mathbf{Q}_{\hat{\mathbf{a}}}}^2 - \ \hat{\mathbf{a}} - \check{\mathbf{a}}\ _{\mathbf{Q}_{\hat{\mathbf{a}}}}^2 \geq c$</p>
<p>F-Ratio Test</p>	<p>Projector Test</p>
<p>accept $\check{\mathbf{a}}$ if : $\frac{\ \hat{\mathbf{e}}\ _{\mathbf{Q}_y}^2 + \ \hat{\mathbf{a}} - \check{\mathbf{a}}\ _{\mathbf{Q}_{\hat{\mathbf{a}}}}^2}{\ \hat{\mathbf{e}}\ _{\mathbf{Q}_y}^2 + \ \hat{\mathbf{a}} - \check{\mathbf{a}}\ _{\mathbf{Q}_{\hat{\mathbf{a}}}}^2} \geq c$</p>	<p>accept $\check{\mathbf{a}}$ if : $\left \frac{(\check{\mathbf{a}}' - \check{\mathbf{a}})^T \mathbf{Q}_{\hat{\mathbf{a}}}^{-1} (\hat{\mathbf{a}} - \check{\mathbf{a}})}{\ \check{\mathbf{a}}' - \check{\mathbf{a}}\ _{\mathbf{Q}_{\hat{\mathbf{a}}}}^2} \right \leq \mu$</p>
<p>$\check{\mathbf{a}}'$: Second-best candidate of AR, c, μ : Test thresholds $\ \mathbf{x}\ _{\mathbf{Q}}^2 = \mathbf{x}^T \mathbf{Q}^{-1} \mathbf{x}$ $\hat{\mathbf{e}} = \mathbf{y} - \mathbf{A}\hat{\mathbf{a}} - \mathbf{B}\hat{\mathbf{b}}$</p>	

Note: The test thresholds are usually selected empirically as a fixed value (for example Ratio Test with $c = 3$). The threshold value, however, is often optimistic or conservative without theoretical basis. In some literatures, variable threshold values are proposed base on fixed-failure rate approach (FF-RT) [2].

- [1] S. Verhagen and P. J. G. Teunissen, New global navigation satellite system ambiguity resolution method compared to exiting approaches, Journal of Guidance, Control and Dynamics, 2006
- [2] S. Verhagen and P. J. G. Teunissen, The ratio test for future GNSS ambiguity resolution, GPS Solution, 2013

WL/NL AR with Iono-free LC

FLOAT Solution and LC Ambiguity *

$$\mathbf{x} = (\mathbf{r}_r^T, T, \mathbf{N}_{LC}^T)^T, \mathbf{y} = (\mathbf{P}_{LC}^T, \Phi_{LC}^T)^T, \mathbf{Q}_y$$

$$\begin{cases} P_{LC} = C_1 P_{L1} + C_2 P_{L2} = \rho + mT + \varepsilon_P \\ \Phi_{LC} = C_1 \Phi_{L1} + C_2 \Phi_{L2} = \rho + mT + N_{LC} + \varepsilon_\Phi \end{cases}$$

$$\rightarrow \hat{\mathbf{x}} = (\hat{\mathbf{r}}_r^T, \hat{T}, \hat{\mathbf{N}}_{LC}^T)^T, \mathbf{Q}_{\hat{\mathbf{x}}}$$

Ionosphere-free

FLOAT WL Ambiguity *

$$\hat{N}_{WL} = \frac{1}{n} \sum_{i=1}^n (MW) = \frac{1}{n} \sum_{i=1}^n (\Phi_{WL} - P_{NL})$$

$$= \frac{1}{n} \sum_{i=1}^n \left(\left(\frac{\Phi_{L1}}{\lambda_1} - \frac{\Phi_{L2}}{\lambda_2} \right) - \left(\frac{P_{L1}}{\lambda_1} + \frac{P_{L2}}{\lambda_2} \right) \right)$$

geometry-free,
ionosphere-free

WL/NL AR by IR **

$$\check{N}_{WL} = \left[\hat{N}_{WL} \right] \quad (\text{WL AR})$$

$$\check{N}_{L1} = \left[\hat{N}_{L1} \right] = \left[\frac{\hat{N}_{LC} - C_2 \lambda_2 \check{N}_{WL}}{\lambda_{NL}} \right] \quad (\text{NL AR})$$

Note:

* DD applied for baseline processing to eliminate clock and initial bias terms. SD applied for PPP-AR with FCB corrections

** Alternatively, ILS or IB can be applied to NL AR considering the VC-matrix of FLOAT LC ambiguities

N_{LC} : Iono-free LC ambiguity (m)

N_{WL} : Wide lane ambiguity (cyc)

m : Mapping function

T : ZTD or ZWD (m)

FIXED Solution *

$$\mathbf{x} = (\mathbf{r}_r^T, T)^T, \mathbf{y} = (\Phi_{LC}^T)^T$$

$$\Phi_{LC} = C_1 \Phi_{L1} + C_2 \Phi_{L2} = \rho + mT + \check{N}_{LC} + \varepsilon_\Phi$$

$$\rightarrow \check{\mathbf{x}} = (\check{\mathbf{r}}_r^T, \check{T})^T, \mathbf{Q}_{\check{\mathbf{x}}}$$

$$C_1 = \frac{\lambda_2^2}{\lambda_2^2 - \lambda_1^2}, C_2 = \frac{-\lambda_1^2}{\lambda_2^2 - \lambda_1^2}$$

$$C_1 \lambda_1 + C_2 \lambda_2 = \frac{\lambda_1 \lambda_2}{\lambda_1 + \lambda_2} = \frac{1}{1/\lambda_1 + 1/\lambda_2} = \lambda_{NL}$$

$$N_{WL} = N_{L1} - N_{L2}$$

$$N_{LC} = C_1 \lambda_1 N_{L1} + C_2 \lambda_2 N_{L2} = (C_1 \lambda_1 + C_2 \lambda_2) N_{L1} - C_2 \lambda_2 N_{WL}$$

$$= \lambda_{NL} N_{L1} - C_2 \lambda_2 N_{WL}$$

TCAR/CIR

TCAR (three-carrier AR) ^[1] /CIR (cascade integer resolution) ^[2]

Sequential conditional rounding EWL -> WL -> NL ambiguities

Geometry-free measurement model

Ionosphere terms can be reduced by short baseline or ionosphere corrections (for PPP)

Many modifications or enhancements including geometry-based models

$$\begin{aligned}
 (1) \quad \check{N}_{EWL} &= \left[\frac{\Phi_{EWL} - P_X}{\lambda_{EWL}} \right] \\
 (2) \quad \check{N}_{WL} &= \left[\frac{\Phi_{WL} - (\Phi_{EWL} - \lambda_{EWL} \check{N}_{EWL})}{\lambda_{WL}} \right] \\
 (3) \quad \check{N}_{NL} &= \left[\frac{\Phi_{NL} - (\Phi_{WL} - \hat{N}_{WL})}{\lambda_{NL}} \right]
 \end{aligned}
 \quad
 \begin{cases}
 P_X = \rho + I_X + T + \varepsilon_P \\
 \Phi_{EWL} = \rho - I_{EWL} + T + \lambda_{EWL} N_{EWL} + \varepsilon_{\Phi_{EWL}} \\
 \Phi_{WL} = \rho - I_{WL} + T + \lambda_{WL} N_{WL} + \varepsilon_{\Phi_{WL}} \\
 \Phi_{NL} = \rho - I_{NL} + T + \lambda_{NL} N_{NL} + \varepsilon_{\Phi_{NL}}
 \end{cases}$$

$$|I_X + I_{EWL}| \ll \lambda_{EWL}, |I_{WL}| \ll \lambda_{WL}, |I_{NL}| \ll \lambda_{NL}$$

Typical Selection of EWL, WL and NL for GPS

$$P_X = \frac{P_{L2}/\lambda_2 + P_{L5}/\lambda_5}{1/\lambda_2 + 1/\lambda_5}, \Phi_{EWL} = \frac{\Phi_{L2}/\lambda_2 - \Phi_{L5}/\lambda_5}{1/\lambda_2 - 1/\lambda_5}, \Phi_{WL} = \frac{\Phi_{L1}/\lambda_1 - \Phi_{L2}/\lambda_2}{1/\lambda_1 - 1/\lambda_2}, \Phi_{NL} = \Phi_{L1}$$

[1] U. Vollath et al., Analysis of three-carrier ambiguity resolution (TCAR) technique for precise relative positioning in GNSS-2, ION GPS-98

[2] J. Jung and P. Enge, Optimization of cascade integer resolution with three civil GPS frequency, ION GPS 2000

Triple Frequency LC

$$\Phi_{(i,j,k)} = \frac{i/\lambda_1 \Phi_{L1} + j/\lambda_2 \Phi_{L2} + k/\lambda_5 \Phi_{L5}}{i/\lambda_1 + j/\lambda_2 + k/\lambda_5} \quad P_{(l,m,n)} = \frac{l/\lambda_1 P_{L1} + m/\lambda_2 P_{L2} + n/\lambda_5 P_{L5}}{l/\lambda_1 + m/\lambda_2 + n/\lambda_5}$$

Type	LC	Coefficients						λ_{LC} (cm)	I_{LC} (wrt P1)	σ_{LC}		Note
		i	j	k	l	m	n			(cm)	(cyc)	
Geometry Based	$\Phi_{(1,0,0)}$	1	-	-	-	-	-	19.0	-1	0.3	0.016	NL
	$\Phi_{(0,1,0)}$	-	1	-	-	-	-	24.4	-1.647	0.3	0.012	NL
	$\Phi_{(0,0,1)}$	-	-	1	-	-	-	25.5	-1.793	0.3	0.012	NL
	$\Phi_{(1,-1,0)}$	1	-1	-	-	-	-	86.1	1.283	1.7	0.020	WL
	$\Phi_{(1,0,-1)}$	1	-	-1	-	-	-	75.1	1.339	1.5	0.020	WL
	$\Phi_{(0,1,-1)}$	-	1	-1	-	-	-	586.1	1.719	10.0	0.017	EWL
	$\Phi_{(1,-6,5)}$	1	-6	5	-	-	-	325.6	0.074	31.1	0.096	EWL
	$\Phi_{(1,-5,4)}$	1	-5	4	-	-	-	209.3	0.662	16.5	0.079	EWL
	$\Phi_{(4,-3,0)}$	4	-3	-	-	-	-	11.4	-0.090	0.8	0.073	NL
$\Phi_{(4,0,-3)}$	4	-	-3	-	-	-	10.8	0.010	0.8	0.072	NL	
Geometry Free	$\Phi_{(1,-1,0)} - P_{(1,1,0)}$	1	-1	-	1	1	-	86.1	0	21.4	0.249	WL
	$\Phi_{(1,0,-1)} - P_{(1,0,1)}$	1	-	-1	1	-	1	75.1	0	21.5	0.286	WL
	$\Phi_{(0,1,-1)} - P_{(0,1,1)}$	-	1	-1	-	1	1	586.1	0	23.4	0.040	EWL
	$\Phi_{(1,-6,5)} - P_{(1,1,1)}$	1	-6	5	1	1	1	325.6	-1.360	35.7	0.110	EWL
	$\Phi_{(1,-6,5)} - P_{(1,1,0)}$	1	-6	5	1	1	-	325.6	-1.209	37.8	0.116	EWL
	$\Phi_{(1,-5,4)} - P_{(1,1,1)}$	1	-5	4	1	1	1	209.3	-0.773	24.1	0.115	EWL
	$\Phi_{(1,-5,4)} - P_{(1,1,0)}$	1	-5	4	1	1	-	209.3	-0.622	27.0	0.129	EWL

$$\lambda_{LC} = \frac{1}{i/\lambda_1 + j/\lambda_2 + k/\lambda_5} \quad N_{LC} = i \cdot N_{L1} + j \cdot N_{L2} + k \cdot N_{L5} \quad I_{LC} = -\frac{i/\lambda_1 + j \cdot \lambda_2/\lambda_1^2 + k \cdot \lambda_5/\lambda_1^2}{i/\lambda_1 + j/\lambda_2 + k/\lambda_5} - \frac{l/\lambda_1 + m \cdot \lambda_2/\lambda_1^2 + n \cdot \lambda_5/\lambda_1^2}{l/\lambda_1 + m/\lambda_2 + n/\lambda_5}$$

$$\sigma_{LC} = \sqrt{\frac{(i/\lambda_1)^2 + (j/\lambda_2)^2 + (k/\lambda_5)^2}{(i/\lambda_1 + j/\lambda_2 + k/\lambda_5)^2} \sigma_{\Phi}^2 + \frac{(l/\lambda_1)^2 + (m/\lambda_2)^2 + (n/\lambda_5)^2}{(l/\lambda_1 + m/\lambda_2 + n/\lambda_5)^2} \sigma_P^2} \quad (\sigma_{\Phi} = 0.3\text{cm}, \sigma_P = 30\text{cm})$$

Partial AR (PAR)

Partial AR (PAR)

Full AR (FAR) indicates low fixing ratio or long TTFF under ill conditions like long BL RTK
 Newly rising satellites or cycle-slips often disturbs FAR with validation
 Degraded accuracy by PAR solutions acceptable in many applications

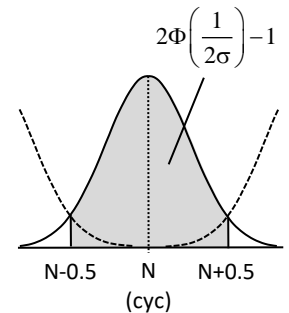
Many criteria how to select subset of ambiguities:

Elevation angle, continuous tracking epochs, SNR, ADOP (ambiguity dilution of precision),
 EWL/WL/NL, success or failure probability of AR

BSR (bootstrapping success rate) Criterion [1]

$$\prod_{i=k}^n \left(2\Phi \left(\frac{1}{2\sigma_{\hat{z}_{i|I}}} \right) - 1 \right) \geq P_0$$

P_0 : Minimum success probability of bootstrapping AR
 $\sigma_{\hat{z}_{i|I}}$: Std-dev of Z-transformed i-th ambiguity of bootstrapping AR
 $\Phi(x)$: CDF (cumulative distribution function) of normal distribution



FF-RT (fixed-failure-rate ratio-test) Criterion [1]

$$\frac{\|\hat{\mathbf{z}}_p - \check{\mathbf{z}}_p'\|_{\mathbf{Q}_{\hat{\mathbf{z}}_p}}^2}{\|\hat{\mathbf{z}}_p - \check{\mathbf{z}}_p\|_{\mathbf{Q}_{\hat{\mathbf{z}}_p}}^2} \geq c(n, P_f)$$

$p = (k, k+1, \dots, n)$: Partial set of Z-transformed ambiguities
 $\hat{\mathbf{z}}_p$: Float Z-transformed ambiguities
 $\check{\mathbf{z}}_p, \check{\mathbf{z}}_p'$: Best-fixed, secondary-best-fixed Z-transformed ambiguities
 $c(n, P_f)$: Threshold of FF-RT (fixed-failure-rate ratio-test)

$$\Phi(x) = \frac{1}{\sqrt{2\pi}} \int_{-\infty}^x \exp\left(-\frac{t^2}{2}\right) dt$$

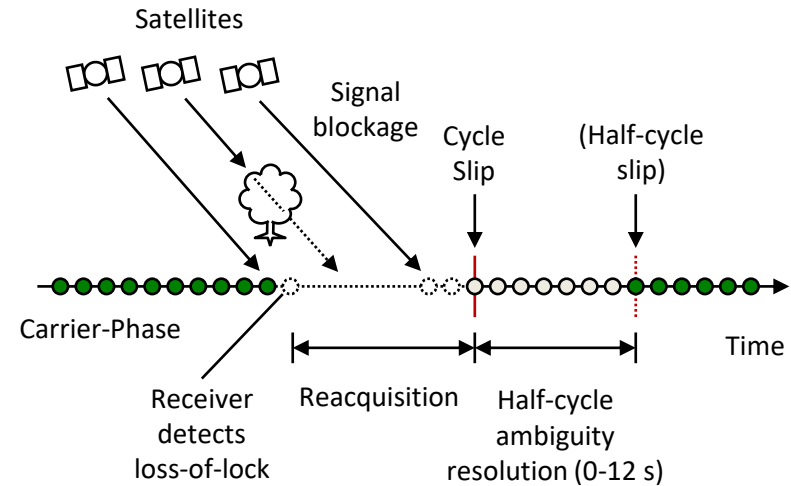
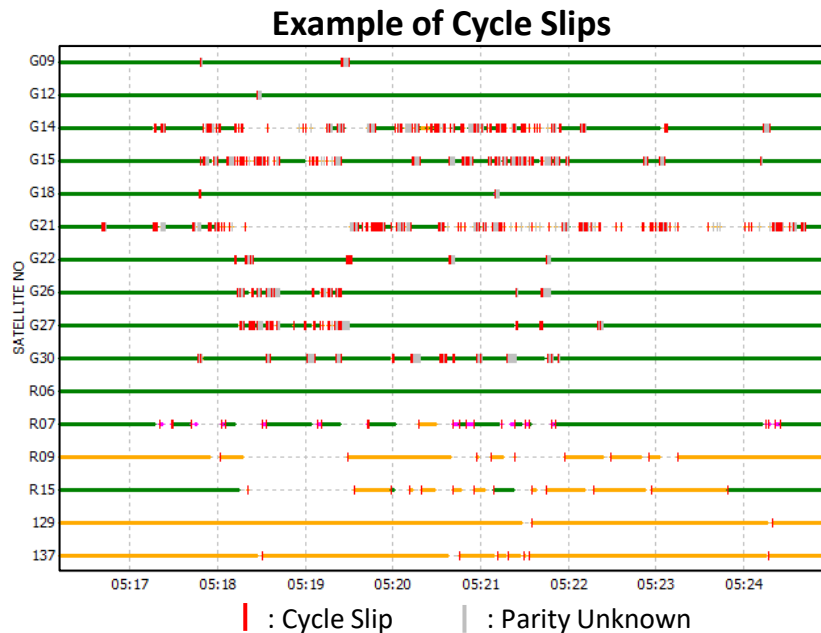
$$= \frac{1}{2} \left(1 - \operatorname{erf}\left(\frac{1}{\sqrt{2}}\right) \right)$$

[1] S. Verhagen et al., GNSS ambiguity resolution: which subset to fix ?, International GNSS Symposium, 2011

Cycle Slip

Definition

A sudden jump in carrier-phase measurements when the phase tracking loop (PLL) in receivers detects a temporary loss of lock due to signal blockage or some other disturbing factor. The carrier-cycle counter in the receiver restarts, causing a jump in the accumulated phase by an integer number of cycles.



Receiver Biases and Phase Shift

DCB (Differential Code Bias)

Biases in pseudorange between different codes tracked (e.g. GPS L1C/A - L1P(Y))

Satellite DCB should be corrected by external DCB info (T_{GB} , P1-C1 DCB, P2-C2 DCB ...)

Receiver DCB usually implicitly estimated as in the receiver clock biases as LC

ISB (Inter System Bias)

Biases in pseudorange and phase between different systems (e.g. GPS L1C/A - GAL E1B)

Hard to incorporated ISB in estimation due to unstable behavior (varied by receiver F/W updates)

IFB (Inter Frequency Bias)

Biases in pseudorange and phase between different FCN GLONASS satellites (e.g. R01 - R02)

IFB in pseudorange should be estimated explicitly or corrected by external calibration data

IFB in phase is hard to be corrected due to instability including antennas and cables

ISTB (Inter Satellite Type Bias) ^[1]

Biases in pseudorange and phase between different BDS satellite types (e.g. BDS GEO - IGSO)

Quarter Cycle Phase Shift

Quarter cycle phase shift in phase between different codes tracked (e.g. GPS L2P(Y) - L2C)

All phases on the same frequency should be aligned by the latest RINEX or RTCM 3, but needs careful handling of OBS data in vendor proprietary formats

[1] N. Nadarajah et al., The mixed-receiver BeiDou inter-satellite-type-bias and its impact on RTK positioning, GPS Solution, 2014

GNSS Data Formats

RINEX (Receiver Independent Exchange Format)

Developed and maintained by IGS since 1990s for PP and data archive

For observation data (OBS), navigation data (NAV), meteorological data (MET) and extensions

RTCM (Radio Technical Commission for Maritime Services)

Developed and maintained by RTCM SC-104 (special-committee 104) for DGNSS, RTK and PPP
RTCM 2 (version 2) and RTCM 3 (version 3). RTCM 3 is not compatible to RTCM 2.

Compact and portable binary format

BINEX (Binary Exchange Format)

Developed and maintained by UNAVCO (university NAVSTAR consortium) for RT or PP and archive

Compact and portable binary format

Proprietary Formats by GNSS Receiver Vendors

RT17/RT27, CMR/CMR+ (Trimble), GREIS (JAVAD), NovAtel, SBF (Septentrio), UBX (u-blox), ...

Example of Data Sizes^{*1}

Format	Data Size (Bytes)					
	RTCM 3 *1	BINEX *1	CMR+ *1	RINEX 2.12 *2	RINEX 3.02 *2	Compressed RINEX *3
OBS Data	2,387,289	5,140,927	1,137,059	83,386,990	29,225,908	6,709,900
NAV Data	-			33,022	32,794	-

*1 GNSS receiver: Trimble BD982, Data sampling: 1 Hz x 1 H, System: GPS/GLO/GAL/BDS/QZS/SBS, *2 Converted from BINEX by RTKCONV 2.4.3 b32, *3 Converted from RINEX 3.02 by RNX2CNX 4.08

RINEX

RINEX Version/
RINEX Type

3.02	OBSERVATION DATA	M (MIXED)	RINEX VERSION / TYPE
NetR9 5.37	Receiver Operator	20190710 000000 UTC	PGM / RUN BY / DATE
...			
G	12 C1C L1C S1C C2W L2W S2W C2X L2X S2X C5X L5X S5X		SYS / # / OBS TYPES
R	12 C1C L1C S1C C1P L1P S1P C2C L2C S2C C3X L3X S3X		SYS / # / OBS TYPES
E	12 C1X L1X S1X C5X L5X S5X C7X L7X S7X C8X L8X S8X		SYS / # / OBS TYPES
...			
END OF HEADER			

> 2019 7 10 0 0 0.0000000 0 35			
R10 21997839.273 7 117260873.451 7		47.800	21997838.297 7 ...
...			
...			

Header Section

Data Records

Sat System (G: GPS, R: GLONASS, E: Galileo, J: QZSS, C: BeiDou, I: IRNSS, S: SBAS, M: Mixed)

RINEX Version	RINEX Type																
	Observation Data ^[1]							Navigation Data ^[1]							MET ^[1]	CLK ^[2]	SBAS ^[3]
	G	R	E	J	C	I	S	G	R	E	J	C	I	S			
2.10	O	O	-	-	-	-	O	N	G	-	-	-	-	H	M	-	B
2.11	O	O	O	-	-	-	O	N	G	-	-	-	-	H	M	-	-
2.12	O	O	O	-	O	-	O	N	G	N	-	-	-	H	M	-	-
3.00	O	O	O	-	-	-	O	N	N	N	-	-	-	N	M	C	-
3.01	O	O	O	-	O	-	O	N	N	N	-	-	-	N	M	C	-
3.02	O	O	O	O	O	-	O	N	N	N	N	N	-	N	M	C	-
3.03	O	O	O	O	O	O	O	N	N	N	N	N	N	N	M	-	-
3.04	O	O	O	O	O	O	O	N	N	N	N	N	N	N	M	-	-

MET: Meteorological data, CLK: RINEX clock extension, SBAS: GEO SBAS broadcast data extension

[1] RINEX - The receiver independent exchange format version 3.04, Nov 2018, [2] RINEX extension to handle clock information, version 3.02, Sep 2010,

[3] Proposal for a new RINEX-type exchange file for GEO SBAS broadcast data, Sep 2004

RINEX 3 OBS

RINEX Version +
RINEX Type(O) +
Sat System

Receiver +
Antenna
#/Type/Version

of OBS Types +
OBS Type List

Phase Shift
Correction
Info

GLONASS FCN

Epoch Flag
(0: OK, >1: Event)

Epoch Time

Satellite ID

3.02	OBSERVATION DATA	M (MIXED)	RINEX VERSION / TYPE
NetR9 5.37	Receiver Operator	20190710 000000 UTC	PGM / RUN BY / DATE
GMSD			MARKER NAME
21749S002			MARKER NUMBER
GEODETIC			MARKER TYPE
OBS	JAXA		OBSERVER / AGENCY
5049K72188	TRIMBLE NETR9	5.37	REC # / TYPE / VERS
4938353448	TRM59800.00	SCIS	ANT # / TYPE
-3607665.3641	4147867.5119	3223716.6949	APPROX POSITION XYZ
0.0000	0.0000	0.0000	ANTENNA: DELTA H/E/N
G 12 C1C L1C S1C C2W L2W S2W C2X L2X S2X C5X L5X S5X			SYS / # / OBS TYPES
R 12 C1C L1C S1C C1P L1P S1P C2C L2C S2C C3X L3X S3X			SYS / # / OBS TYPES
E 12 C1X L1X S1X C5X L5X S5X C7X L7X S7X C8X L8X S8X			SYS / # / OBS TYPES
J 18 C1C L1C S1C C1X L1X S1X C1Z L1Z S1Z C2X L2X S2X C5X			SYS / # / OBS TYPES
L5X S5X C6X L6X S6X			SYS / # / OBS TYPES
C 6 C2I L2I S2I C7I L7I S7I			SYS / # / OBS TYPES
30.000			INTERVAL
2019 7 10 0 0 0.000000	GPS		TIME OF FIRST OBS
G L2X -0.25000			SYS / PHASE SHIFT
R L1P 0.25000			SYS / PHASE SHIFT
R L2C -0.25000			SYS / PHASE SHIFT
J L2X -0.25000			SYS / PHASE SHIFT
DBHZ			SIGNAL STRENGTH UNIT
24 R01 1 R02 -4 R03 5 R04 6 R05 1 R06 -4 R07 5 R08 6			GLONASS SLOT / FRQ #
R09 -2 R10 -7 R11 0 R12 -1 R13 -2 R14 -7 R15 0 R16 -1			GLONASS SLOT / FRQ #
R17 4 R18 -3 R19 3 R20 2 R21 4 R22 -3 R23 3 R24 2			GLONASS SLOT / FRQ #
			GLONASS COD/PHS/BIS
			END OF HEADER
> 2019 7 10 0 0 0.000000	0 35		# of Satellites
R10 21997839.273 7 117260873.451 7	47.800	21997838.297 7 117260869.455 7	46.500 ...
R09 19559207.609 8 104445089.256 8	53.200	19559206.813 8 104445085.259 8	51.400 ...
R19 20027311.109 6 107132605.273 6	41.000	20027309.691 6 107132618.286 6	39.400 ...
G26 23089708.242 6 121337231.800 6	39.700	23089717.098 4 94548509.497 4	26.400 ...
...			
...			
			OBS Data
E15 25080778.563 7 131800394.872 7	46.000	25080786.383 7 98422406.965 7	47.400 ...
E02 24484493.625 7 128666873.439	47.600	24484498.691 8 96082402.437 8	50.300 ...
> 2019 7 10 0 0 30.000000	0 35		
R10 21978389.961 7 117157199.224	47.600	21978388.867 7 117157195.207 7	46.600 ...
...			

ARP Position wrt
Marker Position
H/E/N (m)

OBS Type
(C: Pseudorange,
L: Carrier-phase,
D: Doppler Freq,
S: Raw C/NO) +
Band/Freq +
Attribute
(see Appendix)

Time System
(GPS: GPS Time)

Receiver Clock
Offset (optional)

Header
Section

Data
Records

LLI SSI (LLI: Loss-of-lock Indicator, SSI: Signal Strength Indicator)

[1] IGS RINEX WG and RTCM-SC104, RINEX - The receiver independent exchange format version 3.04, Nov 2018

RINEX 3 NAV

RINEX Version +
RINEX Type(N) +
Sat System

3.03	N: GNSS NAV DATA	M: MIXED	RINEX VERSION / TYPE		
MergeMNFfile.tcl	IGS	20190719 075936 GMT	PGM / RUN BY / DATE		
GPSA 4.6566D-09	1.4901D-08	-5.9605D-08	-1.1921D-07	IONOSPHERIC CORR	
GPSB 8.1920D+04	8.1920D+04	-6.5536D+04	-5.2429D+05	IONOSPHERIC CORR	
...					
GPUP 2.7939677238D-09	1.154631946D-14	405504	2061	TIME SYSTEM CORR	
GLUT -4.6566128731D-10	0.000000000D+00	0	0	TIME SYSTEM CORR	
GAUT 9.3132257462D-09	-5.329070518D-15	172800	2061	TIME SYSTEM CORR	
...					
18	18	1929	7	LEAP SECONDS	
				END OF HEADER	
G01	2019 07 10 00 00 00	-6.297975778580E-05	-1.034550223270E-11	0.00000000000E+00	
	7.40000000000E+01	6.40625000000E+00	4.275535236060E-09	-1.468053231860E+00	
	3.315508365630E-07	9.019587654620E-03	7.307156920430E-06	5.153651456830E+03	
	2.59200000000E+05	1.434236764910E-07	2.552552807090E+00	-4.284083843230E-08	
	9.763611140680E-01	2.432812500000E+02	7.320008488990E-01	-7.944973797190E-09	
	4.535903224290E-10	1.00000000000E+00	2.06100000000E+03	0.00000000000E+00	
	2.00000000000E+00	0.00000000000E+00	5.587935447690E-09	7.40000000000E+01	
	2.52018000000E+05	4.00000000000E+00			
	0	Time_of_Clock(TOC)	SV_clock_bias(s)	SV_Clk_Drift(s/s)	SV_Clk_rate(s/s2)
	1	IODE*1	Crs(m)	Delta_n(rad/s)	M0(rad)
	2	Cuc(rad)	e(eccentricity)	Cus(rad)	sqrt(A)(sqrt(m))
	3	Time_of_ephem(TOE)	Cic(rad)	OMEGA0(rad)	Cis(rad)
	4	i0(rad)	Crc(rad)	omega(rad)	OMEGA_DOT(rad/s)
	5	IDOT(rad/s)	Code_on_L2_ch*2	GPS_week_#*3	L2_P_data_flag*4
	6	SV_accuracy(m)*5	SV_health*6	TGD(s)*7	IODC*8
	7	Transmit_Time	Fit_interval(h)*9	Spare	Spare
	...				
R01	2019 07 10 00 15 00	4.648976027966E-05	0.00000000000E+00	2.60100000000E+05	
	1.750996093750E+04	1.717527389526E+00	-9.313225746155E-10	0.00000000000E+00	
	6.118407226562E+03	1.674188613892E+00	9.313225746155E-10	1.00000000000E+00	
	1.752643945312E+04	-2.299521446228E+00	-1.862645149231E-09	0.00000000000E+00	
	0	Time_of_Clock(TOC)	SV_clock_bias(s)	SV_rel_freq_bias	Msg_frame_time(s)
	1	Sat_position_X(km)	Vel_X_dot(km/s)	X_accel(km/s2)	health
	2	Sat_position_Y(km)	Vel_Y_dot(km/s)	Y_accel(km/s2)	frequency_number
	3	Sat_position_Z(km)	Vel_Z_dot(km/s)	Z_accel(km/s2)	Age_of_oper(days)
	...				

Satellite ID

GPS/GAL/BDS/
QZS Ephemeris
and SV Clock
Parameters

Satellite ID

GLO Ephemeris
and SV Clock
Parameters

Ionospheric Correction
Parameters (optional)

GNSS Time Difference
Parameters (optional)

Leap seconds (optional)

Header
Section

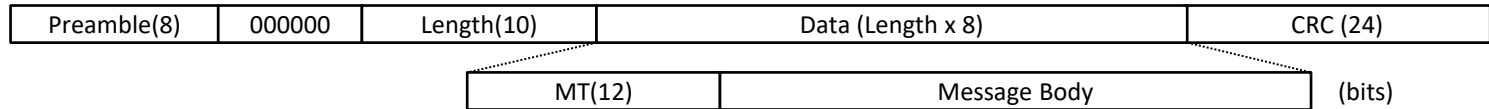
- *1 GAL: IOD_nav
BDS: AODE
- *2 GAL: Data_source
BDS: Spare
- *3 GAL: GAL_week_#
BDS: BDT_week_#
- *4 GAL,BDS: Spare
- *5 GAL: SISA(m)
- *6 BDS: SatH1
- *7 GAL: BGD_E5a/E1(s)
BDS: TGD1_B1/B3(s)
- *8 GAL: BGD_E5b/E1(s)
BGS: TGD2_B2/B3(s)
- *9 GAL: Spare
QZS: Fit_interval_flag
BDS: AODC

Data
Records

[1] IGS RINEX WG and RTCM-SC104, RINEX - The receiver independent exchange format version 3.04, Nov 2018

RTCM 3

RTCM 3 Message [1]

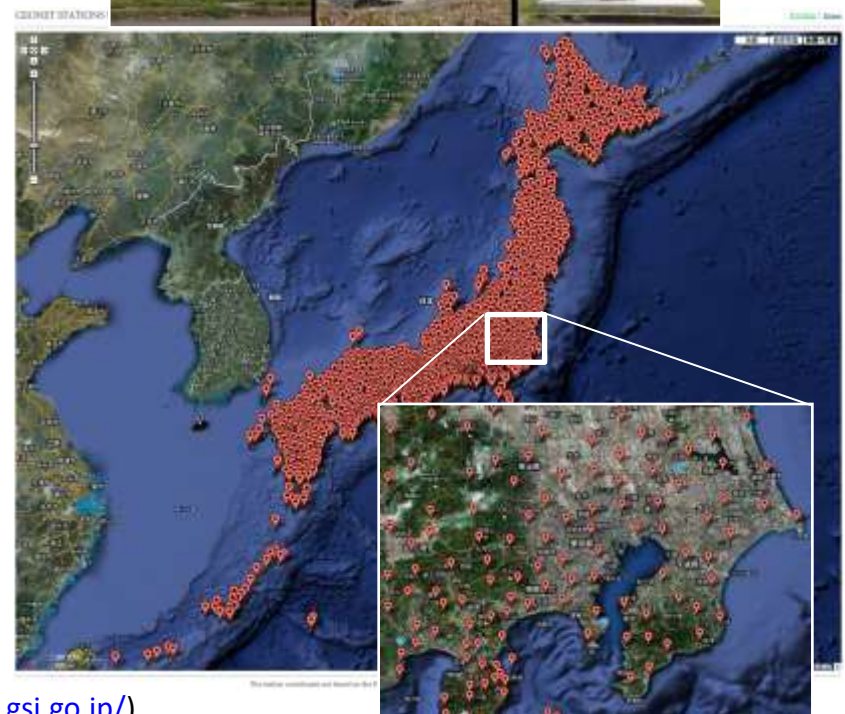


Message		MT (Message Type)					
		GPS	GLONASS	Galileo	QZSS	BeiDou	SBAS
OBS	Basic RTK L1 Only	1001	1009	-	-	-	-
	Extended RTK L1 Only	1002	1010	-	-	-	-
	Basic RTK L1 & L2	1003	1011	-	-	-	-
	Extended RTK L1 & L2	1004	1012	-	-	-	-
Satellite Ephemeris Data		1019	1020	1045, 1046* ²	1044	1042	-
MSM	MSM 1 (Compact P) * ³	1071	1081	1091	1111	1121	1101
	MSM 2 (Compact PR) * ³	1072	1082	1092	1112	1122	1102
	MSM 3 (Compact P+PR) * ³	1073	1083	1093	1113	1123	1103
	MSM 4 (Full P+PR+CN) * ³	1074	1084	1094	1114	1124	1104
	MSM 5 (Full P+PR+PRR+CN) * ³	1075	1085	1095	1115	1125	1105
	MSM 6 (Full P+PR+CN+H) * ³	1076	1086	1096	1116	1126	1106
	MSM 7 (Full P+PR+PRR+CN+H) * ³	1077	1087	1097	1117	1127	1107
SSR	Orbit Correction	1057	1063	1240* ¹	1246* ¹	1258* ¹	1252* ¹
	Clock Correction	1058	1064	1241* ¹	1247* ¹	1259* ¹	1253* ¹
	Code Bias	1059	1065	1242* ¹	1248* ¹	1260* ¹	1254* ¹
	Combined Orbit and Clock	1060	1066	1243* ¹	1249* ¹	1261* ¹	1255* ¹
	URA	1061	1067	1244* ¹	1250* ¹	1262* ¹	1256* ¹
	High-Rate Clock Correction	1062	1068	1245* ¹	1251* ¹	1263* ¹	1257* ¹
Station Coordinates/Antenna Description		1005, 1006, 1007, 1008, 1032, 1033					
Proprietary Information		4070 ~ 4095					

*1 Draft version, *2 1045: F/NAV, 1046: I/NAV, *3 P: Pseudorange, PR: PhaseRange, PRR: PhaseRangeRate, CN: CNR, H: High Resolution

[1] RTCM standard 10403.3, Differential GNSS (global navigation satellite system) services - version 3, Oct 2016

GSI GEONET



(<https://terras.gsi.go.jp/>)

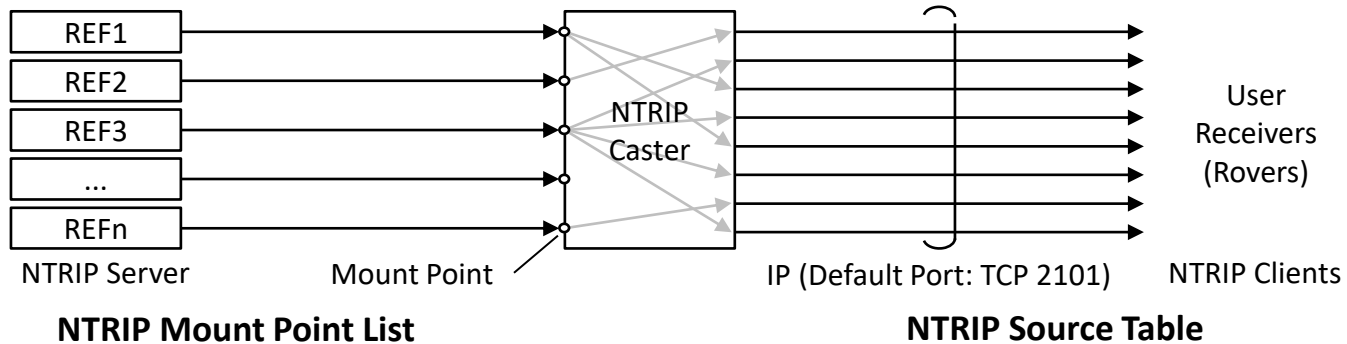
NTRIP (1)

NTRIP (Networked Transport of RTCM via Internet Protocol) [1]

Designed based on HTTP/RTSP to disseminate DGNSS corrections and GNSS data over Internet

Ver. 1.0: Initial version only supporting TCP/IP

Ver. 2.0: Supporting RTP/UDP/IP and other features (chunked transfer enc., source table filtering ...)



NTRIP Mount Point List

NTRIP Source Table

MountPoint ID	Format	Format Details	Co-Ordinate Network	Cont. Latitude	Longitude	IP	So	Demersal
ANP00042	Lea_Abyem	RTCM 3.1 1004(1),1004(30),1004(X),1012(1),1012(30);IC 2	GPS+GLG 302	GLP	16.26	-41.53	0	SEPT POLARIS
ADH103495	Alu_Dhah	RTCM 3.0 1004(1),1012(1)	2 GPS+GLG 302C	ARE	24.38	34.82	0	SEPT POLARIS
AZ0002740	Adha_Ababa	RTCM 3.0 1004(1),1006(3),1007(9),1012(1)	2 GPS+GLG 302	ETH	9.34	36.77	0	GPS LEGACY
AG0000741	A GPS-Abba_Melba	RTCM 3.1 1018	2 GLG 302	ETH	9.83	36.74	0	GPS LEGACY
AG0000460	Appo	RTCM 3.2 1006(30),1018,1020,1023(30),1045,1077(1),108 2	GPS+GLG 302	ARG	-34.87	-58.14	0	SEPT POLARIS/ETH
ARA001870	Ara	RTCM 3.0 1004(1),1012(1),1018,1020,1044,1046,1046	2 GPS+GLG 302	JPN	31.80	130.60	1	NEWS
A1AC00343	Atacoto	RTCM 3.2 1004(1),1006(30),1008(10),1012(1),1012(30);IC 2	GPS+GLG 302	PRA	41.93	8.76	0	LEICA GR25
A1B000340	Albert Head	RTCM 3.2 1006(1),1008(1),1018(30),1019,1020,1023(1) 2	GPS+GLG 302	CAN	46.39	-123.46	0	LEICA GR25
A1C000450	Alca_Springs	RTCM 3.2 1006(1),1008(1),1018(30),1019,1020,1023(1) 2	GPS+GLG 302	AUS	-23.67	153.99	0	LEICA GR25
AF0000490	Afrikash	RTCM 3.1 1006(3),1007(3),1008(30),1013(30),1019,102 2	GPS+GLG 302	PER	-16.47	-71.46	0	SEPT POLARIS
AF0000540	Afrington	RTCM 3.1 1004(1),1004(3),1007(3),1012(1),1033(3),4094 2	GPS+GLG 302C	USA	46.17	-122.14	0	SEPT POLARIS
AF0000490	Afrikash	RTCM 3.1 1006(3),1008(1),1018(30),1019,1020,1023(1) 2	GPS+GLG 302	PER	-16.47	-71.46	0	SEPT POLARIS
A1C000343	Atacoto	RTCM 3.1 1004(1),1006(3),1007(9),1012(1),1012(30);IC 2	GPS+GLG 302	PRA	41.93	8.76	0	LEICA GR25
B40000340	Baker-Lake	RTCM 3.2 1004(1),1006(1),1012(30),1019,1020,1023(1) 2	GPS+GLG 302	CAN	69.10	-68.28	0	GPS NET-G3
B40000340	Baker-Lake	RTCM 3.2 1004(1),1006(1),1012(30),1019,1020,1023(1) 2	GPS+GLG 302	CAN	69.10	-68.28	0	GPS NET-G3
BR0000000	Brisbane	RTCM 3.2 1006(1),1007(1),1008(30),1019,1020,1023(1) 2	GPS+GLG 302	NOZ	42.05	174.83	1	scarenet
BR0000000	Brisbane	RTCM 3.2 1006(1),1007(1),1008(30),1019,1020,1023(1) 2	GPS+GLG 302C	AUS	34.64	152.32	0	SEPT POLARIS
BR0000000	Brisbane	RTCM 3.2 1006(1),1008(1),1012(30),1019,1020,1023(1) 2	GPS+GLG 302	NOZ	2.85	-40.70	0	SEPT POLARIS
BR0000000	Brisbane	RTCM 3.2 1006(1),1008(1),1012(30),1019,1020,1023(1) 2	GPS+GLG 302	NOZ	2.85	-40.70	0	SEPT POLARIS

MountPoint ID	Format	Format Details	Co-Ordinate Network	Cont. Latitude	Longitude	IP	So	Demersal
ANP00042	Lea_Abyem	RTCM 3.1 1004(1),1004(30),1004(X),1012(1),1012(30);IC 2	GPS+GLG 302	GLP	16.26	-41.53	0	SEPT POLARIS
ADH103495	Alu_Dhah	RTCM 3.0 1004(1),1012(1)	2 GPS+GLG 302C	ARE	24.38	34.82	0	SEPT POLARIS
AZ0002740	Adha_Ababa	RTCM 3.0 1004(1),1006(3),1007(9),1012(1)	2 GPS+GLG 302	ETH	9.34	36.77	0	GPS LEGACY
AG0000741	A GPS-Abba_Melba	RTCM 3.1 1018	2 GLG 302	ETH	9.83	36.74	0	GPS LEGACY
AG0000460	Appo	RTCM 3.2 1006(30),1018,1020,1023(30),1045,1077(1),108 2	GPS+GLG 302	ARG	-34.87	-58.14	0	SEPT POLARIS/ETH
ARA001870	Ara	RTCM 3.0 1004(1),1012(1),1018,1020,1044,1046,1046	2 GPS+GLG 302	JPN	31.80	130.60	1	NEWS
A1AC00343	Atacoto	RTCM 3.2 1004(1),1006(30),1008(10),1012(1),1012(30);IC 2	GPS+GLG 302	PRA	41.93	8.76	0	LEICA GR25
A1B000340	Albert Head	RTCM 3.2 1006(1),1008(1),1018(30),1019,1020,1023(1) 2	GPS+GLG 302	CAN	46.39	-123.46	0	LEICA GR25
A1C000450	Alca_Springs	RTCM 3.2 1006(1),1008(1),1018(30),1019,1020,1023(1) 2	GPS+GLG 302	AUS	-23.67	153.99	0	LEICA GR25
AF0000490	Afrikash	RTCM 3.1 1006(3),1007(3),1008(30),1013(30),1019,102 2	GPS+GLG 302	PER	-16.47	-71.46	0	SEPT POLARIS
AF0000540	Afrington	RTCM 3.1 1004(1),1004(3),1007(3),1012(1),1033(3),4094 2	GPS+GLG 302C	USA	46.17	-122.14	0	SEPT POLARIS
AF0000490	Afrikash	RTCM 3.1 1006(3),1008(1),1018(30),1019,1020,1023(1) 2	GPS+GLG 302	PER	-16.47	-71.46	0	SEPT POLARIS
A1C000343	Atacoto	RTCM 3.1 1004(1),1006(3),1007(9),1012(1),1012(30);IC 2	GPS+GLG 302	PRA	41.93	8.76	0	LEICA GR25
B40000340	Baker-Lake	RTCM 3.2 1004(1),1006(1),1012(30),1019,1020,1023(1) 2	GPS+GLG 302	CAN	69.10	-68.28	0	GPS NET-G3
B40000340	Baker-Lake	RTCM 3.2 1004(1),1006(1),1012(30),1019,1020,1023(1) 2	GPS+GLG 302	CAN	69.10	-68.28	0	GPS NET-G3
BR0000000	Brisbane	RTCM 3.2 1006(1),1007(1),1008(30),1019,1020,1023(1) 2	GPS+GLG 302	NOZ	42.05	174.83	1	scarenet
BR0000000	Brisbane	RTCM 3.2 1006(1),1007(1),1008(30),1019,1020,1023(1) 2	GPS+GLG 302C	AUS	34.64	152.32	0	SEPT POLARIS
BR0000000	Brisbane	RTCM 3.2 1006(1),1008(1),1012(30),1019,1020,1023(1) 2	GPS+GLG 302	NOZ	2.85	-40.70	0	SEPT POLARIS
BR0000000	Brisbane	RTCM 3.2 1006(1),1008(1),1012(30),1019,1020,1023(1) 2	GPS+GLG 302	NOZ	2.85	-40.70	0	SEPT POLARIS

[1] RTCM standard 10410.1 with amendment 1, Networked transport of RTCM via internet protocol (Ntrip) - version 2.0, June 2011

NTRIP (2)

Commercial NTRTK/RTK Services in Japan

GPSdata (<https://www.gpsdata.co.jp>)

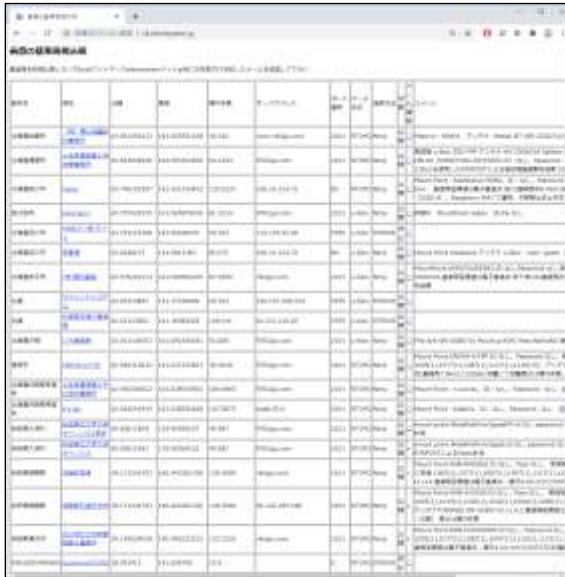
Jenoba (<https://www.jenoba.jp>)

Nihon Terasat (<https://www.terasat.co.jp>)

NTT docomo (https://www.nttdocomo.co.jp/biz/service/highprecision_gnss_positioning)

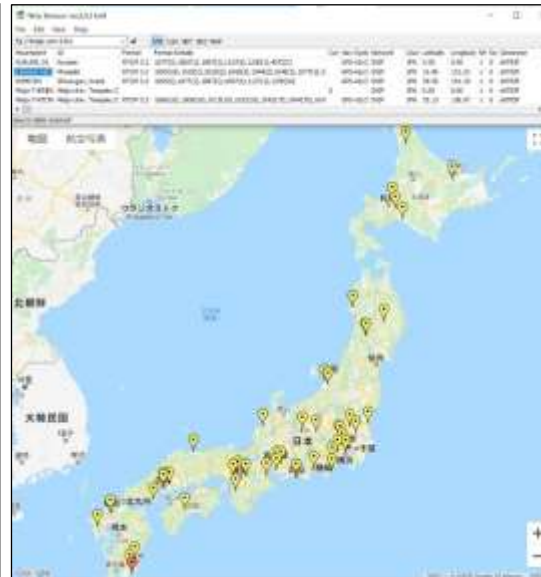
Softbank (<https://www.softbank.jp/biz/iot/service/ichimill>)

Open RTK Reference Stations



名称	ID	緯度	経度	標高	サービス	備考
静岡大学浜松キャンパス	43.000000	138.000000	35.000000	35.000000	RTK	静岡大学浜松キャンパス
静岡大学浜松キャンパス	43.000000	138.000000	35.000000	35.000000	RTK	静岡大学浜松キャンパス
静岡大学浜松キャンパス	43.000000	138.000000	35.000000	35.000000	RTK	静岡大学浜松キャンパス
静岡大学浜松キャンパス	43.000000	138.000000	35.000000	35.000000	RTK	静岡大学浜松キャンパス
静岡大学浜松キャンパス	43.000000	138.000000	35.000000	35.000000	RTK	静岡大学浜松キャンパス

(<http://rtk.silentsystem.jp>)



(<http://www.rtk2go.com>)



The screenshot shows the homepage of the website hamamatsu-gnss.org. The page features a blue header with the site name, a large image of a sky with clouds, and a main heading in Japanese: "静岡大学浜松キャンパス設置の RTK-GNSS用基準局データの常時配信について". Below the heading, there is a detailed announcement in Japanese regarding the real-time distribution of RTK-GNSS reference station data from the Hamamatsu University Shizuoka Campus.

(<https://hamamatsu-gnss.org>)

3. RTK/PPK Practice

RTKLIB

The screenshot displays the RTKLIB website's 'Download' page. It features a table with the following columns: Version, Date, Binary ZIP Package for Windows, and Full Package with Source Programs. The table lists several versions from 2.8.0 to 3.2.0. Below the table, there is a note about downloading the latest version and a table for mirrors. At the bottom, there are sections for 'Subscribe to RSS Feeds' and 'Open Source License Information'.

<http://www.rtklib.com/>

The screenshot shows the GitHub page for the RTKLIB repository. It displays the repository name 'tomojitaku / RTKLIB' and a 'Join GitHub today' button. Below this, there is a list of files and folders with their commit counts and last update times. The repository is described as 'An Open Source Program Package for GNSS Positioning'.

<https://github.com/tomojitaku/RTKLIB>

The advertisement is for the 'センチメートルGPS測位 F9P RTKキット・マニュアル' (Centimeter GPS Positioning F9P RTK Kit & Manual). It features a large image of the green F9P RTK kit with a USB connector. Below the main image, there are smaller images showing the kit being used on a tractor and a person working on a computer. The advertisement includes Japanese text and lists features such as 'スタート・キット発売中!' (Start Kit Available!), '開発スタートアップ&ツール' (Development Start-up & Tools), and '2周波RTK受信機ZED-F9P入門ムービー' (2-Frequency RTK Receiver ZED-F9P Beginner Video). The price is listed as 定価21,500円(税別).

<https://shop.cqpub.co.jp/hanbai/books/MSP/MSP202004.html>

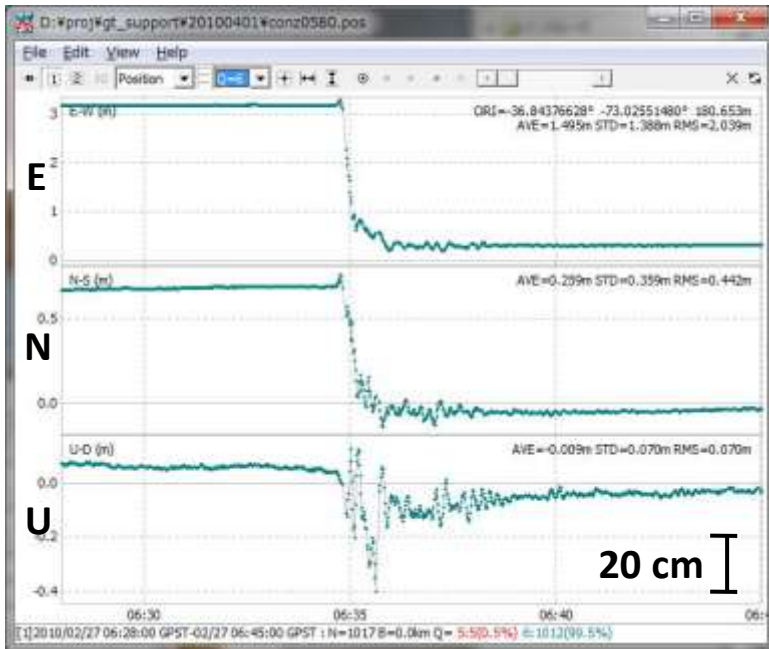
RTK/PPK Practice

(TBD)

4. Theory of PPP

Typical Accuracy of PPP

1 Hz Kinematic PPP

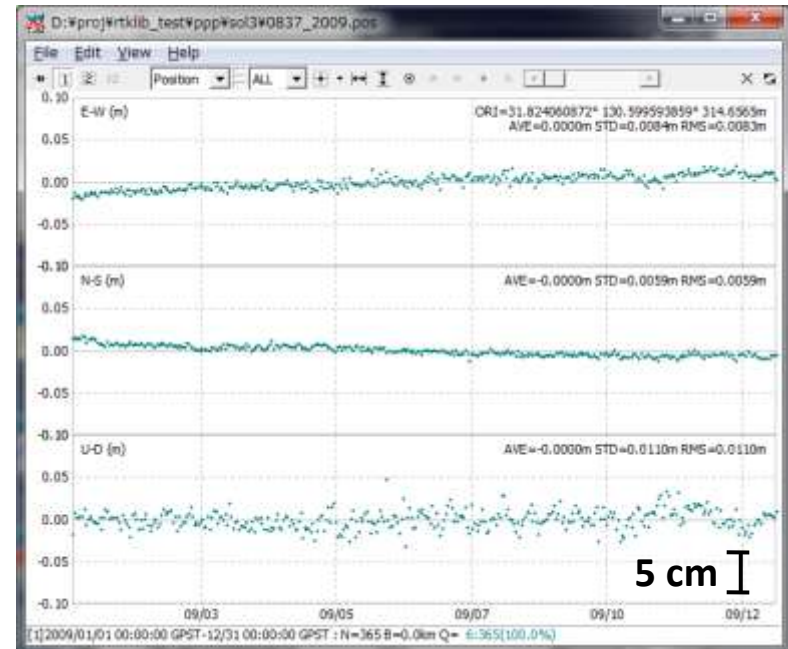


IGS CONZ, 2010/2/27 6:28-6:45 GPST

H-RMS: 1 cm, V-RMS: 2 cm (PP)

H-RMS: 3 cm, V-RMS: 6 cm (RT)

24 H Static PPP



GEONET 0837 (Aira), 2009/1/1-2009/12/31

H-RMS: 3 mm, V-RMS: 6 mm (PP)

PPP Model Error < 1 mm

Pseudorange/Carrier-phase Model

$$\begin{aligned}
 P_r^s &\equiv c\tau \\
 &= c(\bar{t}_r - \bar{t}^s) \\
 &= c((t_r + dt_r) - (t^s + dT^s(t^s))) + \varepsilon_p \\
 &= c(t_r - t^s) + c(dt_r - dT^s(t^s)) + \varepsilon_p \\
 &= (\rho_r^s + I_r^s + T_r^s) + c(dt_r - dT^s(t^s)) + \varepsilon_p \\
 &= \overbrace{\rho_r^s}^{(1)} + \overbrace{c(dt_r - dT^s(t^s))}^{(2)} + \overbrace{I_r^s}^{(3)} + \overbrace{T_r^s}^{(4)} + \overbrace{d_r^s}^{(5)} + \varepsilon_p
 \end{aligned}$$

$$\begin{aligned}
 \phi_r^s &= \phi_r(t_r) - \phi^s(t^s) + N_r^s + \varepsilon_\phi \\
 &= (f(t_r + dt_r - t_0) + \phi_{r,0}) - (f(t^s + dT^s(t^s) - t_0) + \phi_0^s) + N_r^s + \varepsilon_\phi \\
 &= \frac{c}{\lambda}(t_r - t^s) + \frac{c}{\lambda}(dt_r - dT^s(t^s)) + (\phi_{r,0} - \phi_0^s + N_r^s) + \varepsilon_\phi
 \end{aligned}$$

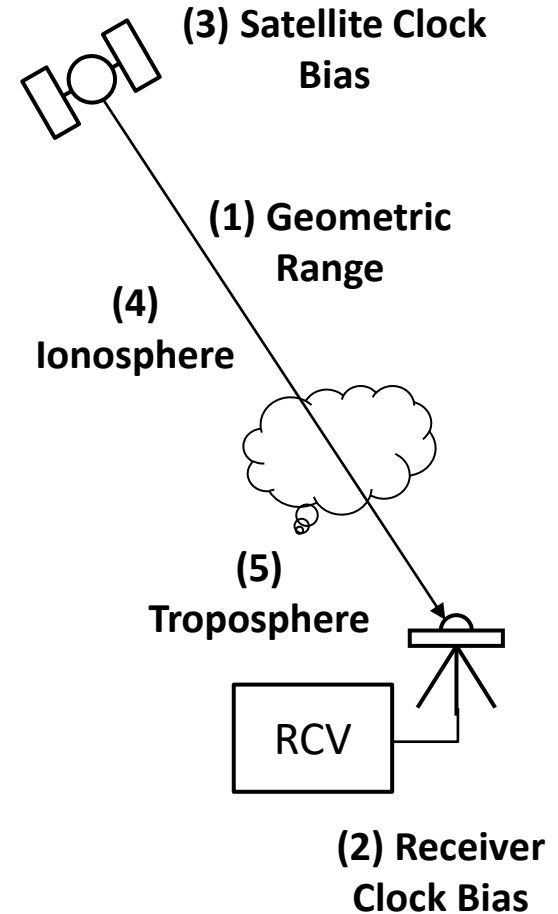
$$\begin{aligned}
 \Phi_r^s &\equiv \lambda\phi_r^s = c(t_r - t^s) + c(dt_r - dT^s(t^s)) + \lambda(\phi_{r,0} - \phi_0^s + N_r^s) + \lambda\varepsilon_\phi \\
 &= \rho_r^s + c(dt_r - dT^s(t^s)) - I_r^s + T_r^s + d_r^s + \lambda d_{pw} + \lambda B_r^s + \varepsilon_\Phi
 \end{aligned}$$

$$d_r^s = d_{r,ant} + d_{ant}^s - \mathbf{d}_{disp}^T \mathbf{e}_{r,enu}^s + d_{rel}$$

$$B_r^s = \phi_{r,0} - \phi_0^s + N_r^s$$

$\phi_{r,0}$: Receiver initial phase (cyc)

ϕ_0^s : Satellite initial phase (cyc)



LC (Linear Combination)

LC of L1, L2, L5 Carrier Phase and Pseudorange

$$LC = a\Phi_{L1} + b\Phi_{L2} + c\Phi_{L5} + dP_{L1} + eP_{L2} + fP_{L5}$$

	LC	Coefficients						Wave Length (cm)	Ionos Effect wrt L1	Typical Noise (cm)
		a	b	c	d	e	f			
L1	L1 Carrier-Phase	1	-	-	-	-	-	19.0	1.0	0.3
L2	L2 Carrier-Phase	-	1	-	-	-	-	24.4	1.6	0.3
L5	L5 Carrier-Phase	-	-	1	-	-	-	25.5	1.8	0.3
LC/L3	L1-L2 Iono-Free Phase	C_1	C_2	-	-	-	-	-	0.0	0.9
LC_{L1-L5}	L1-L5 Iono-Free Phase	C_3	-	C_4	-	-	-	-	0.0	0.8
LG/L4	L1-L2 Geometry-Free Phase	1	-1	-	-	-	-	-	-0.6	0.4
LG_{L2-L5}	L2-L5 Geometry-Free Phase	-	1	-1	-	-	-	-	-0.1	0.4
EWL	Extra-Wide-Lane Phase	-	$\lambda_{EWL}/\lambda_{L2}$	$-\lambda_{EWL}/\lambda_{L5}$	-	-	-	586.1	-0.2	0.4
WL	Wide-Lane Phase	$\lambda_{WL}/\lambda_{L1}$	$-\lambda_{WL}/\lambda_{L2}$	-	-	-	-	86.2	-1.3	1.7
NL	Narrow-Lane Phase	$\lambda_{NL}/\lambda_{L1}$	$\lambda_{NL}/\lambda_{L2}$	-	-	-	-	10.7	1.3	1.7
MW	Melbourne-Wübbena WL	$\lambda_{WL}/\lambda_{L1}$	$-\lambda_{WL}/\lambda_{L2}$	-	$-\lambda_{NL}/\lambda_{L1}$	$-\lambda_{NL}/\lambda_{L2}$	-	86.2	0.0	21
MW_{EWL}	Melbourne-Wübbena EWL	-	$\lambda_{EWL}/\lambda_{L2}$	$-\lambda_{EWL}/\lambda_{L5}$	-	$-\lambda_{ENL}/\lambda_{L2}$	$-\lambda_{ENL}/\lambda_{L5}$	586.1	0.0	21
MP1	L1-Multipath	$2C_2 - 1$	$-2C_2$	-	1	-	-	-	0.0	30
MP2	L2-Multipath	$-2C_1$	$2C_1 - 1$	-	-	1	-	-	0.0	30
MP5	L5-Multipath	$-2C_3$	-	$2C_3 - 1$	-	-	1	-	0.0	30

$$C_1 = \lambda_{L1}^2 \lambda_{L2}^2 / (\lambda_{L2}^2 - \lambda_{L1}^2) = 2.55, C_2 = -\lambda_{L2}^2 \lambda_{L1}^2 / (\lambda_{L2}^2 - \lambda_{L1}^2) = -1.55, C_3 = \lambda_{L1}^2 \lambda_{L5}^2 / (\lambda_{L5}^2 - \lambda_{L1}^2) = 2.26, C_4 = -\lambda_{L5}^2 \lambda_{L1}^2 / (\lambda_{L5}^2 - \lambda_{L1}^2) = -1.26,$$

$$\lambda_{WL} = \lambda_{L1} \lambda_{L2} / (\lambda_{L2} - \lambda_{L1}) = 86.2 \text{ cm}, \lambda_{NL} = \lambda_{L1} \lambda_{L2} / (\lambda_{L1} + \lambda_{L2}) = 10.7 \text{ cm}, \lambda_{EWL} = \lambda_{L2} \lambda_{L5} / (\lambda_{L5} - \lambda_{L2}) = 586.1 \text{ cm}, \lambda_{ENL} = \lambda_{L2} \lambda_{L5} / (\lambda_{L2} + \lambda_{L5}) = 12.5 \text{ cm}$$

Tropospheric Delay

Tropospheric Delay

$$T_r^s = m_h(EI)Z_h + m_w(EI)Z_w \quad (1)$$

$$T_r^s = m_h(EI)Z_h + m_w(EI)(Z_t - Z_h) \quad (2) \quad (m)$$

Zenith hydrostatic delay

$$Z_h = \frac{0.0022768p}{1 - 0.00266 \cos 2\phi - 2.8 \times 10^{-7} H}$$

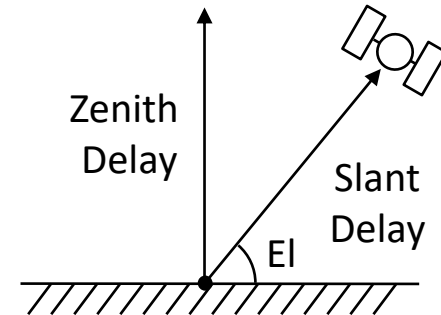
p : Total atmospheric pressure (hPa)

Troposphere Model by Standard Atmosphere

$$p = 1013.25 \times (1 - 2.2557 \times 10^{-5} h)^{5.2568}$$

$$T = 15.0 - 6.5 \times 10^{-3} h + 273.15$$

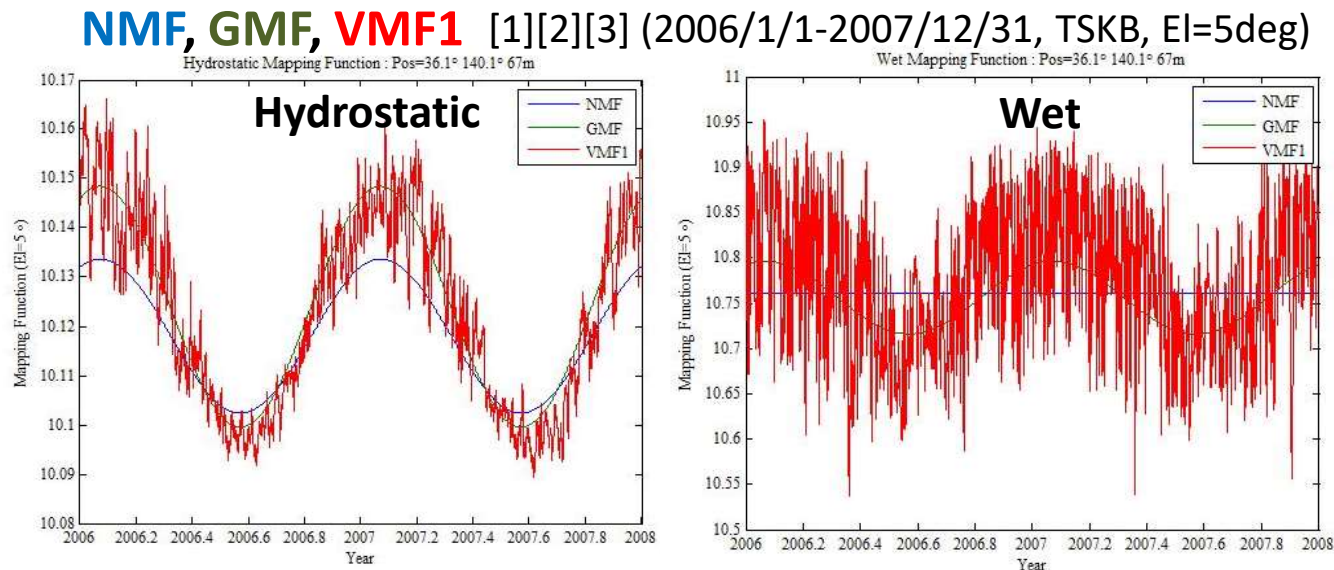
$$e = 6.108 \times \exp\left\{\frac{17.15T - 4684.0}{T - 38.45}\right\} \times \frac{h_{rel}}{100}$$



Mapping Function

$$m_x(\text{El}) = \frac{1 + \frac{a_x}{1 + \frac{b_x}{1 + c_x}}}{\sin(\text{El}) + \frac{a_x}{\sin(\text{El}) + \frac{b_x}{\sin(\text{El}) + c_x}}$$

a_x, b_x, c_x : Mapping Function Coefficients



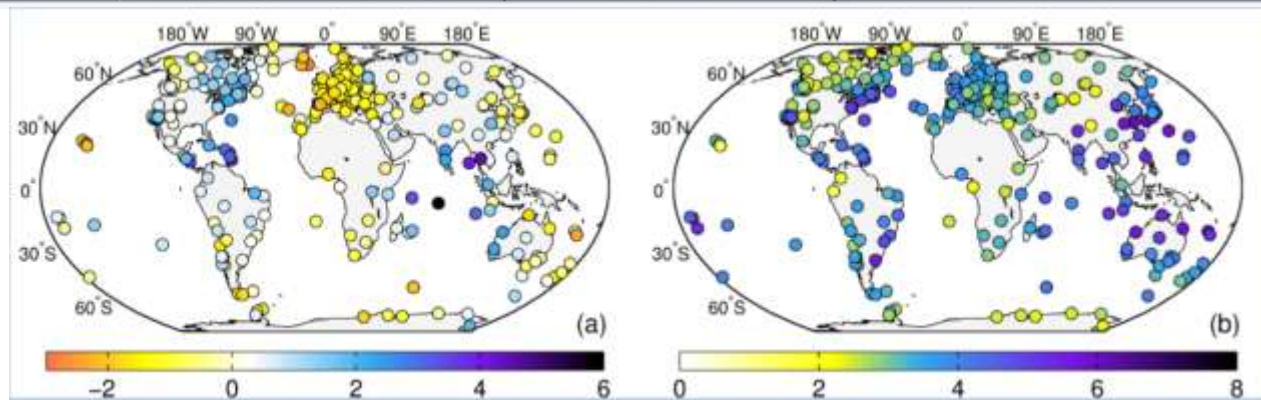
- [1] A.E.Niell, Global mapping functions for the atmosphere delay at radio wavelength, Journal of Geophysical Research, 1996
- [2] J.Boehm, A.Niell, P.Tregoning and H.Shuh, Global Mapping Function (GMF): A new empirical mapping function base on numerical weather model data, G/formeophysical Res Lett, 33, L07304, 2006
- [3] J.Boehm, R.Heinkelmann and H.Schuh, Short note: A global model of pressure and temperature for geodetic applications, Journal of Geodesy, 2007

Empirical Tropospheric Model

Model ZTD Bias and RMS error (cm) (2012)

	mean bias	mean standard deviation
RTCA-MOPS (1999)	-2.50 cm	4.55 cm
ESA (Martellucci 2012)	0.83 cm	3.82 cm
GPT2 (Lagler et al. 2013)	-0.28 cm	3.79 cm
GPT2w (Böhm et al. 2014)	-0.02 cm	3.61 cm

[1]
[2]
[3]



GPT2w
ZTD Bias
and RMS
error (cm)

J. Bohm et al., Development of an improved empirical model for slant delays in the troposphere (GPT2w), GPS Solutions, 2015

[1] RTCA/DO-229, Minimum operational standards for global positioning system/wide area augmentation system airborne equipment. 1999

[2] A. Martellucci, Galileo reference troposphere model for the user receiver. ESA-APPNG-REF/00621-AM v2.7, 2012

[3] K. Lagler et al., GPT2: empirical slant delay model for radio space geodetic techniques. Geophys Res Lett, 2013

Satellite Attitude Model

Nominal Yaw Attitude Model

$$\mathbf{E}^s = (\mathbf{e}_x^{sT}, \mathbf{e}_y^{sT}, \mathbf{e}_z^{sT})^T$$

$$\mathbf{e}_z^s = -\frac{\mathbf{r}^s(t^s)}{\|\mathbf{r}^s(t^s)\|}, \mathbf{e}_{\text{sun}} = \frac{\mathbf{r}_{\text{sun}}(t^s) - \mathbf{r}^s(t^s)}{\|\mathbf{r}_{\text{sun}}(t^s) - \mathbf{r}^s(t^s)\|}$$

$$\mathbf{e}_y^s = \frac{\mathbf{e}_z^s \times \mathbf{e}_{\text{sun}}}{\|\mathbf{e}_z^s \times \mathbf{e}_{\text{sun}}\|}, \mathbf{e}_x^s = \mathbf{e}_y^s \times \mathbf{e}_z^s$$

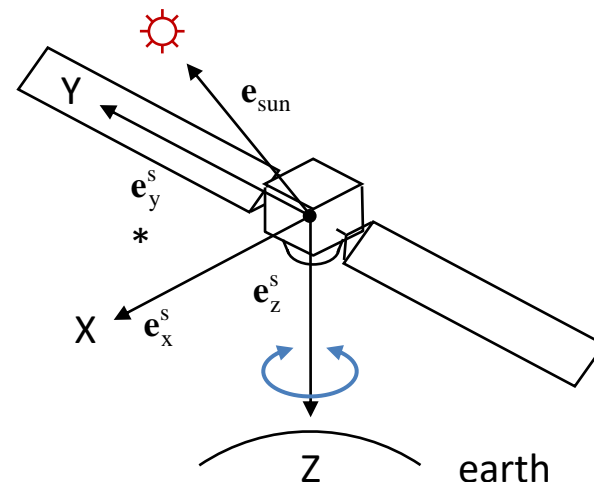
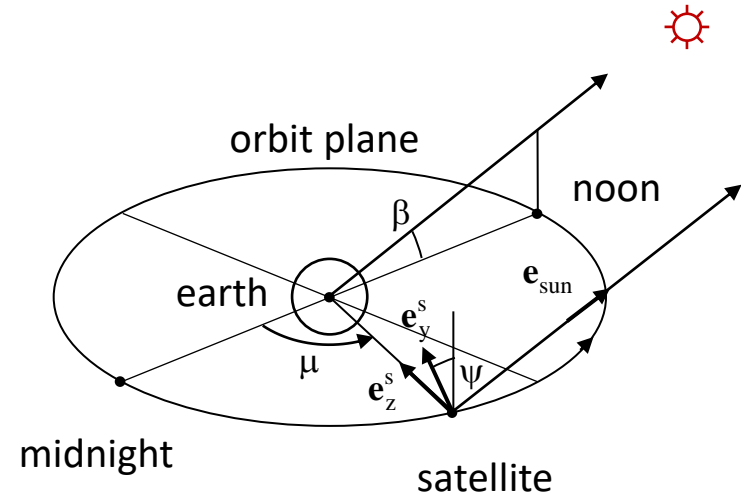
$\mathbf{r}_{\text{sun}}(t)$: Sun position in ECEF (m)

β : Beta angle of orbit plane (rad)

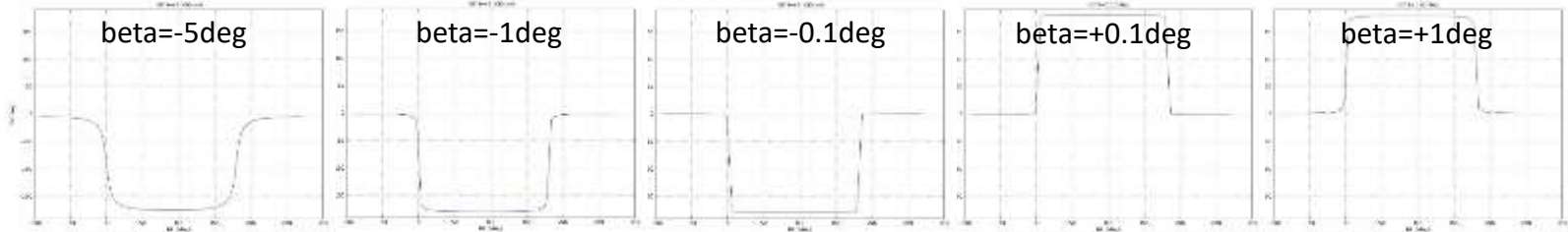
μ : Orbit angle from midnight (rad)

ψ : Yaw angle of satellite attitude (rad)

* Some satellites take opposite direction of Y-axis

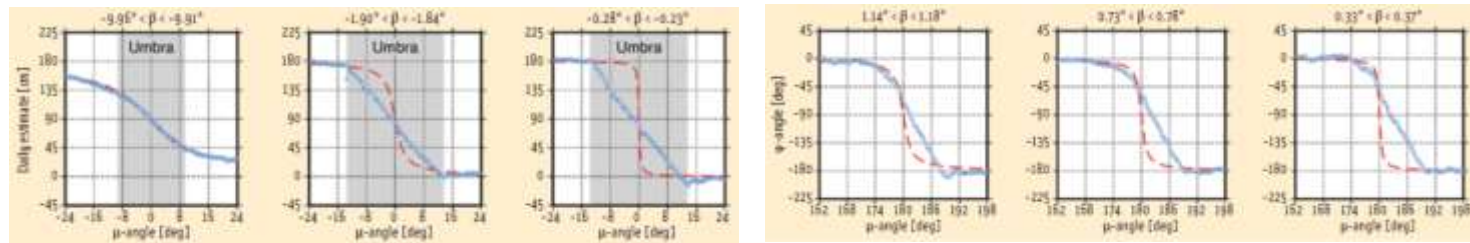


Yaw Attitude of Eclipsing Satellites



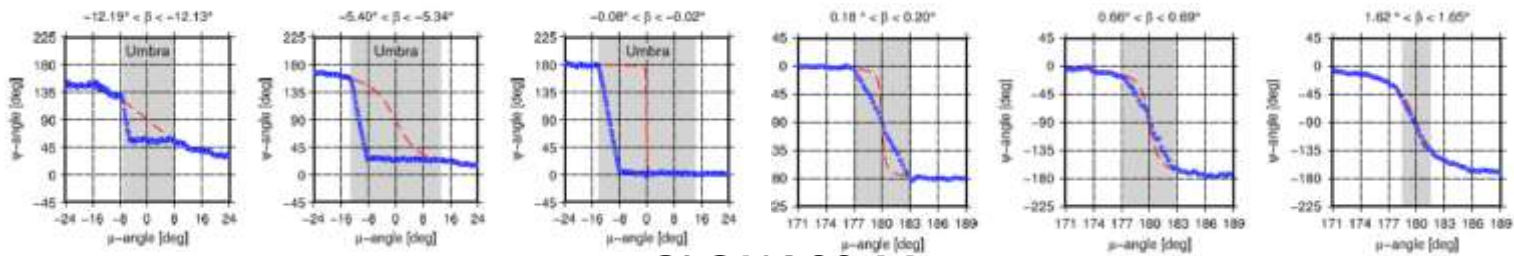
GPS Block IIR

J.Kouba, A simplified yaw-attitude model for eclipsing GPS satellites, GPS Solutions, 2009



GPS Block IIF

F. Dilssner, GPS IIF-1 satellite antenna phase center and attitude modeling, Inside GNSS, 2010



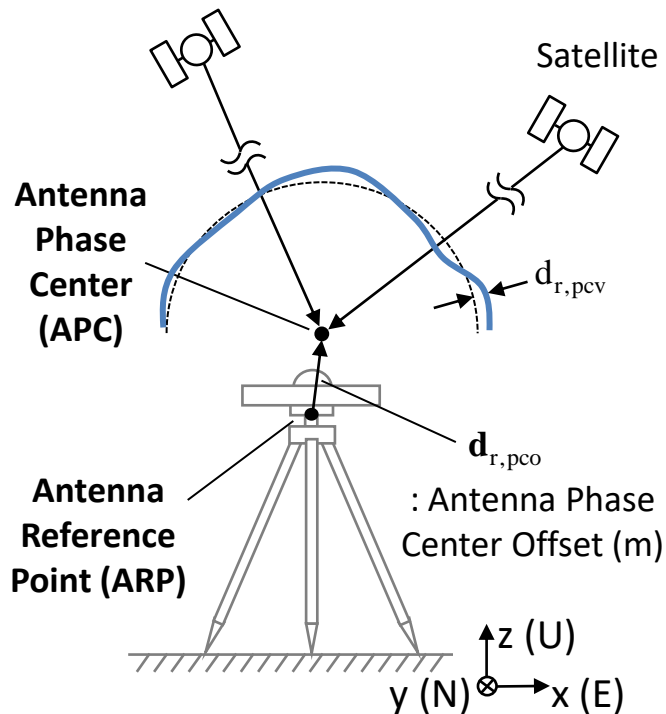
GLONASS-M

F. Dilssner, The GLONASS-M satellite yaw-attitude model, Advances in Space Research, 2010

Antenna Phase Center 1

Receiver Antenna Phase Center Corrections

$$\mathbf{d}_{r,ant} = -\mathbf{d}_{r,pco}^T \mathbf{e}_{r,enu}^s + \mathbf{d}_{r,pcv}(El, Az) \quad (m) \quad (1)$$

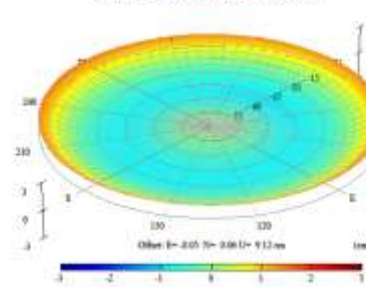


$\mathbf{d}_{r,pcv}$: Antenna Phase Center Variation (PCV)

Choke-Ring Type



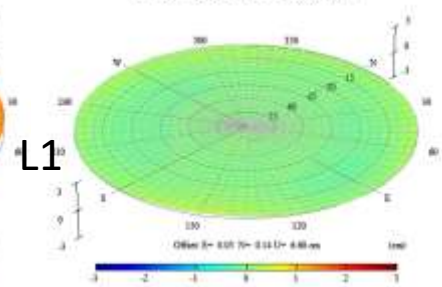
Antenna Phase Center Offset Variation : ADAD3_T (L1)



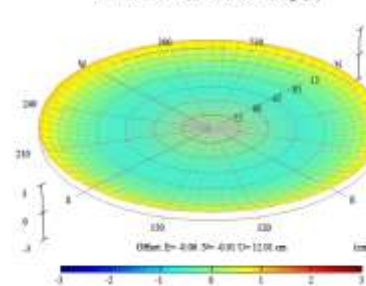
Zero-Offset Type



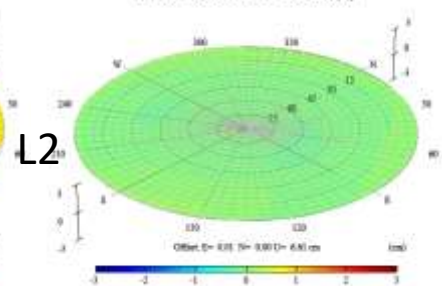
Antenna Phase Center Offset Variation : 30N70300 (L1)



Antenna Phase Center Offset Variation : ADAD3_T (L2)



Antenna Phase Center Offset Variation : 30N70300 (L2)



IGS Absolute Antenna Model (IGS05.PCV)

Antenna Phase Center 2

Satellite Antenna Phase Center Corrections

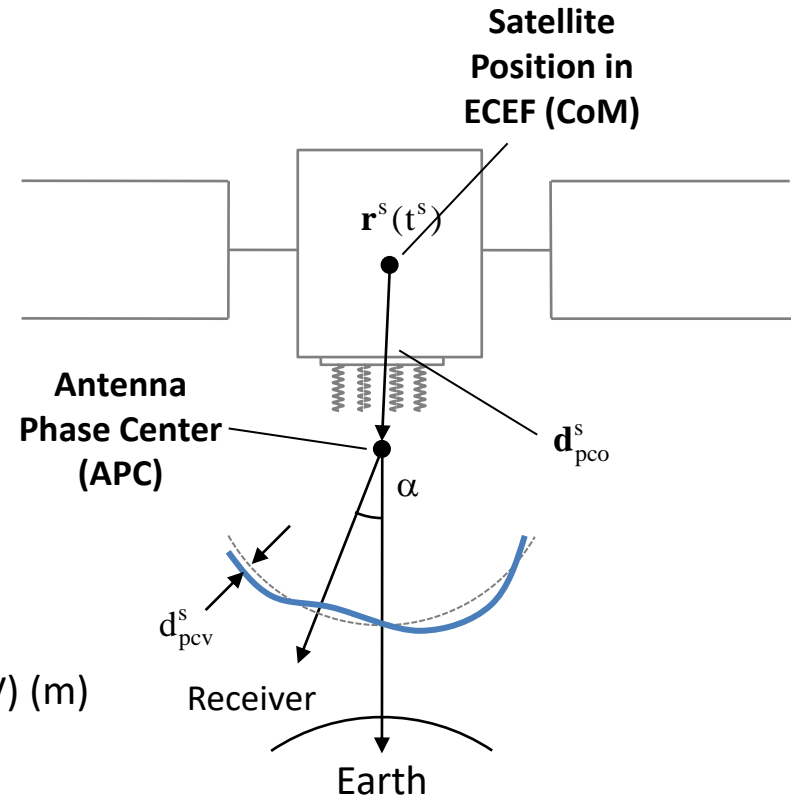
$$\mathbf{d}_{\text{ant}}^s = \left(\mathbf{E}^{sT} \mathbf{d}_{\text{pco}}^s \right)^T \mathbf{e}_r^s + d_{\text{pcv}}^s(\alpha)$$

$$\alpha = \arccos \left(\frac{\mathbf{e}_r^{sT} \mathbf{r}^s(t^s)}{\|\mathbf{r}^s(t^s)\|} \right)$$

$\mathbf{d}_{\text{pco}}^s$: Antenna Phase Center Offset (m)

d_{pcv}^s : Antenna Phase Center Variation (PCV) (m)

α : Off-nadir Angle (rad)



Site Displacement

$$\mathbf{dr}_{\text{tide}} = \mathbf{E}_r^T (\mathbf{dr}_{\text{solid}}(t_r, \mathbf{r}_r) + \mathbf{dr}_{\text{otl}}(t_r, \mathbf{r}_r) + \mathbf{dr}_{\text{pole}}(t_r, \mathbf{r}_r) + \mathbf{dr}_{\text{atmos}}(t_r, \mathbf{r}_r)) \quad (\text{m})$$

- **Displacement of Ground-Fixed Receiver**

- Solid Earth Tide $\mathbf{dr}_{\text{solid}}(t_r, \mathbf{r}_r)$
- Ocean Tide Loading (OTL) $\mathbf{dr}_{\text{otl}}(t_r, \mathbf{r}_r)$
- Pole Tide $\mathbf{dr}_{\text{pole}}(t_r, \mathbf{r}_r)$
- Atmospheric Loading $\mathbf{dr}_{\text{atmos}}(t_r, \mathbf{r}_r)$

- **Tide Models**

- IERS Conventions 1996/2003/2010
- Ocean Loading: Schwiderski, GOT99.2/00.2, CSR 3.0/4.0, FES99/2004, NAO99.b
- $M_2, S_2, N_2, K_2, K_1, O_1, P_1, Q_1, M_1, M_m, S_{sa}$ (11 constituents)

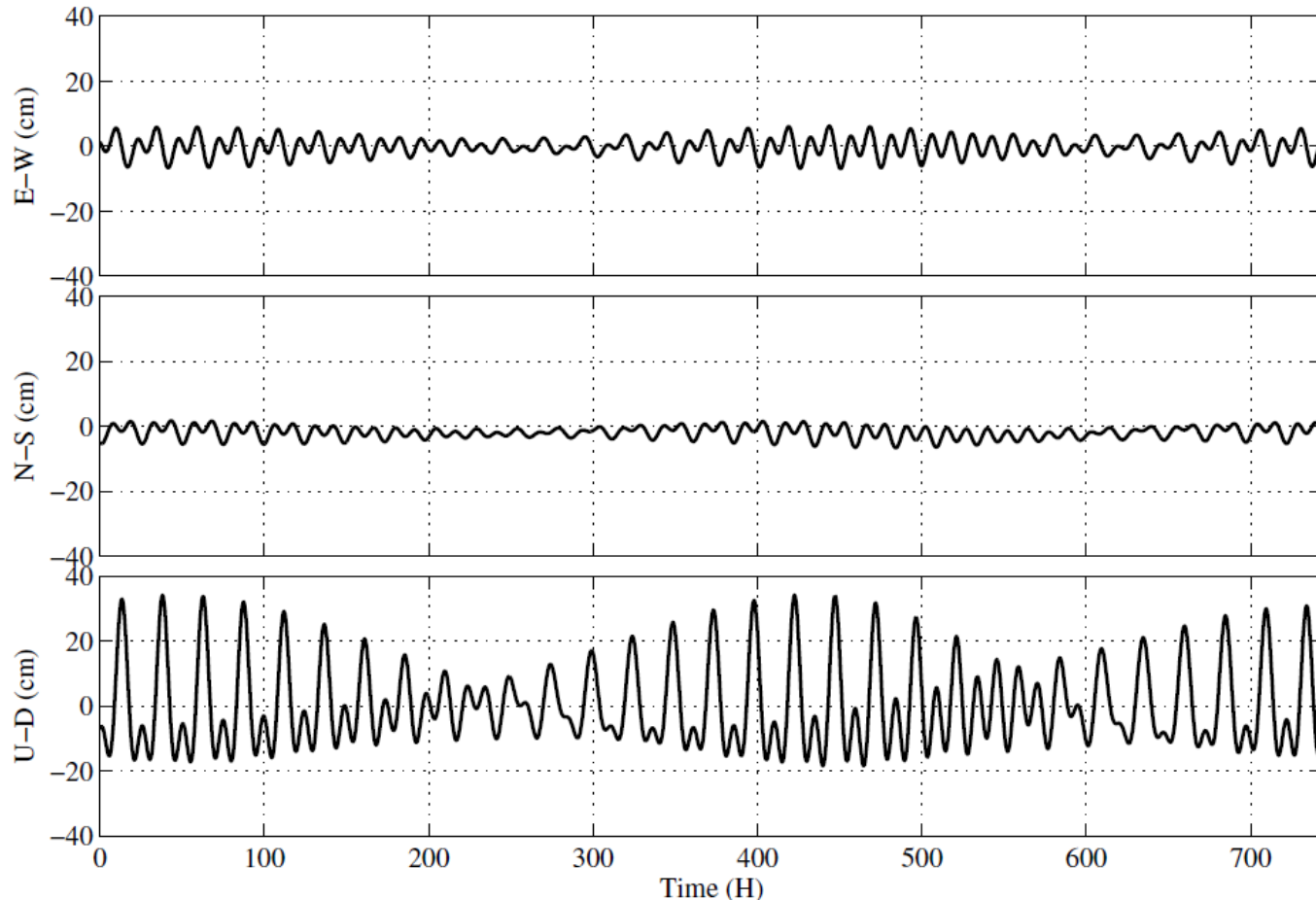
- **IERS Subroutines**

- DEHANTTIDEINEL.F

<http://iers-conventions.obspm.fr/content/chapter7/software/dehanttideinel/DEHANTTIDEINEL.F>

Earth Tides

Earth Tides Model



IERS Conventions 1996 + NAO99.b, 2007/1/1-1/31, TSKB

Phase Wind-up

- Relative rotation between satellite and receiver antennas effect to the measured phase of RHCP signal.

$$d_{pw} = \text{sign}(\mathbf{e}_r^{sT} (\mathbf{D}^s \times \mathbf{D}_r)) \arccos\left(\frac{\mathbf{D}^s \cdot \mathbf{D}_r}{\|\mathbf{D}^s\| \|\mathbf{D}_r\|}\right) / 2\pi + N \quad (\text{cyc})$$

$$\mathbf{E}^s = (\mathbf{e}_x^{sT}, \mathbf{e}_y^{sT}, \mathbf{e}_z^{sT})^T$$

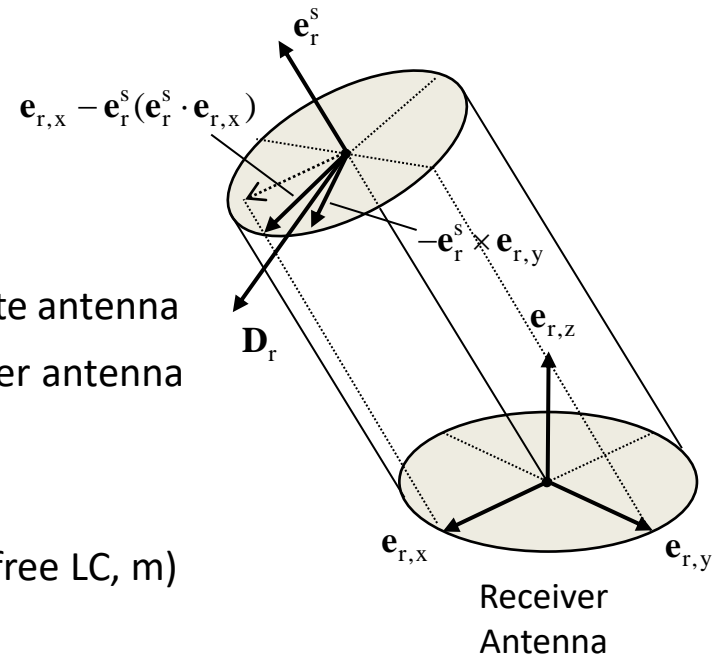
$$\mathbf{E}_r = (\mathbf{e}_{r,x}^T, \mathbf{e}_{r,y}^T, \mathbf{e}_{r,z}^T)^T$$

$$\mathbf{D}^s = \mathbf{e}_x^s - \mathbf{e}_r^s (\mathbf{e}_r^s \cdot \mathbf{e}_x^s) + \mathbf{e}_r^s \times \mathbf{e}_y^s \quad : \text{Dipole vector of satellite antenna}$$

$$\mathbf{D}_r = \mathbf{e}_{r,x} - \mathbf{e}_r^s (\mathbf{e}_r^s \cdot \mathbf{e}_{r,x}) - \mathbf{e}_r^s \times \mathbf{e}_{r,y} \quad : \text{Dipole vector of receiver antenna}$$

N : Integer ambiguity

$$\delta_{pw,LC} = C_1 \lambda_1 d_{pw} + C_2 \lambda_2 d_{pw} = \frac{c}{f_1 + f_2} d_{pw} = \lambda_{NL} d_{pw} \quad (\text{lono-free LC, m})$$



J. T. Wu et al., Effects of antenna orientation on GPS carrier phase, Manuscripta Geodaetica, 1993

IGS Precise Ephemeris

IGS Products (Satellite Orbit, Clock and EOP) [1]

Product		Final (IGS)	Rapid (IGR)	Ultra-Rapid (IGU)		Broadcast	
				Observed	Predicted		
Accuracy	Orbit	GPS	~ 2.5 cm	~ 2.5 cm	~ 3 cm	~ 5 cm	~ 100 cm
		GLONASS	~ 3 cm	-	-	-	-
	Clock (GPS)	RMS	~ 75 ps	~ 75 ps	~ 150 ps	~ 3 ns	~ 5 ns
		STD	~ 20 ps	~ 25 ps	~ 50 ps	~ 1.5 ns	~ 2.5 ns
	EOP	PM	~ 30 uas	~ 50 uas	~ 50 uas	~ 300 uas	-
		PM Rate	~ 150 uas/day	~ 250 uas/day	~ 250 uas/day	~ 300 uas/day	-
LOD		~ 10 us	~ 10 us	~ 10 us	~ 50 us	-	
Sample Interval	Orbit		15 min	15 min	15 min		-
	Clock	Satellite	30 s	5 min	15 min		-
		Station	5 min	-	-		-
	EOP		1 day	1 day	1 day		-
Update Interval		1 week (Thursday)	1 day (17:00 UTC)	6 h (3:00, 9:00, 15:00, 21:00 UTC)		-	
Latency		12 ~ 18 days	17 ~ 41 h	3 ~ 9 h	Realtime	Realtime	
Format		SP3-c, RINEX Clock, IGS ERP ver.2	SP3-c, RINEX Clock, IGS ERP ver.2	SP3-c, IGS ERP ver.2		RINEX 2 (NAV)	
Combination of IGS ACs		COD, EMR, ESA, GFZ, GRG, JPL, MIT, NGS, SIO	COD, EMR, ESA, GFZ, JPL, NGS, SIO, USN, WHU	COD, EMR, ESA, GFZ, NGS, SIO, USN		-	

[1] <http://www.igs.org/products>

SP3

Coordinate System

SP3 Version +
Pos/Vel Flag
(P or V)

```
#cP2019 8 11 0 0 0.00000000 96 ORBIT IGS14 HLM IGS
## 2066 0.00000000 900.00000000 58706 0.00000000000000
+ 32 G01G02G03G04G05G06G07G08G09G10G11G12G13G14G15G16G17
+ G18G19G20G21G22G23G24G25G26G27G28G29G30G31G32 0 0
...
```

of Satellites +
Satellite ID List
(nsat <= 65: SP3-c)

```
++ 2 2 3 0 2 2 2 2 2 3 2 2 2 2 2 2
++ 2 2 2 2 2 2 2 2 2 2 2 2 1 2 1 0 0
...
```

Accuracy

Time System

```
%c G GPS ccc cccc cccc cccc cccc ccccc ccccc ccccc ccccc
%c cc cc ccc ccc cccc cccc cccc cccc ccccc ccccc ccccc ccccc
%f 1.2500000 1.025000000 0.000000000000 0.0000000000000000
%f 0.0000000 0.000000000 0.00000000000 0.0000000000000000
...
```

Base for Pos/Vel,
Clock/Rate

Epoch Header

```
* 2019 8 11 0 0 0.00000000
```

```
PG01 -13937.084103 20599.191872 8651.202344 -92.964795 8 4 7 88
PG02 15724.617716 -1528.775235 -20723.114309 -280.106539 8 6 8 81
PG03 -18296.728356 13096.333779 -14091.595163 -0.633827 14 8 12 68
PG04 -21943.288752 -11533.160188 9959.429407 999999.999999
```

Type Symbol
(P: Pos, V: Vel)
+ Satellite ID

```
... Pos: X, Y, Z-Coordinate (km) Clock (us) Std-devs Flags
... Vel: X, Y, Z-Velocity (dm/s) Clock Rate-Change (10-4 us/s) (P: Predicted)
... (0.000000: Bad or Absent) (999999.999999: Bad or Absent)
...
```

```
* 2019 8 11 0 15 0.00000000
```

End of File
Marker

```
EOF
```

Header
Lines
(# lines =
22: SP3-c,
>=22: SP3-d)

[1] S. Hilla, The extended standard product 3 orbit format (SP3-d), Feb 2016

RINEX Clock

RINEX Version + RINEX Type (C)	3.00 C	RINEX VERSION / TYPE
	CCLOCK IGSACC @ GA and MIT	PGM / RUN BY / DATE
	GPS week: 2065 Day: 0 MJD: 58699	COMMENT
	THE COMBINED CLOCKS ARE A WEIGHTED AVERAGE OF:	COMMENT
	...	
# of Data Types + Data Type List	18	LEAP SECONDS
	2 AR AS	# / TYPES OF DATA
	IGS IGSACC @ GA and MIT	ANALYSIS CENTER
# of Stations + Ref Frame + Station ID List	229 IGS14 : IGS REALIZATION of THE ITRF2014	# OF SOLN STA / TRF
	ABMF 97103M001 2919785785 -5383744963 1774604854	SOLN STA NAME / NUM
	ABPO 33302M001 4097216545 4429119196 -2065771184	SOLN STA NAME / NUM
	ADIS 31502M001 4913652571 3945922819 995383509	SOLN STA NAME / NUM
	...	
# of Satellites + Satellite ID List	31	# OF SOLN SATS
	G01 G02 G03 G05 G06 G07 G08 G09 G10 G11 G12 G13 G14 G15 G16	PRN LIST
	G17 G18 G19 G20 G21 G22 G23 G24 G25 G26 G27 G28 G29 G30 G31	PRN LIST
	G32	PRN LIST
Applied PCV	G igs14_2062.atx	SYS / PCVS APPLIED
		END OF HEADER
	AR GPST 2019 08 04 00 00 0.000000 2 2.031378026801e-08 0.000000000000e+00	
	AR ALBH 2019 08 04 00 00 0.000000 2 2.685697915664e-08 2.647813470470e-11	
	...	
Data Type (AR: Rec Clock, AS: Sat Clock)	AS G01 2019 08 04 00 00 0.000000 2 -8.616827744323e-05 3.362553644680e-11	
	AS G02 2019 08 04 00 00 0.000000 2 -2.750040416487e-04 2.953488394790e-11	
	... ↑ Epoch Time # of Data Clock Bias (s) Clock Bias Sigma (s) Station or Follows (opt) Satellite ID	

[1] J. Ray and W. Gurtner, RINEX extensions to handle clock information, version 3.02, Sep 2010

ANTEX

ANTEX Version +
Sat System

Type + Sate ID +
Sat code(opt)
(Sat Ant)

Start/End of
Validity Period
in GPST (opt)

Sat System +
Freq Code

Type/Serial #
(Rec Ant)

PCO (mm) in
X,Y,Z (Sat Ant),
N,E,U (Rec Ant)

Non-azimuth
dependent
PCV (mm) for
each zenith/
nadir angles

1.4	M	ANTEX VERSION / SYST									
A		PCV TYPE / REFANT									
...		COMMENT									
END OF HEADER											
START OF ANTENNA											
BLOCK IIA	G01	G032	1992-079A	TYPE / SERIAL NO							
0.0		0	29-JAN-17	METH / BY / # / DATE							
0.0	17.0	1.0		DAZI							
2				ZEN1 / ZEN2 / DZEN							
1992	11	22	0	0	0.000000						
2008	10	16	23	59	59.999999						
IGS14_2062											
G01	START OF FREQUENCY										
279.00	0.00	2319.50									
NOAZI	-0.80	-0.90	-0.90	-0.80	-0.40	0.20	0.80	1.30	1.40	1.20	...
G01	END OF FREQUENCY										
G02	START OF FREQUENCY										
279.00	0.00	2319.50									
NOAZI	-0.80	-0.90	-0.90	-0.80	-0.40	0.20	0.80	1.30	1.40	1.20	...
G02	END OF FREQUENCY										
...											
END OF ANTENNA											
START OF ANTENNA											
AOAD/M_B	NONE	TYPE / SERIAL NO									
CONVERTED	TUM	0	29-JAN-17	METH / BY / # / DATE							
5.0				DAZI							
0.0	90.0	5.0		ZEN1 / ZEN2 / DZEN							
2				# OF FREQUENCIES							
IGS14_2062											
G01	START OF FREQUENCY										
0.66	-0.53	59.84									
NOAZI	0.00	-0.23	-0.91	-1.94	-3.24	-4.63	-5.98	-7.11	-7.90	-8.24	...
...	0.0	0.00	-0.26	-0.98	-2.06	-3.40	-4.85	-6.23	-7.40	-8.19	-8.51
...	360.0	0.00	-0.26	-0.98	-2.06	-3.40	-4.85	-6.23	-7.40	-8.19	-8.51
G01	END OF FREQUENCY										
...											
END OF ANTENNA											

Header
Section

Record
Header

Freq 1
Section

Freq 2
Section

Ant
Record

Azimuth
dependent
PCV (mm) for
each zenith/
nadir angles
(opt)

[1] M. Rothacher, R. Schmid and M. Chen, ANTEX: The antenna exchange format, version 1.4, Sep 2010

SSR Orbit and Clock Corrections

SSR Orbit and Clock Corrections [1]

$$(t_0, \text{IOD}, \delta O_{\text{radial}}, \delta O_{\text{along}}, \delta O_{\text{cross}}, \delta \dot{O}_{\text{radial}}, \delta \dot{O}_{\text{along}}, \delta \dot{O}_{\text{cross}}, C_0, C_1, C_2, C_{\text{HR}})$$

Satellite Position and Clock Bias with SSR Corrections [1]

$$t_O = t_{O0} + \text{UDI}_O / 2$$

$$\delta \mathbf{O} = \begin{pmatrix} \delta O_{\text{radial}} \\ \delta O_{\text{along}} \\ \delta O_{\text{cross}} \end{pmatrix} + \begin{pmatrix} \delta \dot{O}_{\text{radial}} \\ \delta \dot{O}_{\text{along}} \\ \delta \dot{O}_{\text{cross}} \end{pmatrix} (t - t_O)$$

$$\mathbf{r}^S(t) = \mathbf{r}_{\text{brdc}}^S(t, \text{IOD}) + (\mathbf{e}_{\text{radial}}, \mathbf{e}_{\text{along}}, \mathbf{e}_{\text{cross}}) \delta \mathbf{O}$$

$$\mathbf{v}_{\text{brdc}}^S(t) = \frac{\mathbf{r}_{\text{brdc}}^S(t + \Delta t, \text{IOD}) - \mathbf{r}_{\text{brdc}}^S(t, \text{IOD})}{\Delta t}$$

$$\mathbf{e}_{\text{along}} = \frac{\mathbf{v}_{\text{brdc}}^S(t)}{|\mathbf{v}_{\text{brdc}}^S(t)|}, \quad \mathbf{e}_{\text{cross}} = \frac{\mathbf{r}_{\text{brdc}}^S(t, \text{IOD}) \times \mathbf{v}_{\text{brdc}}^S(t)}{|\mathbf{r}_{\text{brdc}}^S(t, \text{IOD}) \times \mathbf{v}_{\text{brdc}}^S(t)|}$$

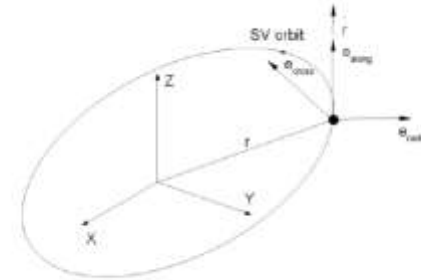
$$\mathbf{e}_{\text{radial}} = \mathbf{e}_{\text{along}} \times \mathbf{e}_{\text{cross}}$$

$$t_C = t_{C0} + \text{UDI}_C / 2$$

$$\delta C = C_0 + C_1(t - t_C) + C_2(t - t_C)^2 + C_{\text{HR}}$$

$$dT^S(t) = dT_{\text{brdc}}^r(t, \text{IOD}) + \frac{\delta C}{c}$$

- t_{O0}, t_{C0} : Epoch time of orbit and clock corrections (s)
- $\text{UDI}_O, \text{UDI}_C$: Update interval of orbit and clock corrections (s)
- IOD : IOD indicating corresponding broadcast ephemeris
- $\delta O_i, \delta \dot{O}_i$: Satellite position/velocity corrections (m, m/s)
- C_0, C_1, C_2 : Satellite clock corrections (m, m/s, m/s²)
- C_{HR} : Satellite high-rate clock correction (m)
- $\mathbf{r}_{\text{brdc}}^S(t, \text{IOD})$: Satellite position by broadcast ephemeris with IOD (m)
- $\mathbf{v}_{\text{brdc}}^S(t)$: Satellite velocity by broadcast ephemeris (m/s)
- $dT_{\text{brdc}}^S(t, \text{IOD})$: Satellite clock bias by broadcast SV clock with IOD (s) *
- $\delta \mathbf{O}$: Satellite orbit corrections (m)
- δC : Satellite clock bias correction (m) * including relativistic correction
- $\mathbf{r}^S(t)$: Satellite position with SSR corrections
- $dT^S(t)$: Satellite clock bias with SSR corrections



[1]

Figure 3.12-1. Radial, along-track and cross-track orbit components

[1] RTCM standard 10403.3, Differential GNSS (global navigation satellite system) services - version 3, Oct 2016 (3.5.13)

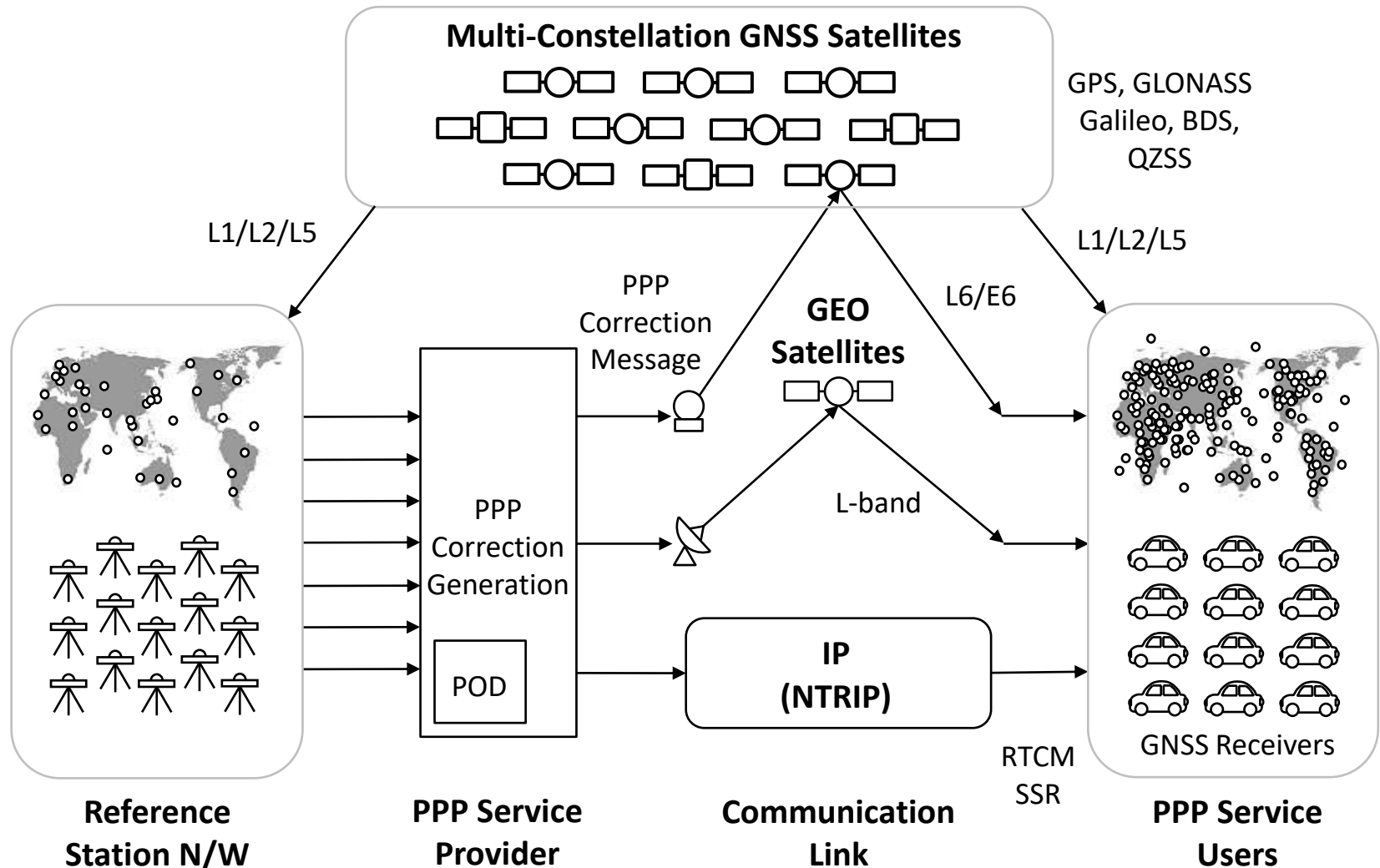
5. PPP Practice

PPP Practice







(TBD)

6. Advanced Topics

PPP Service Architecture

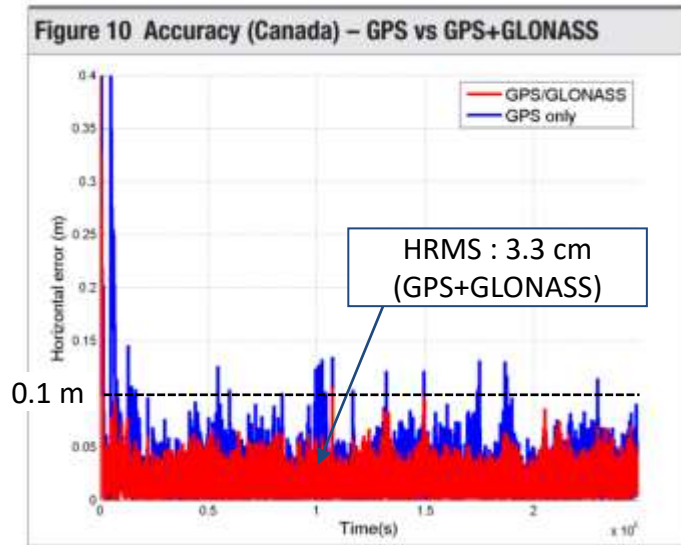


Commercial PPP Services

Service	Provider	Supported GNSS	# of Ref. Stations	Comm. Link	Receivers	Accuracy
StarFire™ [1]	 NAVCOM (US)	GPS, GLO	> 40	3 GEO (L-band), IP	NavCom	< 5 cm
Seastar™ [2]	 FUGRO (NED)	GPS, GLO, GAL, BDS (G4)	~ 80	6 GEO (L-band), IP (NTRIP)	Fugro	10 cm H 15 cm V (95%)
Apex/Ultra [3] TerraStar® [4]	 veripos (UK)	GPS, GLO, GAL, BDS, QZS (Apex ⁵)	~ 80	7 GEO (L-band)	VERIPOS, NovAtel [7], Septentrio [8], TOPCON [9], Hemisphere [10]	< 5 cm H < 12 cm V (95%)
CenterPoint RTX [5]	 Trimble (US)	GPS, GLO, GAL, BDS, QZS	~ 100	6 GEO (L-band), IP (NTRIP)	Trimble, Qualcomm (?)	2 cm H 5 cm V (RMS)
magicGNSS [6]	 gmv (Spain)	GPS, GLO, GAL, BDS, QZS	~ 80	IP (NTRIP)	(RTCM SSR)	5 cm H 8 cm V (RMS)
GEOFLEX [11]	 geoflex (France)	GPS, GLO, (GAL, BDS)	~ 100	GEO, IP, GPRS/UMTS	(RTCM SSR)	4 cm (2D-95%)

[1] <https://www.navcomtech.com>, [2] <https://www.fugro.com>, [3] <https://veripos.com>, [4] <https://www.terrestar.net>,
 [5] <https://positioningservices.trimble.com>, [6] <https://magicgnss.gmv.com>, [7] <https://www.notavel.com>,
 [8] <https://www.septentrio.com>, [9] <https://www.topconpositioning.com>, [10] <https://www.hemispheregnss.com>,
 [11] <http://www.geoflex.fr>

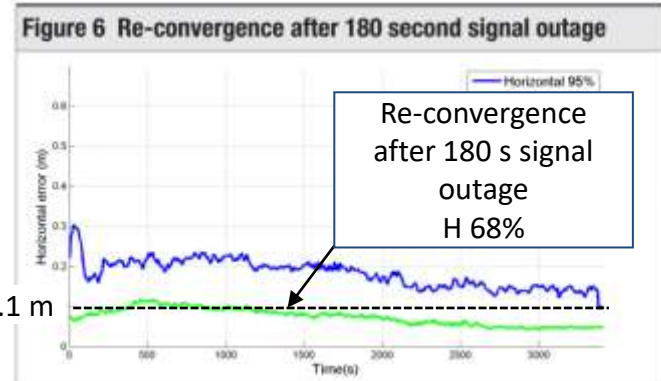
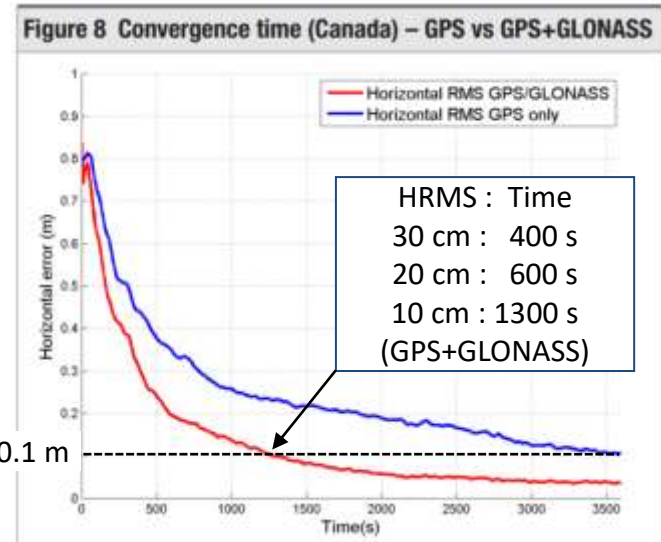
PPP Service Performance



(3 days)

Table 5: Error Statistics at the Canada Station

PPP Correction Source	Horizontal RMS Error (cm)	Vertical RMS Error (cm)
TerraStar-C (GPS/GLONASS)	3.3	4.9
TerraStar-C (GPS only)	4.4	6.5



(NovAtel Correct with TerraStar-C in 2015)

[1] NovAtel White Paper, Precise Positioning with NovAtel CORRECT Including Performance Analysis, April 2015 (<https://www.novatel.com/assets/Documents/Papers/NovAtel-CORRECT-PPP.pdf>)

PPP for Next-Gen Vehicle Positioning

Qualcomm
Snapdragon Automotive
4G/5G Platform:
supporting
GPS, GLONASS, Galileo, BDS
and QZSS (L1, L2, L5)

+

Trimble
RTX Auto:
ASIL and ASPICE compliant
RTX precise positioning
software library



**Absolute In-lane positioning for
ADAS/autonomous-driving**

GPS WORLD GNSS POSITIONING NAVIGATION TIMING

Follow Us: [Social Media Icons]

Search the Site: [Search Bar] subscribe

GNSS OEM UAV Survey Mapping Transportation Defense Mobile Machine Control/Ag More

Trimble, Qualcomm partner on connected vehicle positioning

September 26, 2019 - By Tracy Lazzaris 0 Comments Estimated time: 1:00

Companies aim to provide sub-lane-level accuracy to automotive OEMs and Tier 1 suppliers

Trimble and Qualcomm Technologies, a subsidiary of Qualcomm Inc., will be working together to produce precise-positioning solutions for select automotive applications.

Trimble will work with Qualcomm Technologies to integrate Trimble's RTX technology with select Qualcomm Snapdragon Automotive 4G and 5G platforms to deliver a highly accurate positioning solution essential for maintaining absolute in-lane positioning.

Image: Trimble

The new solution will accelerate the adoption of multi-level navigation and emergency services applications, as well as safety requirements for developing advanced driver-assistance systems (ADAS) and autonomous driving solutions.

The Snapdragon 4G and 5G automotive platforms feature integrated multi-frequency and multi-constellation high-precision GNSS technology. They also support all major global and regional GNSS satellite constellations including GPS, GLONASS, Galileo, BeiDou, and QZSS, operating concurrently in the L1, L2, and L5 frequency bands, including a precise positioning framework.

The framework ensures consistency in access and use of precise positioning information and incorporates the use of GNSS correction technology.

Tight integration of GNSS functionality in conjunction with the modern reception of the correction allows for minimum latencies and optimal performance of the precise-positioning solution from the telematics system and provides automakers with a global location platform to meet the requirements of next-generation vehicles.

Take the pulse of the GNSS market

Read the GSA GNSS Market Report now

DOWNLOAD

2019 edition just released

USA GNSS Market Report

LINKING SPACE TO YOUR NEEDS

GPS World, Trimble, Qualcomm partner on connected vehicle positioning, September 26, 2019 (<https://www.gpsworld.com>)

Faster Convergence for PPP-AR

PPP-RTK

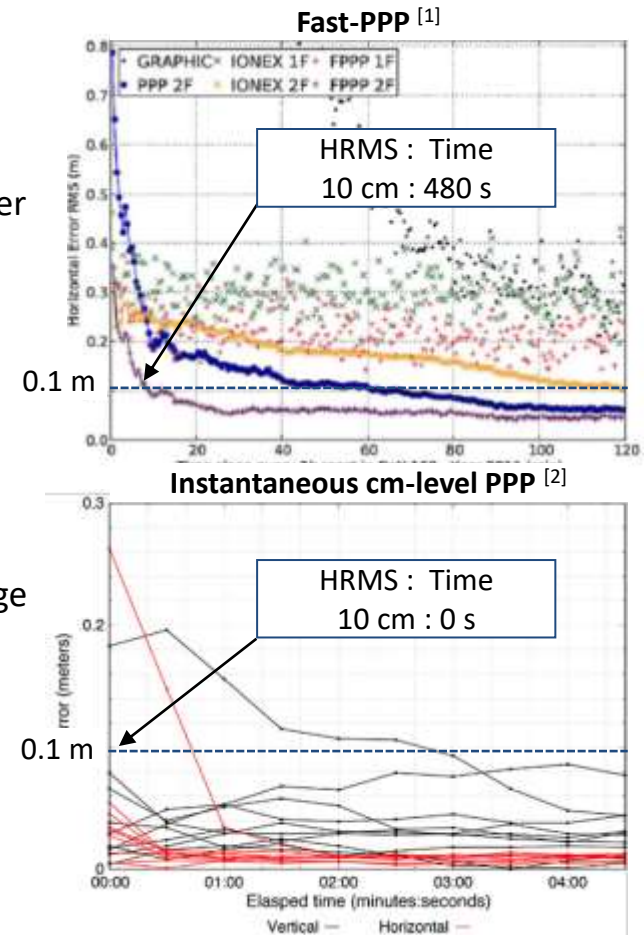
- PPP-AR with local STEC and troposphere corrections
- High bandwidth required to support broad coverage larger than nation-wide
- Dense CORS N/W required for local corrections
- Supported by CLAS and some commercial PPP services

Fast-PPP [1]

- PPP-AR with global VTEC corrections
- Multi-layer model for global VTEC model
- Low bandwidth to transmit corrections for global coverage

Instantaneous cm-level PPP [2]

- No local or global TEC corrections
- Cascading PPP-AR with triple or quad frequencies (L1-L2-L5, E1-E5a-E5b-E6)



- [1] A. R. Garcia et al., A worldwide ionospheric model for fast precise point positioning, IEEE Transaction on Geoscience and Remote Sensing, 2015
- [2] D. Laurichesse and S. Banville, Innovation: Instantaneous centimeter-level multi-frequency precise point positioning, GPS World, 2018

QZSS L6 (1)

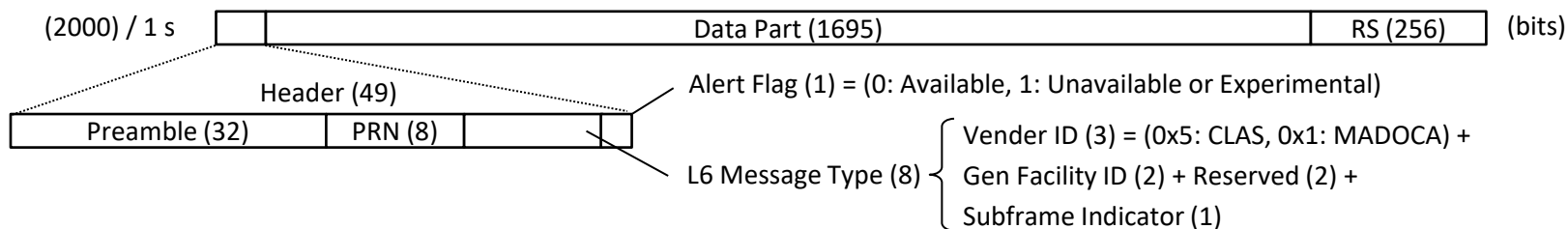
QZSS L6 Signal Specifications

Satellite	QZS-1 (Block I)		QZS-2, 3, 4 (Block II)	
Carrier Frequency	1278.75 MHz		1278.75 MHz	
Modulation	BPSK(5), TDM		BPSK(5), TDM	
Min Received Power	- 155.7 dBW		- 156.82 dBW	
Component	Data	Pilot	Data	Data
PRN number	193	193	194 ~ 197 (QZO) 199 ~ 201 (GEO)	204 ~ 207 (QZO) 209 ~ 211 (GEO)
Chip Rate	2.5575 Mcps	2.5575 Mcps	2.5575 Mcps	2.5575 Mcps
Code Length	4 ms	410 ms	4 ms	4 ms
Data	L6D	-	L6D	L6E
Data Modulation	CSK (8 bit/sym)	-	CSK (8 bit/sym)	CSK (8 bit/sym)
Symbol Rate	250 sym/s	-	250 sym/s	250 sym/s
Data Rate	2 kbps	-	2 kbps	2 kbps
Frame Length	2000 bits	-	2000 bits	2000 bits
Frame Rate	1 frame/s	-	1 frame/s	1 frame/s
FEC	RS(255,223)	-	RS(255,223)	RS(255,223)
Contents	CLAS	-	CLAS	MADOCA
Status	Available (2018/11/1~)	-	Available (2018/11/1~)	Experimental (2019/10)

IS-QZSS-L6-001, Quasi-Zenith Satellite System Interface Specification Centimeter Level Augmentation Service, Nov 5, 2018

QZSS L6 (2)

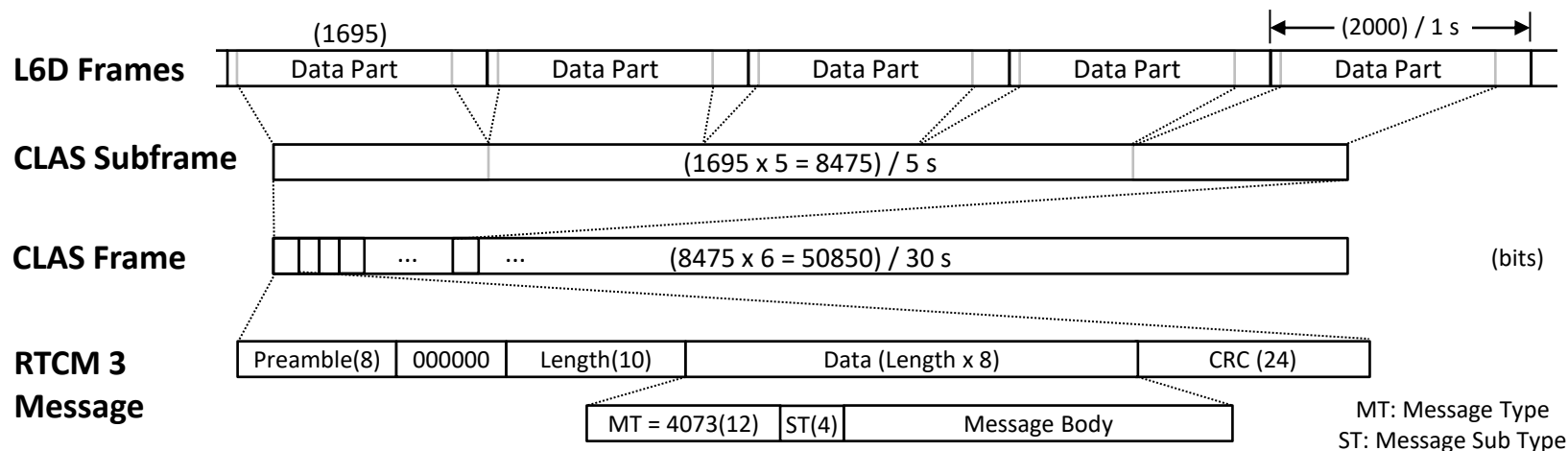
QZSS L6 L6D, L6E Frame



	CLAS	MADOCA
Positioning Mode	PPP-RTK	PPP
Service Area	Japanese Island	All areas covered by QZSS
Accuracy	H: < 6 cm, V: < 12 cm (static, 95%) H: < 12 cm, V: < 24 cm (kinematic, 95%)	Not Specified
TTFF/Convergence Time	< 60 s (95%)	Not Specified
Target GNSS (Signals) *1	GPS (L1C/A, L2P(Y), L2C, L5), GAL (E1, E5a), QZS (L1C/A, L2C, L5)	GPS (L1C/A, L2P(Y)), GLO (L1C/A, L2P), QZS-1 (?)
Corrections	Mask, Orbit Correction, Clock Correction, Code Bias, Phase Bias, URA, STEC Correction, Gridded Correction	Orbit Correction, High-Rate Clock Correction, Code Bias, URA
Format	Compact SSR (CSSR) on RTCM 3 Proprietary (MT 4073)	RTCM 3 SSR + Draft SSR (w/o preamble, length, CRC)

*1 in October 2019

Compact SSR (CSSR)

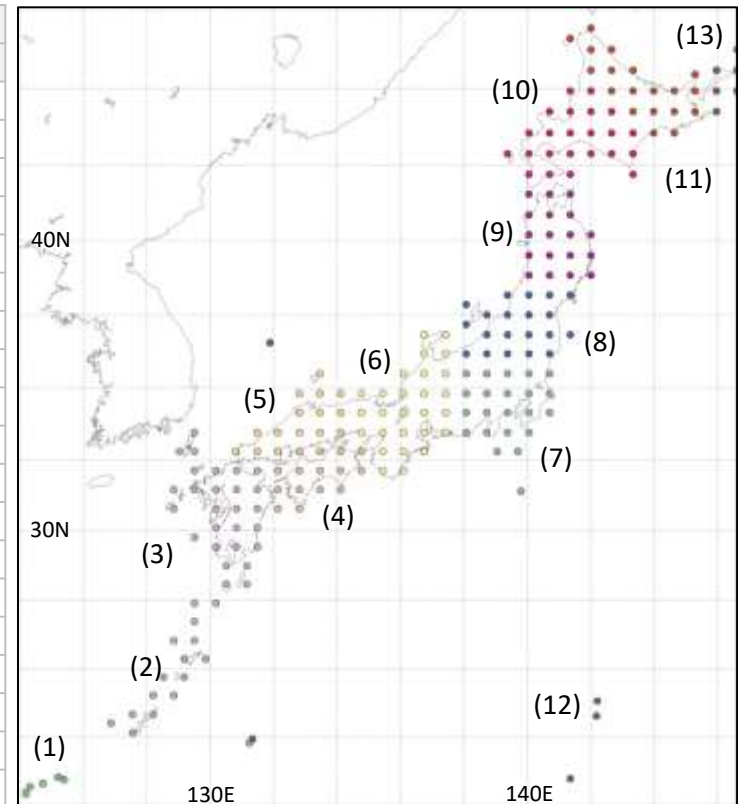


RTCM 3 Message	MT	ST	Contents
Compact SSR Mask	4073	1	Satellite Mask, Cell Mask, Signal Mask
Compact SSR Orbit Corrections	4073	2	IODE, Delta-Orbit (Radial, Along-Track, Cross-Track)
Compact SSR Clock Corrections	4073	3	Delta-Clock C0
Compact SSR Code Bias	4073	4	Code Bias
Compact SSR Phase Bias	4073	5	Phase Bias, Phase Discount. Indicator.
Compact SSR Code and Phase Bias	4073	6	Code Bias, Phase Bias, Phase Discount. Indicator, (N/W ID, N/W SV Mask)
Compact SSR URA	4073	7	URA
Compact SSR STEC Correction	4073	8	STEC Quality Indicator, Polynomial Coefficients, N/W ID, N/W SV Mask
Compact SSR Gridded Correction	4073	9	(Tropos. Hydro-Static Vertical Delay, Tropos. Wet Vertical Delay), STEC Residual Correction, N/W ID, N/W SV Mask, # of Grids
CLAS Service Information	4073	10	TBD
Compact SSR GNSS Combined Correction	4073	11	IODE, Delta-Orbit (Radial, Along-Track, Cross-Track), Delta-Clock C0

[1] IS-QZSS-L6-001 Quasi-Zenith Satellite System Interface Specification Centimeter Level Augmentation Service, November 5, 2018

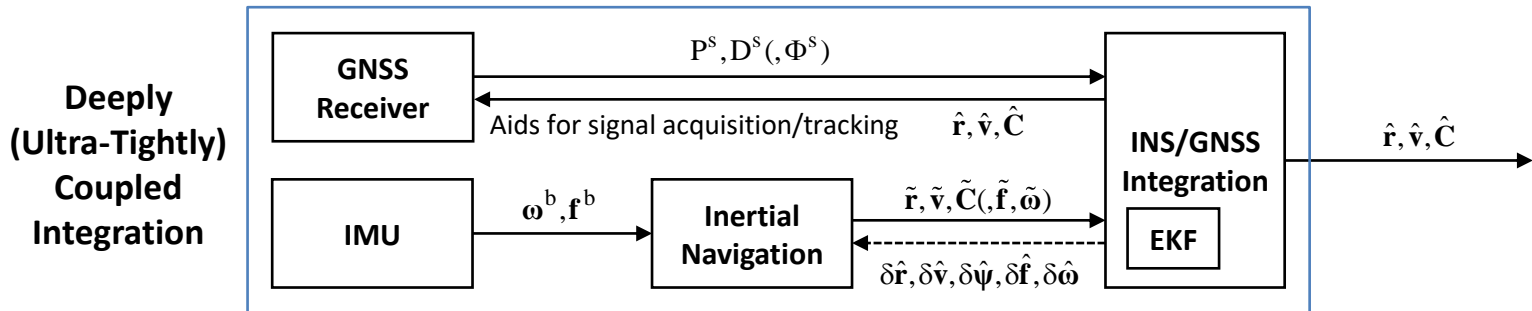
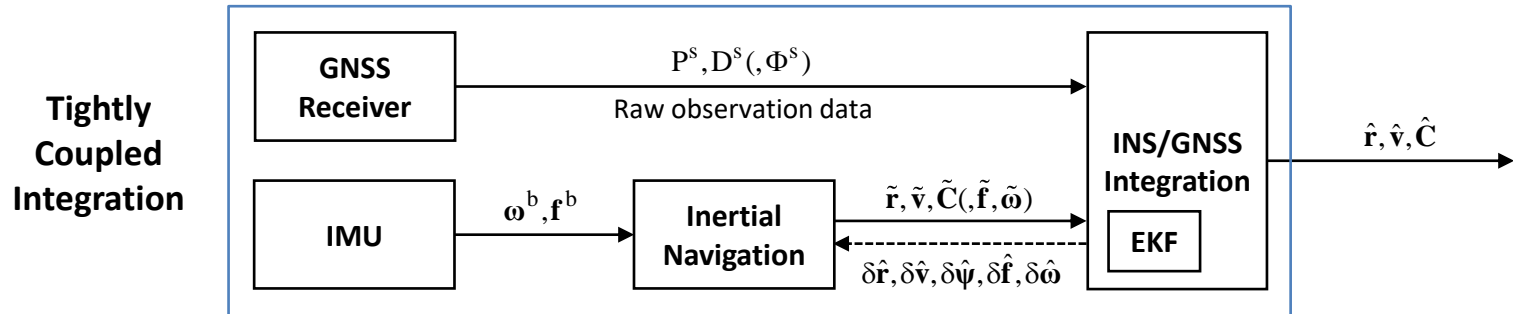
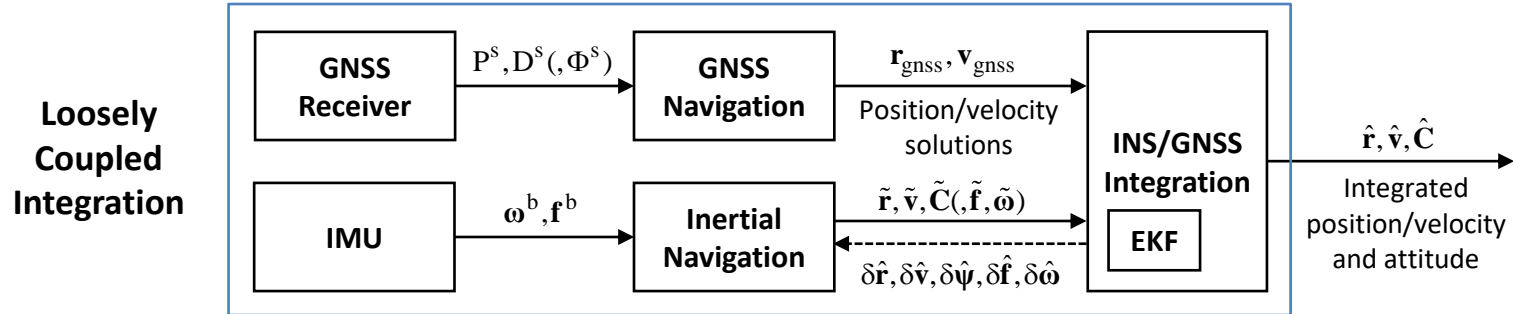
CSSR Networks and Grids

N/W ID	N/W	# of Grids	Area	
			Latitude (deg)	Longitude (deg)
1	Ishigaki	8	24.06 - 24.83 N	122.94 - 125.37 E
2	Okinawa	11	25.83 - 28.30 N	126.87 - 131.23 E
3	Kyusyu	32	28.84 - 34.77 N	128.84 - 131.47 E
4	Shikoku	15	32.62 - 34.23 N	132.13 - 134.76 E
5	Chugoku	15	34.23 - 36.39 N	130.82 - 134.11 E
6	Kansai	27	34.23 - 37.47 N	134.76 - 137.40 E
7	Kanto	22	33.11 - 36.39 N	138.05 - 140.69 E
8	Tohoku South	20	36.93 - 38.55 N	138.05 - 141.34 E
9	Tohoku North	18	39.09 - 41.24 N	140.03 - 142.00 E
10	Hokkaido West	23	41.78 - 43.94 N	139.37 - 143.32 E
11	Hokkaido East	19	42.86 - 45.55 N	141.34 - 145.29 E
12	Ogasawara	2	26.64 - 27.07 N	142.16 - 142.20 E
13	Hokkaido Island	13	43.40 - 45.55 N	145.95 - 149.24 E
14	Island	1	37.24 N	131.87 E
15	Island	1	25.96 N	131.31 E
16	Island	1	25.73 N	123.54 E
17	Island	1	24.77 N	141.34 E
18	Island	1	24.28 N	153.99 E
19	Island	1	20.44 N	136.09 E



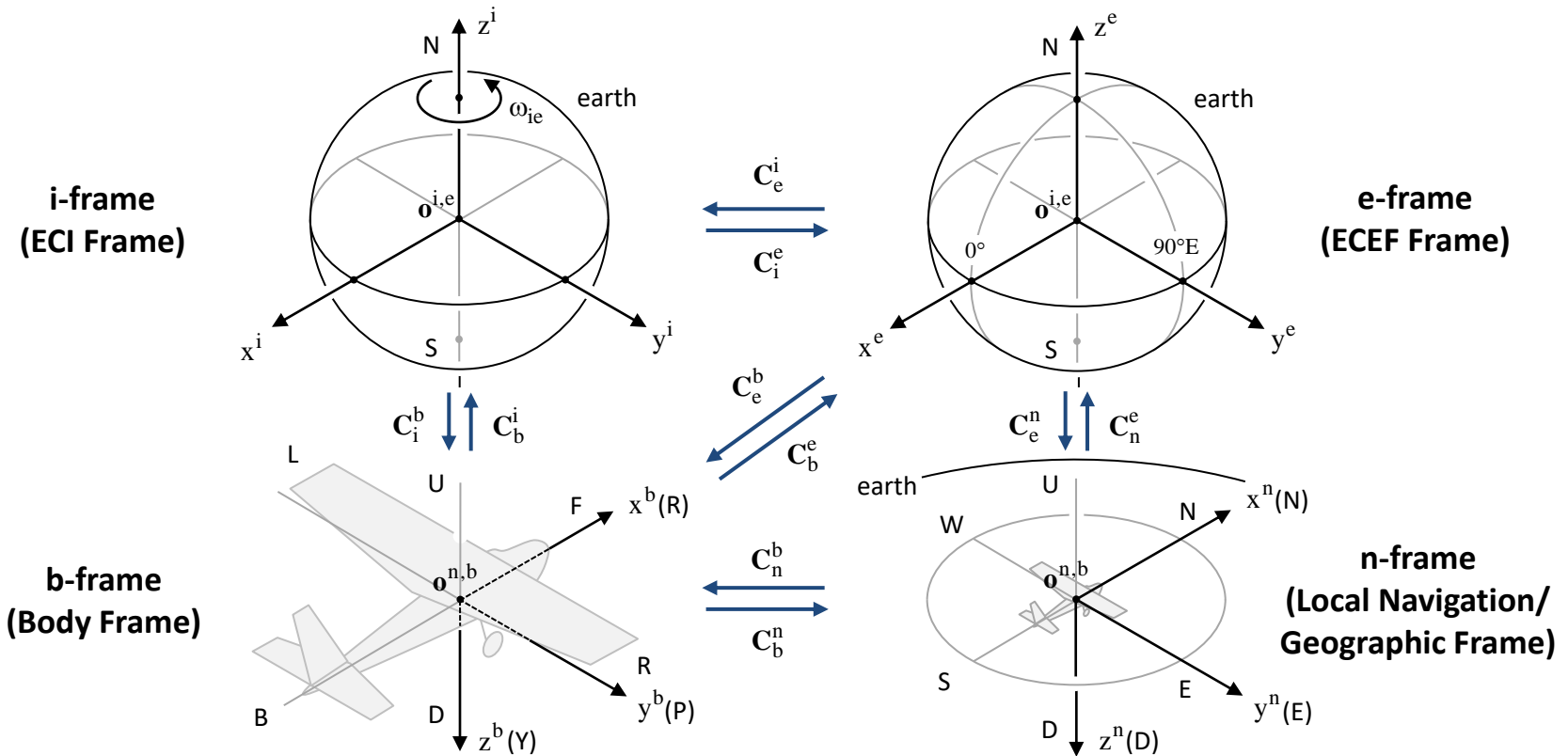
[1] IS-QZSS-L6-001 Quasi-Zenith Satellite System Interface Specification Centimeter Level Augmentation Service, November 5, 2018

INS/GNSS Integration Architecture



$\leftarrow \text{-----}$: Closed-loop INS/GNSS integration

Coordinate Frames



Frame Transformations

$$C_i^e = \mathbf{R}_z(\omega_{ie}(t - t_0)), C_e^n = \mathbf{R}_y(-\pi/2 - L_{en})\mathbf{R}_z(\lambda_{en}), C_n^b = \mathbf{R}_x(\phi_{nb})\mathbf{R}_y(\theta_{nb})\mathbf{R}_z(\psi_{nb}),$$

$$C_e^b = C_n^b C_e^n, C_i^b = C_e^b C_i^e, C_e^i = C_i^{eT}, C_n^e = C_e^{nT}, C_b^n = C_n^{bT}, C_b^e = C_e^{bT}, C_b^i = C_i^{bT}$$

C_β^α : Transformation from β -frame to α -frame
 $o^{i,e}$: i- and e-frame origin (earth mass center)
 $o^{n,b}$: n- and b-frame origin

ω_{ie} : Earth rotation rate (rad/s)
 L_{en} : Latitude of n- and b-frame origin (rad)
 λ_{en} : Longitude of n- and b-frame origin (rad)

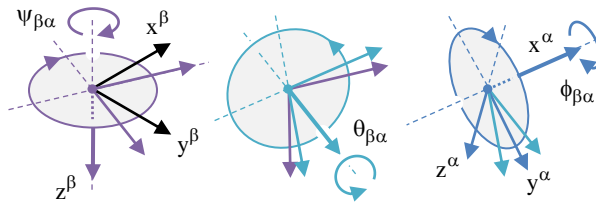
ϕ_{nb} : Roll angle of b- wrt n-frame (rad)
 θ_{nb} : Pitch angle of b- wrt n-frame (rad)
 ψ_{nb} : Yaw angle of b- wrt n-frame (rad)

Attitudes and Rotations

(1) Euler Angles/Attitude

$$\Psi_{\beta\alpha} = (\phi_{\beta\alpha}, \theta_{\beta\alpha}, \psi_{\beta\alpha})^T$$

$\phi_{\beta\alpha}, \theta_{\beta\alpha}, \psi_{\beta\alpha}$: Roll, Pitch and Yaw angles of α -frame wrt β -frame

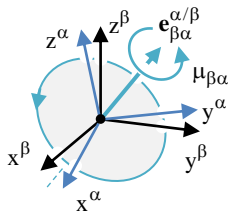


$$(1) \text{ to } (2) : \mathbf{C}_{\beta}^{\alpha} = \mathbf{R}_x(\phi_{\beta\alpha})\mathbf{R}_y(\theta_{\beta\alpha})\mathbf{R}_z(\psi_{\beta\alpha})$$

(3) Rotation Vector

$$\rho_{\beta\alpha}^{\alpha/\beta} = \mu_{\beta\alpha} \mathbf{e}_{\beta\alpha}^{\alpha/\beta}$$

$\mu_{\beta\alpha}$: Rotation angle of α -frame wrt β -frame
 $\mathbf{e}_{\beta\alpha}^{\alpha/\beta}$: Unit vector of rotation axis



(3) to (4) :

$$\mathbf{q}_{\beta}^{\alpha} = \begin{pmatrix} \cos(\mu_{\beta\alpha}/2) \\ \mathbf{e}_{\beta\alpha}^{\alpha/\beta} \sin(\mu_{\beta\alpha}/2) \end{pmatrix}$$

Note:
The $\mathbf{e}_{\beta\alpha}^{\alpha/\beta}$ is one of the eigenvectors of the $\mathbf{C}_{\beta}^{\alpha}$

$\mathbf{x}_{\beta\alpha}^{\gamma}$: \mathbf{x} of α -frame wrt β -frame expressed in γ -frame axes

$$\mathbf{R}_x(\theta) = \begin{pmatrix} 1 & 0 & 0 \\ 0 & \cos\theta & \sin\theta \\ 0 & -\sin\theta & \cos\theta \end{pmatrix}, \mathbf{R}_y(\theta) = \begin{pmatrix} \cos\theta & 0 & -\sin\theta \\ 0 & 1 & 0 \\ \sin\theta & 0 & \cos\theta \end{pmatrix}, \mathbf{R}_z(\theta) = \begin{pmatrix} \cos\theta & \sin\theta & 0 \\ -\sin\theta & \cos\theta & 0 \\ 0 & 0 & 1 \end{pmatrix}, \boldsymbol{\Omega} = (\boldsymbol{\omega} \times) = \begin{pmatrix} 0 & -\omega_z & \omega_y \\ \omega_z & 0 & -\omega_x \\ -\omega_y & \omega_x & 0 \end{pmatrix} : \text{Skew-symmetric matrix of angular rate vector } \boldsymbol{\omega} = (\omega_x, \omega_y, \omega_z)^T$$

(2) DCM/CTM

$$\mathbf{C}_{\beta}^{\alpha} = \begin{pmatrix} c_{11} & c_{12} & c_{13} \\ c_{21} & c_{22} & c_{23} \\ c_{31} & c_{32} & c_{33} \end{pmatrix}$$

$\mathbf{C}_{\beta}^{\alpha}$: Transformation from β -frame to α -frame

(1) to (2)

(2) to (1)

(2) to (3) (4) to (2)

$$(2) \text{ to } (1) : \Psi_{\beta\alpha} = \begin{pmatrix} \text{ATAN2}(c_{23}, c_{33}) \\ -\arcsin(c_{13}) \\ \text{ATAN2}(c_{12}, c_{11}) \end{pmatrix}$$

$$\mu_{\beta\alpha} = \arccos(1/2(c_{11} + c_{22} + c_{33} - 1))$$

$$(2) \text{ to } (3) : \mathbf{e}_{\beta\alpha}^{\alpha/\beta} = \frac{1}{2\sin\mu_{\beta\alpha}} \begin{pmatrix} c_{23} - c_{32} \\ c_{31} - c_{13} \\ c_{12} - c_{21} \end{pmatrix}$$

(4) Quaternion

$$\mathbf{q}_{\beta}^{\alpha} = (q_0, q_1, q_2, q_3)^T$$

$$(q_0^2 + q_1^2 + q_2^2 + q_3^2 = 1)$$

(4) to (2) :

$$\mathbf{C}_{\beta}^{\alpha} = \begin{pmatrix} q_0^2 + q_1^2 - q_2^2 - q_3^2 & 2(q_1q_2 + q_3q_0) & 2(q_1q_3 - q_2q_0) \\ 2(q_1q_2 - q_3q_0) & q_0^2 - q_1^2 + q_2^2 - q_3^2 & 2(q_2q_3 + q_1q_0) \\ 2(q_1q_3 + q_2q_0) & 2(q_2q_3 - q_1q_0) & q_0^2 - q_1^2 - q_2^2 + q_3^2 \end{pmatrix}$$

IMU (Inertial Measurement Unit)

Gyroscopes

Mechanical: RIG (rate integrating gyro), DTG (dynamically tuned gyro), ...
 Vibratory: HRG (hemispherical resonator gyro), Wine grass resonator, ...
 Optical: RLG (ring laser gyro), FOG (fiber optic gyro), ...

Accelerometers

Mechanical: Force-feedback pendulous accelerometer, Vibrating beam, ...
 Solid-state: Silicon sensors, Optical accelerometers, ...



Apollo IMU [2]

IMU Vendors [1]



Gyro Bias Stability - IMU Grades [1]

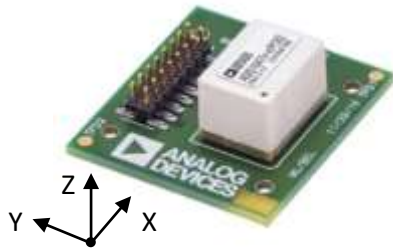


[1] Yole Development, High-end gyroscopes, accelerometers and IMUs for defense, aerospace & industrial, 2015

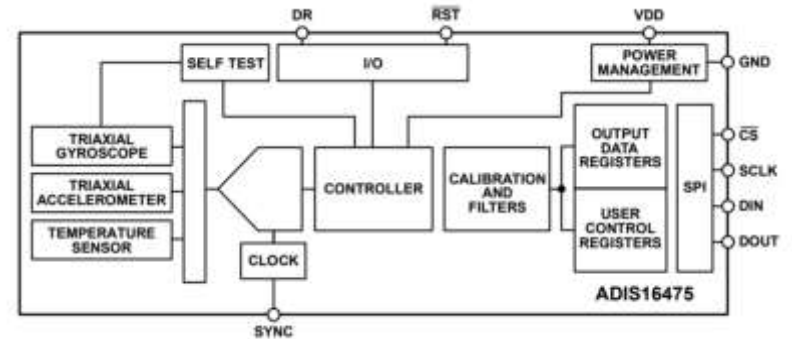
[2] https://en.wikipedia.org/wiki/Inertial_measurement_unit

MEMS IMU

ADI ADIS16475-1 [1]



Triaxial Gyro: +/- 125 deg/s
 Triaxial Accelerometer: +/- 8 g
 Size: 11 x 15 x 11 mm
 Factory Calibrated Bias, Alignment
 Sample Price: \$499.87 (Digi-key)



Specifications [2]

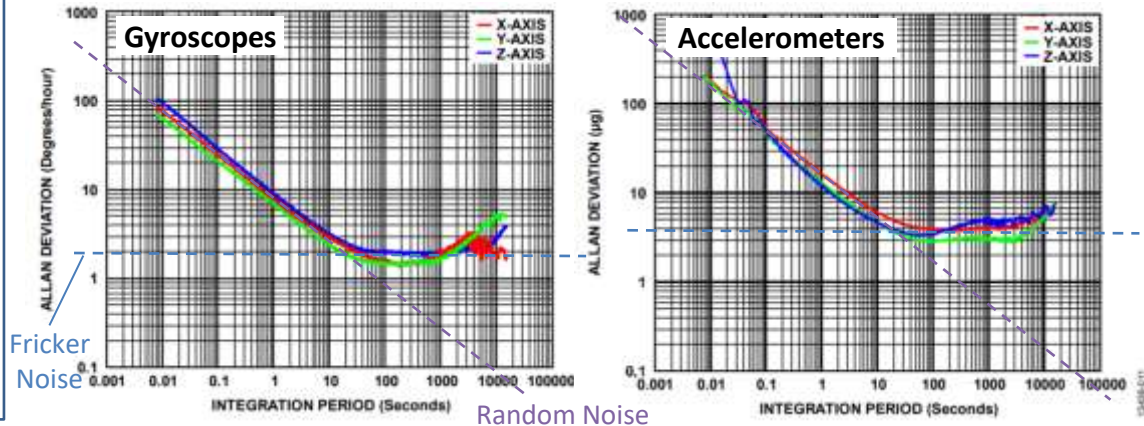
Gyroscopes

Misalignment Error : +/- 0.1°
 Nonlinearity : 0.2 % FS
 In-Run Bias Stability : 2 °/hr
 Angular Random Walk : 0.15 °/√hr

Accelerometers

Misalignment Error : +/- 0.05°
 Nonlinearity (+/- 2g) : 0.25 % FS
 In-Run Bias Stability : 3.6 μg
 Velocity Random Walk : 0.012 m/s/√hr

Gyro/Accelerometer Bias Stability [2]



Expected Position Error due to IMU Noise (t = 60 s, v = 60 km/h)

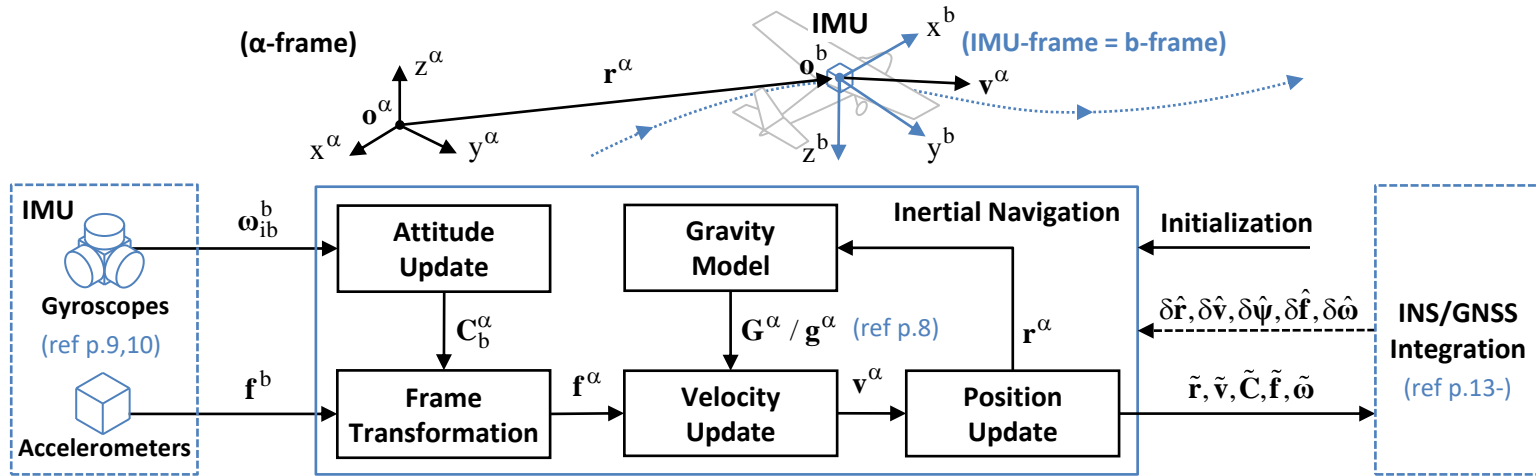
Cross-Track: $(2 \times \pi / 180 / 3600 \times 60 / 2) \times (60 \times 10^3 / 3600 \times 60) = 0.291 \text{ (m)}$ Along-Track: $(3.6 \times 10^{-6} \times 9.8) \times 60^2 / 2 = 0.064 \text{ (m)}$
 gyro stability (rad/s) time (s) distance (m) accelerometer stability (m/s²) time (s)

[1] <https://www.analog.com/en/products/adis16475.html>

[2] Analog Devices, Precision, Miniature MEMs IMU ADIS16475 Data Sheet, Rev.C, 2019

Inertial Navigation

Strapdown Inertial Navigation



Attitude, velocity and position update in i-frame

$$C_b^i(t + \tau) = C_b^i(t) \exp\left(\left((\omega_{ib}^b - \delta\omega) \times\right) \tau\right) \quad (\text{ref p.7})$$

$$f^i = \frac{1}{2} \left(C_b^i(t) + C_b^i(t + \tau) \right) (f^b - \delta f)$$

$$v^i(t + \tau) = v^i(t) + \left(f^i + G^i(r^i(t)) \right) \tau \quad (\text{acceleration})$$

$$r^i(t + \tau) = r^i(t) + \frac{1}{2} \left(v^i(t) + v^i(t + \tau) \right) \tau$$

Attitude, velocity and position update in e-frame

$$C_b^e(t + \tau) = C_b^e(t) \exp\left(\left((\omega_{ib}^b - \delta\omega - C_b^e(t)^T \omega_{ie}^e) \times\right) \tau\right) \quad (\text{earth rotation})$$

$$f^e = \frac{1}{2} \left(C_b^e(t) + C_b^e(t + \tau) \right) (f^b - \delta f)$$

$$v^e(t + \tau) = v^e(t) + \left(f^e + g^e(r^e(t)) - 2\omega_{ie}^e \times v^e(t) \right) \tau \quad (\text{Coriolis force})$$

$$r^e(t + \tau) = r^e(t) + \frac{1}{2} \left(v^e(t) + v^e(t + \tau) \right) \tau$$

r^α : Position in α -frame(m)

v^α : Velocity in α -frame (m/s)

C_b^α : Transformation from b- to α -frame

ω_{ib}^b : Angular rate measurement (rad/s)

f^b : Specific force measurement (m/s^2)

f^α : Specific force in α -frame (m/s^2)

δf : Accelerometer bias (m/s^2)

$\delta\omega$: Gyro bias (rad/s)

G^α : Gravitational acceleration (m/s^2)

g^α : Acceleration due to gravity (m/s^2)

ω_{ie}^e : Earth rotation vector (rad/s)

τ : Update interval (s)

INS/GNSS Integration (1)

State Vector and their Propagation in e-frame

$$\mathbf{x}_{\text{ins}} = (\delta\mathbf{r}^T, \delta\mathbf{v}^T, \delta\psi^T, \delta\mathbf{f}^T, \delta\boldsymbol{\omega}^T)^T$$

$$\dot{\mathbf{x}}_{\text{ins}} = \begin{pmatrix} \mathbf{0} & \mathbf{I} & \mathbf{0} & \mathbf{0} & \mathbf{0} \\ \partial\mathbf{g}^e/\partial\mathbf{r}^e & -2\boldsymbol{\Omega}_{ie}^e & -(\mathbf{C}_b^e\mathbf{f}^b)\times & \mathbf{C}_b^e & \mathbf{0} \\ \mathbf{0} & \mathbf{0} & -\boldsymbol{\Omega}_{ie}^e & \mathbf{0} & \mathbf{C}_b^e \\ \mathbf{0} & \mathbf{0} & \mathbf{0} & \mathbf{0} & \mathbf{0} \\ \mathbf{0} & \mathbf{0} & \mathbf{0} & \mathbf{0} & \mathbf{0} \end{pmatrix} \mathbf{x}_{\text{ins}} + \mathbf{q}_{\text{ins}}$$

$$\mathbf{r}^e = \tilde{\mathbf{r}}^e - \delta\mathbf{r}, \mathbf{v}^e = \tilde{\mathbf{v}}^e - \delta\mathbf{v}$$

$$\mathbf{f}^b = \tilde{\mathbf{f}}^b - \delta\mathbf{f}, \boldsymbol{\omega}_{ib}^b = \tilde{\boldsymbol{\omega}}_{ib}^b - \delta\boldsymbol{\omega}$$

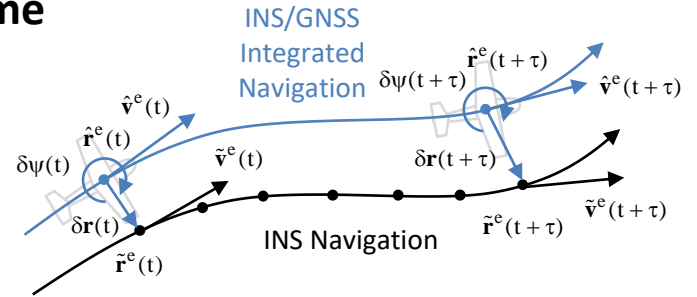
$$\mathbf{C}_b^e = (\mathbf{I} - (\delta\psi\times))\tilde{\mathbf{C}}_b^e$$

State Transition and Process Noise Matrix

$$\Phi_{\text{ins}} \approx \begin{pmatrix} \mathbf{I} & \mathbf{I}\tau & \mathbf{0} & \mathbf{0} & \mathbf{0} \\ \partial\mathbf{g}^e/\partial\mathbf{r}^e\tau & \mathbf{I} - 2\boldsymbol{\Omega}_{ie}^e\tau & -(\mathbf{C}_b^e\mathbf{f}^b)\times\tau & \mathbf{C}_b^e\tau & \mathbf{0} \\ \mathbf{0} & \mathbf{0} & \mathbf{I} - \boldsymbol{\Omega}_{ie}^e\tau & \mathbf{0} & \mathbf{C}_b^e\tau \\ \mathbf{0} & \mathbf{0} & \mathbf{0} & \mathbf{I} & \mathbf{0} \\ \mathbf{0} & \mathbf{0} & \mathbf{0} & \mathbf{0} & \mathbf{I} \end{pmatrix} \quad (\text{1st-order approx.})^*$$

$$\mathbf{Q}_{\text{ins}} \approx \text{blkdiag}(\mathbf{0}, \sigma_a^2\mathbf{I}, \sigma_g^2\mathbf{I}, \sigma_{ab}^2\mathbf{I}, \sigma_{gb}^2\mathbf{I})\tau$$

* To minimize the integration error in high-dynamic environment with fast attitude change, high-order approximation or finer step integration is desirable to generate a precise state transition matrix.



$\delta\mathbf{r}$: INS position error in e-frame (m)

$\delta\mathbf{v}$: INS velocity error in e-frame (m/s)

$\delta\psi$: INS attitude error in e-frame (rad)

$\delta\mathbf{f}$: Accelerometer bias (m/s²)

$\delta\boldsymbol{\omega}$: Gyro bias (rad/s)

$\tilde{\mathbf{r}}^e$: INS position in e-frame (m)

$\tilde{\mathbf{v}}^e$: INS velocity in e-frame (m/s)

$\tilde{\mathbf{C}}_b^e$: INS attitude in e-frame

$\tilde{\boldsymbol{\omega}}_{ib}^b$: INS angular rate measurement (rad/s)

$\tilde{\mathbf{f}}^b$: INS specific force measurement (m/s²)

\mathbf{r}^e : Corrected position in e-frame (m)

\mathbf{v}^e : Corrected velocity in e-frame (m/s)

\mathbf{C}_b^e : Corrected attitude in e-frame

$\boldsymbol{\omega}_{ib}^b$: Corrected angular rate (rad/s)

\mathbf{f}^b : Corrected specific force (m/s²)

σ_a : Std-dev of accelerometer noise (m/s²)

σ_g : Std-dev of gyro noise (rad/s)

σ_{ab} : Std-dev of accelerometer bias (m/s²)

σ_{gb} : Std-dev of gyro bias (rad/s)

τ : Update interval of EKF (s)

INS/GNSS Integration (2)

Loosely Coupled Integration in e-frame

$$\mathbf{x} = \mathbf{x}_{\text{ins}} = (\delta\mathbf{r}^T, \delta\mathbf{v}^T, \delta\boldsymbol{\psi}^T, \delta\mathbf{f}^T, \delta\boldsymbol{\omega}^T)^T$$

Time Update of EKF

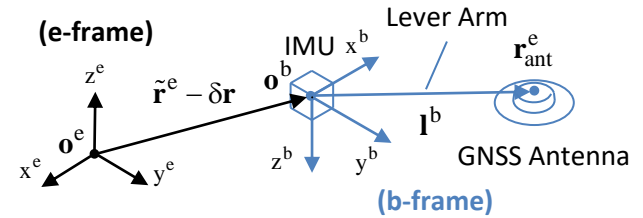
$$\hat{\mathbf{x}}_k^- = \boldsymbol{\Phi}_k \hat{\mathbf{x}}_{k-1}^+, \mathbf{P}_k^- = \boldsymbol{\Phi}_k \mathbf{P}_{k-1}^+ \boldsymbol{\Phi}_k^T + \mathbf{Q}_k \quad (\boldsymbol{\Phi}_k = \boldsymbol{\Phi}_{\text{ins}}, \mathbf{Q}_k = \mathbf{Q}_{\text{ins}})$$

Measurement Update of EKF

$$\mathbf{K}_k = \mathbf{P}_k^- \mathbf{H}_k^T (\mathbf{H}_k \mathbf{P}_k^- \mathbf{H}_k^T + \mathbf{R}_k)^{-1}$$

$$\hat{\mathbf{x}}_k^+ = \hat{\mathbf{x}}_k^- + \mathbf{K}_k (\mathbf{y}_k - \mathbf{h}(\hat{\mathbf{x}}_k^-)), \mathbf{P}_k^+ = (\mathbf{I} - \mathbf{K}_k \mathbf{H}_k) \mathbf{P}_k^-$$

$$\left\{ \begin{array}{l} \mathbf{y}_k = \begin{pmatrix} \mathbf{r}_{\text{gnss}} \\ \mathbf{v}_{\text{gnss}} \end{pmatrix}, \mathbf{R}_k = \begin{pmatrix} \mathbf{Q}_r & \\ & \mathbf{Q}_v \end{pmatrix} \\ \mathbf{h}(\mathbf{x}) = \begin{pmatrix} \mathbf{r}_{\text{ant}}^e \\ \mathbf{v}_{\text{ant}}^e \end{pmatrix}, \mathbf{H}_k = \begin{pmatrix} -\mathbf{I} & \mathbf{0} & (\delta\mathbf{r}_{\text{ant}} \times) & \mathbf{0} & \mathbf{0} \\ \mathbf{0} & -\mathbf{I} & (\delta\mathbf{v}_{\text{ant}} \times) & \mathbf{0} & \mathbf{C}_b^e (\mathbf{I}^b \times) \end{pmatrix} \\ \mathbf{C}_b^e = (\mathbf{I} - (\delta\boldsymbol{\psi} \times)) \tilde{\mathbf{C}}_b^e \\ \delta\mathbf{r}_{\text{ant}} = \mathbf{C}_b^e \mathbf{I}^b \\ \delta\mathbf{v}_{\text{ant}} \approx \mathbf{C}_b^e ((\tilde{\boldsymbol{\omega}}_{ib}^b - \delta\boldsymbol{\omega}) \times \mathbf{I}^b) \\ \mathbf{r}_{\text{ant}}^e = \tilde{\mathbf{r}}^e - \delta\mathbf{r} + \delta\mathbf{r}_{\text{ant}} \\ \mathbf{v}_{\text{ant}}^e = \tilde{\mathbf{v}}^e - \delta\mathbf{v} + \delta\mathbf{v}_{\text{ant}} \end{array} \right.$$



- $\tilde{\mathbf{r}}^e$: INS position in e-frame (m)
- $\tilde{\mathbf{v}}^e$: INS velocity in e-frame (m/s)
- $\tilde{\mathbf{C}}_b^e$: INS attitude in e-frame
- $\tilde{\boldsymbol{\omega}}_{ib}^b$: INS angular rate measurement (rad/s)
- $\tilde{\mathbf{f}}^b$: INS specific force measurement (m/s²)
- $\delta\mathbf{r}$: INS position error in e-frame (m)
- $\delta\mathbf{v}$: INS velocity error in e-frame (m/s)
- $\delta\boldsymbol{\psi}$: INS attitude error in e-frame (rad)
- $\delta\mathbf{f}$: Accelerometer bias (m/s²)
- $\delta\boldsymbol{\omega}$: Gyro bias (rad/s)
- \mathbf{I}^b : Lever-arm vector in b-frame (m)
- $\mathbf{r}_{\text{ant}}^e$: Antenna position in e-frame (m)
- $\mathbf{v}_{\text{ant}}^e$: Antenna velocity in e-frame (m/s)
- \mathbf{r}_{gnss} : GNSS position solution (ECEF) (m)
- \mathbf{v}_{gnss} : GNSS velocity solution (ECEF) (m/s)
- \mathbf{Q}_r : VC-matrix of GNSS position solution
- \mathbf{Q}_v : VC-matrix of GNSS velocity solution

Integrated INS/GNSS Performance

Applanix POS LV [1]



PCS (POS computer system) + IMU +
DMI (Distance measurement instrument) +
GNSS (Trimble BD960 and Zephyr II antenna)
Price range: \$100,000 ~ \$200,000

INERTIAL MEASUREMENT UNIT (IMU) [2]

Type	Operational Temperature °C	Models Used In	Maximum Data Rate	Dimensions (L x W x H) mm	Weight kg
IIMU-7 ²	-54 to +71	POSLV 420	200 Hz	158 x 158 x 124	2.5
IMU-17 ²	-40 to +60	POSLV 210/220	100 Hz	158 x 158 x 124	2.5
IMU-21 ¹	-40 to +60	POSLV 610/620	200 Hz	213 x 172 x 172	4.8
IMU-42 ²	-20 to +55	POSLV 210/220	200 Hz	158 x 158 x 124	2.6
IMU-80 ²	-20 to +55	POSLV 510/520	200 Hz	161 x 120 x 126	1.9
IMU-57 ²	-20 to +55	POSLV 610/620	200 Hz	179 x 126 x 127	2.6
IMU-64 ²	-20 to +55	POSLV 420	200 Hz	158 x 158 x 124	2.6
IMU-82 ²	-40 to +65	POSLV 210/220	200 Hz	158 x 158 x 124	2.3

PERFORMANCE SPECIFICATIONS - GNSS OUTAGE, 60 SECONDS* [2]

POS LV	220 PP	220 IARTK	220 DGPS	420 PP	420 IARTK	420 DGPS	510/520 PP	510/520 IARTK	510/520 DGPS	610/620 PP	610/620 IARTK	610/620 DGPS
X,Y Position (m)	0.240	0.690	0.880	0.120	0.340	0.450	0.100	0.300	0.420	0.100	0.280	0.410
Z Position (m)	0.130	0.350	0.610	0.100	0.270	0.560	0.070	0.100	0.530	0.070	0.100	0.510
Roll & Pitch (deg)	0.060	0.060	0.060	0.020	0.020	0.020	0.005	0.008	0.008	0.005	0.005	0.005
True Heading (deg)	0.030	0.070	0.070	0.020	0.030	0.030	0.015	0.020	0.020	0.015	0.020	0.020

* All accuracy values given as RMS. Assumes typical road vehicle dynamics for initialization.

[1] <https://www.applanix.com/products/poslv.htm>

[2] Applanix, POS LV - designed for integration, built for performance - Data Sheet, 2017

Appendix

GNSS Signals (1/3)

System	Carrier Freq (MHz)	Signal	I/Q	Min Received Power (dBW)	Modulation	Spreading Code				Navigation Data			Notes
						Length (chips)	Chip Rate (Mcps)	Overlay Code (chips)	Period (ms)	Data	Bit Rate (bps)	FEC	
GPS [1][2]	1575.42	L1C/A	Q	-158.5	BPSK(1)	1023	1.023	-	1	LNAV	50	-	
		L1P(Y)*1	I	-161.5	BPSK(10)	1week	10.23	-	?	LNAV	50	-	
		L1M	I	?	BOC(10,5)	?	5.115	?	?	?	?	?	Block IIR-M~
		L1C-D	I	-163.0	BOC(1,1)	10230	1.023	-	10	CNAV-2	50	1/2	GPS III~
		L1C-P	I	-158.25	TMBOC(6,1,4/33)	10230	1.023	1800	18000	-	-	-	
	1227.6	L2C/A	Q	-164.5	BPSK(1)	1023	1.023	-	1	LNAV	50	-	Block IIR-M~
		L2P(Y)*1	I	-164.5/-161.5	BPSK(10)	1week	10.23	-	?	LNAV	50	-	
		L2M	I	?	BOC(10,5)	?	5.115	?	?	?	?	?	Block IIR-M~
		L2C-M	Q/I	-160.0/-158.5	BPSK(1), TDM	10230	0.5115	-	20	LNAV	50	-	Block IIR-M~
		L2C-L				767250	0.5115	-	1500	-	-	-	
1176.45	L5-I	I	-157.9/-157.0	BPSK(10)	10230	10.23	10 (NH)	10	CNAV	50	1/2	Block IIF~	
	L5-Q	Q	-157.9/-157.0	BPSK(10)	10230	10.23	20 (NH)	20	-	-	-		
GLONASS [3][4][5][6]	1602.0 + 0.5625K*2	L1C/A	I	-161.0	BPSK	511	0.511	-	1	NAV	50	-	
		L1P	Q	?	BPSK	5110000	5.11	-	1000	?	?	-	
	1600.995	L1OCd	Q	?	BPSK(1), TDM	1023	0.5115	2	4	NAV	125	1/2	GLO-K2~
		L1OCp				4092	2.046	4 (MS)	8	-	-	-	
	1246.0 + 0.4375K*2	L2C/A	I	-167.0	BPSK	511	0.511	-	1	NAV	50	-	
		L2P	Q	?	BPSK	5110000	5.11	-	1000	?	?	-	
	1248.06	L2CSI	Q	?	BPSK(1), TDM	?	0.5115	?	?	?	?	?	GLO-K2~
		L2OCp				10230	0.5115	50	1000	-	-	-	
1202.025	L3OCd	I	?	BPSK(10)	10230	10.23	5 (BC)	5	NAV	100	1/2	GLO-K1~	
	L3OCp	Q	?	BPSK(10)	10230	10.23	10 (NH)	10	-	-	-		

*1 AS ON, *2 K = {-7 ... +6}

[1] IS-GPS-200K, Navstar GPS space segment/navigation user interfaces - interface specification, 2019, [2] IS-GPS-800F, Navstar GPS space segment/user segment L1C interface - interface specification, 2019, [3] GLONASS interface control document - navigation radiosignal in bands L1, L2, version 5.1, 2008, [4] GLONASS interface control document - code division multiple access open service navigation signal in L1 frequency band, edition 1.0, 2016, [5] GLONASS interface control document - code division multiple access open service navigation signal in L2 frequency band, edition 1.0, 2016, [6] GLONASS interface control document - code division multiple access open service navigation signal in L3 frequency band, edition 1.0, 2016

GNSS Signals (2/3)

System	Carrier Freq (MHz)	Signal	I/Q	Min Received Power (dBW)	Modulation	Spreading Code				Navigation Data			Notes
						Length (chips)	Chip Rate (Mcps)	Overlay Code (chips)	Period (ms)	Data	Bit Rate (bps)	FEC	
Galileo [7]	1575.42	E1-A	Q	?	BOC(15,2.5)	?	2.5575	?	?	G/NAV	?	?	PRS
		E1-B	I	-157.0	CBOC(6,1,1/11)	4092	1.023	-	4	I/NAV	125	1/2	OS, SoL, CS
		E1-C	Q		CBOC(6,1,1/11)	4092	1.023	25	100	-	-	-	
	1176.45	E5a-I	I	-155.0	BPSK(10)	10230	10.23	20	20	F/NAV	50	1/2	OS, CS
		E5a-Q	Q		BPSK(10)	10230	10.23	100	100	-	-	-	
	1207.14	E5b-I	I	-155.0	BPSK(10)	10230	10.23	4	4	I/NAV	125	1/2	OS, SoL, CS
		E5b-Q	Q		BPSK(10)	10230	10.23	100	100	-	-	-	
	1191.795	E5a+b*3	-	(-152.0)	8-PSK(10)	10230	10.23	100	100	-	-	-	
	1278.75	E6-A	Q	?	BOC(10,5)	?	5.115	?	?	G/NAV	?	?	PRS
		E6-B	I	-155.0	BPSK(5)	5115	5.115	-	1	C/NAV	500	1/2	CS, HAS
E6-C		Q	BPSK(5)		5115	5.115	100	100	-	-	-		
QZSS [8][9][10][11]	1575.42	L1C/A	I/Q	-158.5*4	BPSK(1)	1023	1.023	-	1	LNAV	50	-	
		L1C-D	I	-163.0*5	BOC(1,1)	10230	1.023	-	10	CNAV2	50	1/2	
		L1C-P	Q	-158.25	BOC(1,1)	10230	1.023	1800	18000	-	-	-	Block I
			I	-158.25*6	TMBOC(6,1,4/33)	10230	1.023	1800	18000	-	-	-	Block II
		L1S	I	-161.0/-158.5	BPSK(1)	1023	1.023	-	1	L1S	250	1/2	SLAS
	1227.6	L2C-M	I	-160.0/-158.5	BPSK(1), TDM	10230	0.5115	-	20	CNAV	25	1/2	
		L2C-L				767250	0.5115	-	1500	-	-	-	
	1176.45	L5-I	I	-157.9/-157.0	BPSK(10)	10230	10.23	10 (NH)	10	CNAV	50	1/2	
		L5-Q	Q	-157.9/-157.0	BPSK(10)	10230	10.23	20 (NH)	20	-	-	-	
		L5S-I	I	-157.0*7	BPSK(10)	10230	10.23	10 (NH)	10	L5S	250	1/2	
		L5S-Q	Q		BPSK(10)	10230	10.23	20 (NH)	20	-	-	-	
	1278.75	L6	I	-155.7	BPSK(5), TDM	10230	2.5575	-	4	L6D	2000	RS	
						1048575	2.5575	-	410	-	-	-	Block I
10230						2.5575	-	4	L6E	2000	RS	Block II	

*3 AltBOC *4 -164.0 dBW (SVID=7), *5 -167.2 dBW (SVID=7), *6 -162.4 dBW (SVID=7), *7 -162.6 dBW (SVID=3)

[7] European GNSS (Galileo) open service signal-in-space interface control document (OS SIS ICD), Issue 1, Revision 3, 2016, [8] Quasi-Zenith satellite system interface specification - satellite positioning, navigation and timing service (IS-QZSS-PNT-003), 2018, [9] Quasi-zenith satellite system interface specification - sub-meter level augmentation service (IS-QZSS-L1S-003), 2018, [10] Quasi-zenith satellite system interface specification - centimeter level augmentation service (IS-QZSS-L6-003), 2018, [11] Quasi-zenith satellite system interface specification - positioning technology verification service (IS-QZSS-TV-002), 2018,

GNSS Signals (3/3)

System	Carrier Freq (MHz)	Signal	I/Q	Min Received Power (dBW)	Modulation	Spreading Code				Navigation Data			Notes
						Length (chips)	Chip Rate (Mcps)	Overlay Code (chips)	Period (ms)	Data	Bit Rate (bps)	FEC	
BeiDou [12][13][14][15]	1561.098	B1I	I	-163.0	BPSK(2)	2046	2.046	20 (NH)	20	D1* ¹⁰	50	BCH	BDS-2* ¹²
		B1Q	Q	?	BPSK(2)	?	2.046	-	1	D2* ¹¹	500	BCH	
	1575.42	B1C-D	I	-159.0/-161.0	BOC(1,1)	10230	1.023	-	10	B-CNAV1	50	1/2	BDS-3
		B1C-P	Q		QMBOC(6,1,4/33)	10230	1.023	1800	18000	-	-	-	
		B1A-D* ⁸	I	?	BOC(14,2)	?	?	?	?	?	50	?	
		B1A-P* ⁸	Q	?	BOC(14,2)	?	?	?	?	?	-	-	
	1207.14	B2I	I	?	BPSK(2)	2046	2.046	20 (NH)	20	D1* ¹⁰	50	BCH	BDS-2
		B2Q* ⁸	Q	?	BPSK(10)	10230	10.23	-	1	D2* ¹¹	500	BCH	
	1176.45	B2a-D	I	-156.0/-158.0	BPSK(10)	10230	10.23	5	5	B-CNAV2	25	1/2	BDS-3
		B2a-P	Q		BPSK(10)	10230	10.23	100	100	-	-	-	
	1207.14	B2b-I	I	?	BPSK(10)	10230	10.23	?	?	?	500	-	BDS-3
		B2b-Q	Q	?	BPSK(10)	10230	10.23	?	?	?	500	-	
	1191.795	B2a+b* ⁹	-	?	8-PSK(10)	10230	10.23	?	?	-	-	-	
	1268.52	B3I	I	-163.0	BPSK(10)	10230	10.23	-	1	D1* ¹⁰	50	BCH	BDS-2* ¹²
		B3Q* ⁸	Q	?	BPSK(10)	?	10.23	?	?	?	?	?	
B3A-D* ⁸		I	?	BPSK(10)	?	10.23	?	?	?	50	?	BDS-3	
B3A-P* ⁸		Q	?	BPSK(10)	?	10.23	?	?	-	-	-		
SBAS	1575.42	L1C/A	I	-	BPSK(1)	1023	1.023	-	1	SBAS	250	1/2	
		L5-I	I	-	BPSK(10)	10230	10.23	10 (NH)	10	SBAS	250	1/2	
	1176.45	L5-Q	Q	-	BPSK(10)	10230	10.23	20 (NH)	20	-	-	-	

*8 Authorized signal, *9 ACE-BOC, *10 IGSO/MEO satellites, *11 GEO satellites *12 B1I and B3I signals are also transmitted by BDS-3

[12] BeiDou navigation satellite system signal in space interface control document - open service signal B1I, version 3, 2019, [13] BeiDou navigation satellite system signal in space interface control document - open service signal B1C, version 1.0, 2017, [14] BeiDou navigation satellite system signal in space interface control document - open service signal B2a, version 1.0, 2017, [15] BeiDou navigation satellite system signal in space interface control document - open service signal B3I, version 1.0, 2018

GNSS Signal ID (1/4)

System	Carrier Frequency (MHz)	Channel or Code	RINEX *								RTCM3 MSM ^[9]	BINEX ^[10]
			2.10 ^[1]	2.11 ^[2]	2.12 ^[3]	3.00 ^[4]	3.01 ^[5]	3.02 ^[6]	3.03 ^[7]	3.04 ^[8]		
GPS	L1/ 1575.42	C/A	C1	C1	CA	1C	1C	1C	1C	1C	2	1
		L1C(D)	-	-	CB	1S	1S	1S	1S	1S	30	6
		L1C(P)	-	-	CB	1L	1L	1L	1L	1L	31	6
		L1C(D+P)	-	-	CB	1X	1X	1X	1X	1X	32	6
		P (AS off)	P1	P1	P1	1P	1P	1P	1P	1P	3	2
		Z-tracking and similar (AS on)	P1	P1	P1	1W	1W	1W	1W	1W	4	3
		Y	-	-	-	1Y	1Y	1Y	1Y	1Y	-	4
		M	-	-	-	1M	1M	1M	1M	1M	-	5
		codeless	-	-	-	1N	1N	1N	1N	1N	-	7
	L2/ 1227.60	C/A	-	-	-	2C	2C	2C	2C	2C	8	11
		L1(C/A)+(P2-P1) (semi-codeless)	P2	P2	C2	2D	2D	2D	2D	2D	-	12
		L2C(M)	-	C2	CC	2S	2S	2S	2S	2S	15	13
		L2C(L)	-	C2	CC	2L	2L	2L	2L	2L	16	14
		L2C(M+L)	-	C2	CC	2X	2X	2X	2X	2X	17	15
		P (AS off)	P2	P2	P2	2P	2P	2P	2P	2P	9	16
		Z-tracking and similar (AS on)	P2	P2	P2	2W	2W	2W	2W	2W	10	17
		Y	-	-	-	2Y	2Y	2Y	2Y	2Y	-	18
		M	-	-	-	2M	2M	2M	2M	2M	-	19
	codeless	-	-	-	2N	2N	2N	2N	2N	-	20	
	L5/ 1176.45	I	-	C5	C5	5I	5I	5I	5I	5I	22	24
Q		-	C5	C5	5Q	5Q	5Q	5Q	5Q	23	25	
I+Q		-	C5	C5	5X	5X	5X	5X	5X	24	26	
GLONASS	G1/ 1602+K*9/16	C/A	C1	C1	CA	1C	1C	1C	1C	1C	2	1
		P	P1	P1	P1	1P	1P	1P	1P	1P	3	2
	G1a/ 1600.995	L1OCd	-	-	-	-	-	-	-	4A	-	-
		L1OCp	-	-	-	-	-	-	-	4B	-	-
		L1OCd+L1OCp	-	-	-	-	-	-	-	4X	-	-

GNSS Signal ID (2/4)

System	Carrier Frequency (MHz)	Channel or Code	RINEX *								RTCM3 MSM ^[9]	BINEX ^[10]
			2.10 ^[1]	2.11 ^[2]	2.12 ^[3]	3.00 ^[4]	3.01 ^[5]	3.02 ^[6]	3.03 ^[7]	3.04 ^[8]		
GLONASS (cont.)	G2/ 1246+K*7/16	C/A (GLONASS-M)	-	C2	CD	2C	2C	2C	2C	2C	8	11
		P	P2	P2	P2	2P	2P	2P	2P	2P	9	12
	G2a/ 1248.06	L2CSI	-	-	-	-	-	-	-	6A	-	-
		L2OCp	-	-	-	-	-	-	-	6B	-	-
		L2CSI+L2OCp	-	-	-	-	-	-	-	6X	-	-
	G3/ 1202.025	I	-	-	-	-	-	3I	3I	3I	-	14
		Q	-	-	-	-	-	3Q	3Q	3Q	-	15
		I+Q	-	-	-	-	-	3X	3X	3X	-	16
	Galileo	E1/ 1575.42	A PRS	-	C1	C1	1A	1A	1A	1A	1A	3
B I/NAV OS/CS/SoL			-	C1	C1	1B	1B	1B	1B	1B	4	2
C			-	C1	C1	1C	1C	1C	1C	1C	2	3
B+C			-	C1	C1	1X	1X	1X	1X	1X	5	4
A+B+C			-	C1	C1	1Z	1Z	1Z	1Z	1Z	6	5
E5a/ 1176.45		I F/NAV OS	-	C5	C5	5I	5I	5I	5I	5I	22	7
		Q no data	-	C5	C5	5Q	5Q	5Q	5Q	5Q	23	8
		I+Q	-	C5	C5	5X	5X	5X	5X	5X	24	9
E5b/ 1207.14		I I/NAV OS/CS/SoL	-	C7	C7	7I	7I	7I	7I	7I	14	11
		Q no data	-	C7	C7	7Q	7Q	7Q	7Q	7Q	15	12
		I+Q	-	C7	C7	7X	7X	7X	7X	7X	16	13
E5a+b/ 1191.795		I	-	C8	C8	8I	8I	8I	8I	8I	18	15
		Q	-	C8	C8	8Q	8Q	8Q	8Q	8Q	19	16
		I+Q	-	C8	C8	8X	8X	8X	8X	8X	20	17
E6/ 1278.75		A PRS	-	C6	C6	6A	6A	6A	6A	6A	9	19
		B C/NAV CS	-	C6	C6	6B	6B	6B	6B	6B	10	20
		C no data	-	C6	C6	6C	6C	6C	6C	6C	8	21
		B+C	-	C6	C6	6X	6X	6X	6X	6X	11	22
		A+B+C	-	C6	C6	6Z	6Z	6Z	6Z	6Z	12	23

GNSS Signal ID (3/4)

System	Carrier Frequency (MHz)	Channel or Code	RINEX *								RTCM3 MSM ^[9]	BINEX ^[10]
			2.10 ^[1]	2.11 ^[2]	2.12 ^[3]	3.00 ^[4]	3.01 ^[5]	3.02 ^[6]	3.03 ^[7]	3.04 ^[8]		
BeiDou	B1-2/ 1561.098	I	-	-	C2	-	2I	1I	2I	2I	2	1
		Q	-	-	C2	-	2Q	1Q	2Q	2Q	3	2
		I+Q	-	-	C2	-	2X	1X	2X	2X	4	3
	B1/ 1575.42 (BDS-3)	Data	-	-	-	-	-	-	-	1D	-	13
		Pilot	-	-	-	-	-	-	-	1P	-	14
		Data+Pilot	-	-	-	-	-	-	-	1X	-	15
		B1A	-	-	-	-	-	-	-	1A	-	-
	B2a/ 1176.45 (BDS-3)	Codeless	-	-	-	-	-	-	-	1N	-	-
		Data	-	-	-	-	-	-	-	5D	-	17
		Pilot	-	-	-	-	-	-	-	5P	-	18
	B2b/ 1207.14 (BDS-2)	Data+Pilot	-	-	-	-	-	-	-	5X	-	19
		I	-	-	C7	-	7I	7I	7I	7I	14	5
		Q	-	-	C7	-	7Q	7Q	7Q	7Q	15	6
	B2b/ 1207.14 (BDS-3)	I+Q	-	-	C7	-	7X	7X	7X	7X	16	7
		Data	-	-	-	-	-	-	-	7D	-	-
		Pilot	-	-	-	-	-	-	-	7P	-	-
	B2a+b/ 1191.795	Data+Pilot	-	-	-	-	-	-	-	7Z	-	-
		Data	-	-	-	-	-	-	-	8D	-	-
		Pilot	-	-	-	-	-	-	-	8P	-	-
	B3/ 1268.52	Data+Pilot	-	-	-	-	-	-	-	8X	-	-
		I	-	-	C6	-	6I	6I	6I	6I	8	9
Q		-	-	C6	-	6Q	6Q	6Q	6Q	9	10	
I+Q		-	-	C6	-	6X	6X	6X	6X	10	11	
	B3A	-	-	-	-	-	-	-	6A	-	-	

GNSS Signal ID (4/4)

System	Carrier Frequency (MHz)	Channel or Code	RINEX *								RTCM3 MSM ^[9]	BINEX ^[10]
			2.10 ^[1]	2.11 ^[2]	2.12 ^[3]	3.00 ^[4]	3.01 ^[5]	3.02 ^[6]	3.03 ^[7]	3.04 ^[8]		
QZSS	L1/ 1575.42	C/A	-	-	-	-	-	1C	1C	1C	2	1
		L1C(D)	-	-	-	-	-	1S	1S	1S	30	2
		L1C(P)	-	-	-	-	-	1L	1L	1L	31	3
		L1C(D+P)	-	-	-	-	-	1X	1X	1X	32	4
		L1-SAIF/L1S	-	-	-	-	-	1Z	1Z	1Z	6	30
	L2/ 1227.60	L2C(M)	-	-	-	-	-	2S	2S	2S	15	8
		L2C(L)	-	-	-	-	-	2L	2L	2L	16	9
		L2C(M+L)	-	-	-	-	-	2X	2X	2X	17	10
	L5/ 1176.45	I	-	-	-	-	-	5I	5I	5I	22	14
		Q	-	-	-	-	-	5Q	5Q	5Q	23	15
		I+Q	-	-	-	-	-	5X	5X	5X	24	16
		L5D (L5S)	-	-	-	-	-	-	-	5D	-	-
		L5P (L5S)	-	-	-	-	-	-	-	5P	-	-
	L5(D+P) (L5S)	-	-	-	-	-	-	-	5Z	-	-	
	L6/ 1278.75	L6D	-	-	-	-	-	6S	6S	6S	9	20
L6P		-	-	-	-	-	6L	6L	6L	10	21	
L6(D+P)		-	-	-	-	-	6X	6X	6X	11	22	
L6E		-	-	-	-	-	-	-	6E	-	-	
L6(D+E)		-	-	-	-	-	-	-	6Z	-	-	
SBAS	L1/ 1575.42	C/A	C1	C1	C1	1C	1C	1C	1C	1C	2	1
	L5/ 1176.45	I	-	C5	C5	5I	5I	5I	5I	5I	22	7
		Q	-	C5	C5	5Q	5Q	5Q	5Q	5Q	23	8
		I+Q	-	C5	C5	5X	5X	5X	5X	5X	24	9

* observation code of pseudorange (RINEX 2), band/frequency + attribute (RINEX 3)

[1] RINEX: The receiver independent exchange format version 2.10, Dec 2007, [2] RINEX: The receiver independent exchange format version 2.11, June 2007, [3] RINEX: The receiver independent exchange format version 2.12, June 2009, [4] RINEX - The receiver independent exchange format version 3.00, Nov 2007, [5] RINEX - The receiver independent exchange format version 3.01, June 2009, [6] RINEX - The receiver independent exchange format version 3.02, April 2013, [7] RINEX - The receiver independent exchange format version 3.03, July 2015, [8] RINEX - The receiver independent exchange format version 3.04, Nov 2018, [9] RTCM standard 10403.3, Differential GNSS (global navigation satellite system) services - version 3, Oct 2016, [10] BINEX: Binary exchange format - BINEX record 0x7f-05: GNSS observable prototyping (<https://www.binex.unavco.org/binex.html>)